Modulation of Mammalian Cell Behavior for Enhancing Polymer-mediated Transgene Expression

by

Matthew Christensen

A Dissertation Presented in Partial Fulfillment
of the Requirements for the Degree
Doctor of Philosophy

Approved July 2016 by the
Graduate Supervisory Committee:

Kaushal Rege, Chair
David Nielsen
Matthew Green
Karmella Haynes
Jitendran Muthuswamy

ARIZONA STATE UNIVERSITY

August 2016

ABSTRACT

Gene delivery is a broadly applicable tool that has applications in gene therapy, production of therapeutic proteins, and as a study tool to understand biological pathways. However, for successful gene delivery, the gene and its carrier must bypass or traverse a number of formidable obstacles before successfully entering the cell's nucleus where the host cell's machinery can be utilized to express a protein encoded by the gene of interest. The vast majority of work in the gene delivery field focuses on overcoming these barriers by creative synthesis of nanoparticle delivery vehicles or conjugation of targeting moieties to the nucleic acid or delivery vehicle, but little work focuses on modifying the target cell's behavior to make it more amenable to transfection.

In this work, a number of kinase enzymes have been identified by inhibition to be targets for enhancing polymer-mediated transgene expression (chapter 2), including the lead target which appears to affect intracellular trafficking of delivered nucleic acid cargo. The subsequent sections (chapters 3 and 4) of this work focus on targeting epigenetic modifying enzymes to enhance polymer-mediated transgene expression, and a number of candidate enzymes have been identified. Some mechanistic evaluation of these targets have been carried out and discussion of ongoing experiments and future directions to better understand the mechanistic descriptions behind the phenomena are discussed. The overall goal is to enhance non-viral (polymer-mediated) transgene expression by modulating cellular behavior for general gene delivery applications.

ACKNOWLEDGMENTS

I would first like to thank my advisor, Dr. Kaushal Rege, for the immeasurable impact he has had guiding me through my graduate career both through scientific dialogue as well as through deeply insightful general conversations and lessons shaping a broader skill set I will use well beyond graduation. The amalgamation of these endeavors as a Ph.D. student, including the ultimate highs of research and the tough lessons that come from the inevitable adversity encountered in the laboratory, have combined for an invaluable set of experiences that will equip me for my future profession, whatever it may be.

Many employees and students at Arizona State University have been extremely helpful with their technical insight and instrument training over my career. I would like to thank Dr. Honor Glenn of the Biodesign Institute and Dr. Debra Baluch of the Keck Bioimaging Facility for training on confocal microscopy. Dr. Tong Fu of the Biodesign Institute was instrumental in training me experimentally on flow cytometry. Dr. Karmella Haynes of the bioengineering department has been tremendously helpful as a collaborator and mentor, by both taking the time to train me on quantitative PCR and providing useful experimental advice, and through many long enlightening scientific discussions. Dr. Laura Gonzalez and Seron Eaton of the Biodesign Institute have been essential as collaborators, contributing in countless ways to multiple major projects. Phillip Schultz and Brian Thompson of the department of chemical engineering at ASU have been indispensable in providing protocols and advising on techniques that I now frequently use in the laboratory. On a day-to-day basis, nobody has been more helpful than my past and present fellow group members in the Rege lab. A special thanks to

former lab members Dr. Jacob Elmer, with whom I worked very closely for two years, and Dr. Sutapa Barua, who mentored me for the first year of my graduate career. Also a special thanks to collaborating graduate student Rene Davis as well as my Rege lab colleagues Dr. Sheba Goklany, Dr. Sudhakar Godeshala, Dr. Sai Pavan, Rajesh Niti, and Melika Meraji for their assistance in wrapping up my recent and ongoing experiments to assure that this work continues on a positive trajectory.

Dr. Christina Voelkel-Johnson, a collaborator from the Medical University of South Carolina, has been extremely perceptive and readily available in providing research direction, sharing her expertise in cancer biology. I would like to acknowledge grant funding from the National Institutes of Health, National Science Foundation, the Arizona Biomedical Research Commission, as well as the Arizona State University Dean's Fellowship. Also, a special thanks to my dissertation committee members, Dr. David Nielsen, Dr. Jitendran Muthuswamy, Dr. Matthew Green, and Dr. Karmella Haynes for their helpful guidance in the successful completion of the remainder of my thesis.

Most importantly, I would like to thank my parents David and Kris, as well as my sister Jamie and her husband Ryan. They have provided me with immense unconditional support throughout my graduate career, always ready with words of wisdom and encouragement, not to mention the often perfectly-timed visits from Iowa and/or home-cooked meals. Finally, I would like to thank my Yiayia Maria, who has always been my greatest inspiration to continue my academic path from preschool through my Ph.D., always preaching "education, education" and supporting me both financially and through articulating numerous invaluable life lessons over the years.

TABLE OF CONTENTS

Page

LIST OF TABLES

LIST OF FIGURES

Figure Page

CHAPTER 1 - INTRODUCTION

1.1 GENE DELIVERY IN MAMMALIAN SYSTEMS

The transfer of nucleic acids from an exogenous source to a target cell for the expression of a desired protein, or gene delivery, is a concept which has value in a broad range of applications. In biotechnology, gene delivery both for transient and stable recombinant protein expression, is utilized in mammalian systems for the purpose of expressing proteins that can be used as therapeutics. This approach was carried out in 2002 for the first successful production of a fully human antibody, HUMIRA, used as a therapeutic for eliminating the inflammatory response associated with the autoimmune disorder rheumatoid arthritis [2]. Mammalian production systems have also been applied to produce protein vaccines, such as Provenge, approved for the treatment of prostate cancer in 2010 [3], and a new seasonal flu vaccine produced in canine kidney cells [4]. While most mammalian-produced commercial protein therapeutics are synthesized in stably-expressing cell lines, the development of stable and high-producing cell lines is a time and cost intensive process. Consequently, it is valuable to carry out transient expression for the rapid production and screening of protein products prior to stable cell line development [5] [6]. It is important to acknowledge that production of relatively simple proteins is commonly carried out in non-mammalian cell hosts (such as bacteria), and these cell systems are important in protein production given their ease of use and, in the case of bacteria, short generational time. However, mammalian cells are capable of carrying out posttranslational modifications, such as glycosylation, that are often necessary for active proteins used as human therapeutics [7]. Taking together the advantages associated with the use of mammalian systems for protein production and the

modes in which proteins are produced in these systems, the importance of research both into stable and transient expression strategies for improving commercial (as well as lab-scale) mammalian protein production is evident.

In addition to applications in commercial protein production, in which recombinant protein products are processed for downstream applications, nucleic acid delivery is also useful for gene therapy. In gene therapy, the host cell in which the recombinant protein product is expressed is the target destination for activity. This activity can be the correction of a genetic mutation that rescues a cell or organ system; examples include the delivery of a gene expressing an enzyme facilitating proper cytosol to sarcoplasmic reticulum calcium signaling in patients with advanced heart failure [8] and correction of a mutation causing choroideremia, a condition commonly leading to legal blindness between 40 and 50 years of age [9].

Another gene therapeutic use is the destruction of target cells, as opposed to their rescue as referenced above. This is a common approach in cancer gene therapy, which constitutes over 64% of all current gene therapy clinical trials [10]. The delivery of an oncolytic virus is one approach for targeted cancer gene therapy. While the virus does not express a transgene, it contains its own genome and becomes lethal towards the tumor target through replication. This scheme works in a two-fold manner: first, the delivered virus replicates in cancer cells, resulting in cell lysis and release of newly produced virus to surrounding tumor cells which may not have taken up the virus initially. Second, the aforementioned lysis of the cancer cells results in release of immune signals, initiating an immune response against the tumor cells [11]. Herpes simplex virus, commonly employed for oncolysis, has been shown to have applications in treatment of

glioblastoma [12] and prostate cancer [13], among other malignancies. Additional gene therapeutic tactics for cell ablation involve delivery of a suicide gene, which initiates targeted cell death upon treatment with a second agent, or transfer of a tumor repressor gene, which itself has growth reduction or toxic effects on the target cells; both of these techniques are common in cancer gene therapy.

A prominent example of the delivery of a cancer-targeted "suicide" gene therapy is the combination treatment with the herpes simplex virus thymidine kinase (HSV-TK) gene and the anti-viral drug, ganciclovir [14, 15]. Briefly, cells are transfected with a vector expressing HSV-TK which phosphorylates the prodrug ganciclovir, ultimately leading to the formation of ganciclovir triphosphate in future steps. This incorporates into DNA and acts as a poor substrate for chain elongation during DNA replication, ultimately leading to cell apoptosis. This effect is imposed most prominently on cancer cells, which divide rapidly and must replicate DNA quickly. An alternative to the delivery of suicide genes is wild type tumor suppressor gene delivery to correct a mutated or deleted form of a gene, whose modification activates or promotes cancerous character. A few genes that are commonly affected through loss-of-function mutation or deletion and have been studied *in vivo* or in clinical trials for cancer gene therapy applications are p53 [16, 17], breast cancer 1, early onset (BRCA1) [18], and phosphatase and tensin homolog (PTEN) [19, 20].

Another use for nucleic acid delivery is for target gene silencing, which can be used as a study tool to determine protein function, as well as for therapeutic applications. Gene silencing can be carried out using the process of RNA interference (RNAi) using small interfering RNA (siRNA) or small hairpin RNA (shRNA)-expressing nucleic acids.

The activity of siRNA occurs in the cytoplasm, where it is processed into an active molecule that binds with and degrades mRNA of the target protein. shRNA is generally expressed in the nucleus from a DNA cassette, before being processed and exported to the cytoplasm for further processing and silencing of target protein expression. There are many informative review articles on the mechanism of RNA interference [21-23]. RNAi through nucleic acid delivery has been studied for use in treatments for cancer [24, 25], HIV [26], and rheumatoid arthritis [27], along with many other diseases.

1.2 INTRACELLULAR BARRIERS TO GENE DELIVERY

Gene delivery is a dynamic strategy that can clearly be useful in a plethora of applications, but successful gene delivery suffers from a multitude of physical hurdles. With the exception of cases in which a delivered nucleic acid's activity occurs in the cytoplasm, successful gene delivery requires the delivered cargo's successful traverse or circumvention of several intracellular barriers, including most prominently overcoming exclusion from the target cell nucleus. Gene delivery vectors are classified, at the most general level, as *viral* and *non-viral*. Viral gene delivery boasts the major advantage of efficacy over non-viral gene delivery, but certain safety and nucleic acid size limit issues associated with viral gene delivery warrant deeper exploration into improving non-viral gene delivery vectors and methods. The focus henceforth will be on *non-viral* gene delivery and its barriers (**Figure 1.1**). Non-viral gene delivery vectors constitute a wide range of cationic materials, including lipids[28], polymers [29, 30], functionalized carbon nanotubes [31], and calcium phosphate nanoparticles [32], among many others.

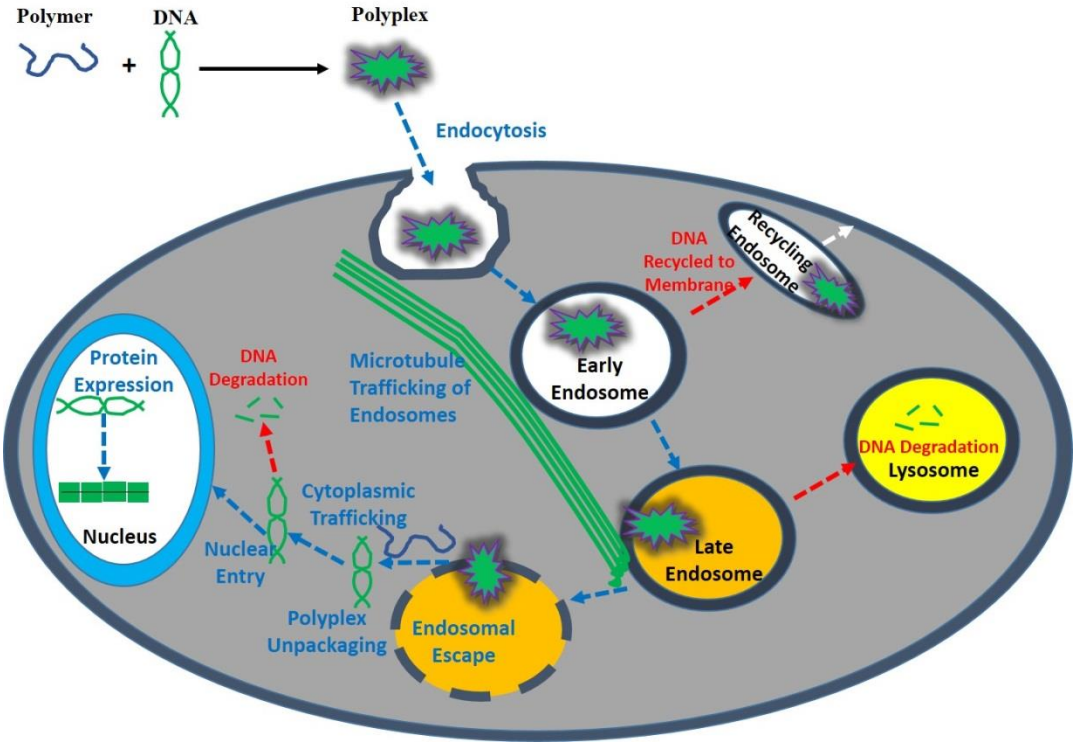

Figure 1.1 Intracellular barriers to successful endocytic non-viral gene delivery, with cationic polymer used as delivery vector: Cationic gene delivery vehicles (liposomes, polymers, calcium, and many others) can be used to condense negatively charged DNA to form deliverable nanoparticles. In addition to condensing the DNA to be delivered, cationic delivery vehicles can assist in binding to negatively charged proteoglycans on the cell membrane to facilitate uptake and shielding DNA from degrading enzymes [1]. Once the cargo enters the cell, it must escape the vesicle which facilitated its cellular entry before it fuses with degradative lysosome compartments. Following vesicle escape, DNA must traffic toward and enter the nucleus, the latter which is commonly acknowledged as the most formidable barrier to successful gene delivery

1.2.1 Pre-Cellular Uptake Barriers

Depending on the application being executed, a variety of obstacles may be present for successful gene delivery that precede uptake of the recombinant nucleic acid into the target cell. For gene therapy applications, the injection site or delivery site will vary depending on the ultimate treatment goal, and this will drastically affect the success of target cell transfection. However, two major issues generally arise when carrying out

systemic gene delivery; detection and elimination by the reticuloendothelial (RES) system, in which phagocytic cells eliminate the delivered DNA (discussed later) and delivery vector destabilization by serum albumin [33]. Strategies by which these issues are overcome will be discussed in Section 1.3.

1.2.2 Cellular Uptake

Cellular uptake mechanisms can be endocytic or non-endocytic. Creative non-endocytic strategies, such as microinjection, electroporation, and chemical pore-forming have been employed for successful gene delivery, allowing nucleic acids to bypass many barriers associated with endocytic gene delivery, including the need to escape endocytic vesicles following cellular uptake. However, applications of these invasive methods are limited, especially in the scope of gene therapy and industrial scale protein production.

Cargo entering cells in an endocytic manner can enter through phagocytosis, clathrin-mediated endocytosis, caveolae-mediated endocytosis, or pinocytosis. The pathway by which cargo enters a target cell is a complex function of the cell itself as well as the size and charge of the delivery vehicle/nucleic acid complex, and due to the heterogeneity of these delivery particles, multiple cell entry mechanisms can simultaneously occur [34].

Phagocytosis is a specialized method of endocytosis, in which cells engulf surrounding cargo. This is most commonly carried out by cells of the immune system, which engulf large particles, greater than 0.5 μm (eg. pathogens) in a vesicle referred to as a "phagosome", ultimately fusing with the lysosome and degrading the engulfed contents [35]. However, phagocytosis can occur in cells outside of the immune system, and may potentially be applied for gene delivery particles that are too large to be taken up

by the other processes discussed below; a model has been proposed for phagocytic uptake of cationic polyethyleneimine (PEI) – DNA nanoparticles into HeLa cells [36], an epithelial cell line not directly associated with the immune system. However, while phagocytosis may be useful for gene delivery applications, the presence of phagocytic cells in the immune system can actually limit the efficacy on systemic *in vivo* gene delivery by scavenging delivered DNA present in the blood [37].

Clathrin-mediated endocytosis is a receptor-dependent mode of cellular uptake, in which complexes of the protein clathrin enable invagination of the cell membrane and facilitates cargo uptake. In response to binding of ligands to cell surface receptors, adaptor associated protein complexes which simultaneously bind receptors, membrane lipids, and clathrin facilitate the formation of clathrin coats around cargo to be taken up by the cell [38]. Dynamin-2 then polymerizes and results in the detachment of the clathrin-coated vesicle, containing the newly endocytosed cargo, from the cell membrane [39]. This vesicle ultimately loses its clathrin-coating and fuses with other similar vesicles to form early endosomes [40], ultimately leading to cargo degradation in the lysosome unless it can escape the vesicle (discussed in next section). Additionally, some cargo may be recycled to the cell membrane by recycling endosomes, which could detrimentally affect gene delivery efficacy. The most prominent example of a protein taken up by this receptor-dependent pathway is transferrin [41].

Caveolae-mediated endocytosis is a clathrin-independent and receptor-mediated mechanism of cargo uptake, facilitated by the formation of cave-like structures called caveosomes. The protein caveolin-1 oligomerizes in the cell and locates to the cell membrane at areas of high sphingolipid and cholesterol content (lipid raft domain) [42],

to which it binds and assists in formation of caveosomes. In a similar manner as clathrin-mediated endocytosis, dynamin appears to be involved with the pinching off of the endocytic vesicles, but the intracellular fate is different in that cargo taken up by the caveolae pathway generally can be transported directly to the Golgi or ER for sorting, thus avoiding the degradative lysosomal pathway associated with clathrin-mediated endocytosed materials [43]. However, there are reports contrary to this notion, supporting that cases do exist in which caveolae-endocytosed materials can interface with the endolysosomal pathway [44, 45]. Common receptors involved in caveolae-mediated endocytosis are insulin and TGF-β.

While a significant amount of research efforts have been focused on associating particular systems with corresponding modes of cellular cargo entry, there remains much to be learned. Interestingly, DNA carried by related delivery vectors can be taken up by cells and trafficked in the cell in different manners. For instance, DNA delivered in Chinese Hamster Ovary (CHO) cells using two commercially available cationic liposomes displayed very different modes of cellular uptake. In the case of DMRIE-C, DNA enters cells through a caveolae pathway subsequently dependent on intracellular microtubule trafficking; however, when Lipofectamine LTX was used as a carrier, DNA was taken up via clathrin mediated endocytosis [46]. In another study in HeLa cells, DOTAP-DNA lipoplexes were taken up exclusively by clathrin-mediated endocytosis, however PEI polyplex uptake proceeded by both clathrin-mediated endocytosis and caveolae mediated endocytosis [47]. These observations indicate that subtle differences in the delivery vector can alter the manner in which materials enter cells.

Mode of endocytosis has also been demonstrated to have dependence on the size of the internalized cargo. In a murine melanoma cell line, latex beads of less than 200 nm were taken up by clathrin-coated pits, while larger beads (up to 500 nm) were taken up by caveolae [48]. Given that caveolae dependent endocytosis generally bypasses degradative lysosomes, this pathway can be advantageous in preserving nucleic acid cargo en route to the nucleus.

Pinocytosis, is another mode of cellular uptake which differs from clathrin and caveolae-mediated pathways in that receptors are not involved. This mode of uptake generally facilitates entry of larger materials than the former pathways.

1.2.3 Endosomal Escape and Cytoplasmic Trafficking

As was acknowledged in the previous section, genes taken up by clathrin-mediated endocytosis and in some cases caveolae-mediated endocytosis must escape the vesicles through which they entered the cell before endosomal maturation/lysosomal fusion occur, resulting in cargo degradation. As early endosomes fuse with late endosomes, eventually maturing into lysosomes, a concomitant drop in pH occurs. While this promotes a rugged environment for the transgene cargo, this very property can be used to assist in endosomal escape (discussed in following section).

Transport of gene delivery vectors has also been associated with trafficking along microtubules, although in many cases, it is not clear whether this occurs while vectors are inside or outside of endocytic vesicles. PEI polyplexes have demonstrated the capability to be actively transported through the cytoplasm along microtubules through interactions with cytoskeleton-dependent motor proteins [49], further evidenced by the alteration of exogenously delivered cargo trafficking by disruption of microtubules with nocodazole

[50]. This process has been shown to play a role in transgene expression, and two ways to improve cytoplasmic trafficking to the nucleus will be discussed in Section 1.3.

1.2.4 Nuclear Entry

Transgenes which successfully reach the doorstep of the nucleus by overcoming the aforementioned intracellular obstacles must ultimately enter the nucleus to allow transcription of the gene of desire; this step is extremely inefficient for non-viral vectors. The nuclei of cells that are actively dividing are generally more permeable to exogenous DNA, possibly by the nuclear membrane breakdown which occurs prior to each cell division [33]. However, the nuclei of cells which are not actively dividing are extremely difficult to penetrate, as diffusion through nuclear pore complexes only allow particles of about 9 nm in size to enter without energy-facilitated transport [51].

1.2.5 Delivery Vector/Nucleic Acid Dissociation

The aforementioned barriers to gene delivery are the preeminent barriers to gene delivery. However, unpackaging of the transgene from the delivery vehicle has also been acknowledged as a formidable barrier to successful gene delivery, as the gene must be accessible by the transcription machinery of the target cell in order for successful transgene expression. This is a very tricky obstacle in gene delivery that must be taken into account when synthesizing delivery vectors, as it works against the preceding steps of gene delivery, in which nucleic acid protection through strong carrier/exogenous DNA interaction is desirable [1]. Interestingly, RNA present in the cytoplasm [52] and chromosomal DNA in the nucleus [53] have both demonstrated the ability to remove cationic carriers from exogenous DNA through ion-exchange, suggesting that delivery

vehicle-nucleic acid nanoparticles can be dissociated either in the cytoplasm or following nuclear entry.

1.3 METHODS FOR OVERCOMING GENE DELIVERY BARRIERS

1.3.1 Non-viral Delivery Vehicles and Vector Modifications

1.3.1A Use of Efficient Delivery Vehicles –

Although naked nucleic delivery has its applications in specific *in vivo* applications and for siRNA delivery (which does not require nuclear entry) [54], for most purposes a delivery vector is required to obtain efficacious transgene expression. Generally, gene delivery vectors are polycations, and by far the most common non-viral vector classes are cationic lipids and cationic polymers, which can spontaneously complex with DNA through electrostatic interactions. Although polycations have been used for delivering DNA to target cells (E. coli) since the 1970s [55], the introduction in the mid-1990s of polyethyleneimine (PEI), an efficacious cationic polymer gene delivery vehicle initiated an unmistakable effort towards discovering and designing new gene delivery vehicles, as well as improving on PEI. PEI is especially attractive as a gene delivery vector because of its ability to escape from endosomes via the "proton sponge effect" due to its high cationic charge through the presence of protonable amines. The proton sponge effect is a controversial theory in the gene delivery field, albeit with strong evidence. Briefly, molecules with protonable amines, with pKa nearly neutral, will become more protonated as the pH decreases from just above neutral to acidic along the endocytic pathway (early endosome to lysosome). The abundance of protonable amines

will continue to "absorb" protons, increasing their flux into the endosome, bringing about negative counterions (Cl^-), ultimately leading to an increase in osmotic pressure compromising the endosomal membrane and releasing the polyplex [56]. Due to the relatively high efficiency of PEI as a vector, many studies have been conducted to improve on the parental structure of PEI to improve transfection efficacy and reduce toxicity [57, 58], including jetPEI, a linear (unbranched) PEI derivative. Another group of delivery vectors, fusogenic peptides, are efficient at inducing endosomal escape through fusing with lipid membranes and facilitating cargo release into the cytoplasm. These commonly employed peptides mimic a membrane fusion domain common in viruses [59].

In addition to PEI and other synthetic polymers, natural polymers (including polypeptides) such as collagen [60], histones [61, 62], and chitosan [63] have been successfully used for carrying out transfections. These polymers have the advantage of being biocompatible [64] given they are found in humans or other eukaryotes (in the case of chitosan). Rational high throughput polymer design and screening approaches have been applied to discover non-viral polymer vectors [30, 65], combined with quantitative structure activity relationship (QSAR) regression modeling to not only identify effective delivery vectors, but to ascertain physicochemical characteristics that make the polymers efficacious to assist in future polymer design [66].

In addition to cationic polymers, cationic lipids are very commonly used as gene delivery vehicles. Lipids are advantageous in that they possess hydrophobic moieties that can interact with cell and endosomal membranes. The most common cationic gene delivery lipid used for lipoplexes is 1,2-Dioleoyl-3-trimethylammonium-propane

(DOTAP), and the helper lipid 1,2-Dioleoyl-*sn*-glycerol-3-phosphoethanolamine (DOPE) is often added to improve transfection [67]. Lipofectamine® is a commercially available cationic lipid based transfection reagent manufactured by Thermo-Fisher with very high transfection efficiencies, often used as a standard when comparing other gene delivery vehicles.

1.3.1B Functionalization of Delivery Vehicles -

Even the most efficacious cationic gene delivery vehicles can be modified to improved general transfection, or modified to cater to specific applications such as cell targeted gene delivery. For gene delivery applications that must deal with systemic barriers such as RES clearance or aggregation due to interactions with serum proteins, delivery vehicles can be functionalized to mitigate these issues. The most common modification is the addition of polyethylene glycol (PEG), a process referred to as PEGylation. The addition of this hydrophilic group shields the cationic vehicle's charge from surrounding proteins and reduces interaction with surrounding erythrocytes [68], ultimately increasing circulation time and increasing the probability of cellular uptake. While PEGylation is a well-studied and commonly employed tactic for improving *in vivo* gene delivery, due to potential problems with oxidation, the introduction of zwitterions to delivery vehicles can be employed to buffer or absorb any non-specific interactions with serum proteins [33].

Cellular localization/uptake can be improved by conjugating antibodies or other ligands that are recognized by cell receptors. For example, transferrin, generally taken into cells via clathrin-mediated endocytosis, has been shown to improve gene delivery when conjugated to liposomes [69]. A similar approach has also been carried out by

conjugating recombinant epidermal growth factor (EGF) to the polymer poly-L-lysine, improving gene delivery to lung cancer cells which overexpress EGF receptor (EGFR) [70], an example of modifying a vector to carry out cancer-targeted gene delivery.

Modifications can be made to cationic delivery vehicles to overcome endosomal entrapment, such as the addition of imidazole groups, which contain protonable amines to efficient gene delivery polymers such as cyclodextrin as carried out by Davis et al [71]. However, a common approach for overcoming this barrier is the direct addition to cells of 4-amino quinoline molecules such as chloroquine [72], which themselves have protonable amines and can have drastic enhancing effects on transgene expression by promoting the proton sponge effect.

Unpackaging of cationic delivery vehicles and nucleic acids is essential for transcription to occur, which generally requires compromise in using a vehicle that sufficiently protects the nucleic acid cargo, but liberates it prior to or following nuclear entry. It is very difficult to change molecular structure to decrease DNA binding capabilities in such a way that will not affect other key factors such as cellular uptake or endosomal escape. Potential methods to overcome this issue include use of environmentally sensitive carriers, such as those that may release DNA in low pH environment (eg. in cancer cells or in late endosomes) or temperature sensitive environment that will only dissociate in response to an external heat stimulus [73]. Although it is difficult to account for this barrier in parallel with many others, it is important that vectors are designed with eventual release of its nucleic acid cargo in mind.

1.3.1C Modification of Exogenous DNA Sequence or Addition of Biologically Relevant Amino Acid Sequence -

In addition to modifying delivery vectors, transgene expression can be improved by incorporating particular nucleic acid sequences on the delivered DNA that can promote trafficking towards the nucleus or nuclear translocation. One strategy that has been employed by Dean et al is the utilization of transcription factor binding sites. In these studies, it has been shown that plasmid DNA indirectly interacts with microtubules during gene transfer [74] and plasmids containing binding sites for the transcription factor cyclic AMP response-element binding protein (CREB, present on the CMV promoter), displayed increased trafficking velocity toward the nucleus and ultimately increased rate of nuclear entry following microinjection [75] (i.e. avoiding endocytic vesicles altogether). This is a potentially promising strategy, essentially allowing DNA to piggyback a transcription factor to the nucleus.

The most common strategy for overcoming the nuclear exclusion hurdle is conjugation to the DNA vector or cationic carrier of a nuclear localization signal (NLS), a short peptide sequence originally found in the SV40 large T antigen that interacts with karyopherins, promoting nuclear entry through the nuclear pore. While this NLS-conjugation strategy has shown potential when applied to linear DNA in HeLa and NIH 3T3 cells[76], it lacks promise when delivering plasmid DNA [77, 78]. Additionally the SV40 enhancer DNA sequence, which binds many transcription factors containing NLS sequences [75], is a useful sequence for gene delivery; this sequence is provided on many commercially available DNA plasmids, facilitating increased nuclear uptake. Also important in efficacious transgene expression are promoter choice and codon optimization for the gene of interest. In many cases, a constitutive promoter such as

CMV, ubiquitin, or EF1α is desired in order to drive expression to its highest possible level. However, careful promoter selection can also be enforced for efficacious and *targeted* transgene expression. For example, Hochberg et al created the BC-819 plasmid, now in clinical trials, which expresses the potent diphtheria toxin A (DTA) under the control of the H19 long non-coding RNA promoter which is only active in cancer cells [79], allowing for selective ablation of cancer cells. Finally, codon-optimization is an important consideration when carrying out gene delivery when delivering a gene originating from one species to a cell of another. Certain codons are highly present in one species and rare in another, and the efficiency of transcription if transferring a gene from the former species to a cell of the latter may be reduced, because the codon in the target cell matching the recombinant DNA codon may be lacking. Species specific codon optimization can circumvent this issue, with one example being the successful production by Zolotuhkin et al in 1996 of humanized green fluorescent protein (GFP), a gene originally from jellyfish [80].

1.3.2 Modification of Mammalian Cell Behavior by Intracellular Protein Activation, Inhibition, or Silencing

Much investigation in the field of gene delivery has focused on enhancing efficacy by synthesis and optimization of nucleic acid delivery vehicles or nucleic acids, but fewer investigations have studied the effects of modulating cell behavior for enhancing transgene expression. The current general approach is to tailor gene delivery vectors to fit the cell's machinery, but a second approach is to tailor the cell's machinery in such a manner that the cell becomes conducive to transfection through activation, inhibition, or silencing of proteins.

One example of this approach is through modulating cell cycle for optimal transgene expression. Polyplex transgene expression has been reported by Brunner et al to be optimal in the late G2 or S phase (just preceding mitosis), and relatively poor in the G1 phase (just following mitosis) [81]. Growth arrest and DNA-damage-inducible protein Gadd45 is expressed in response to DNA damage, leading to G2/M arrest. Kim et al produced a Chinese hamster ovary (CHO) cell line that inducibly over-expressed Gadd45, leading simultaneously to G2/M cell cycle arrest and enhanced PEI-mediated transgene expression [82]. A study carried out in 2012 indicated that hyperacetylation of microtubules by inhibition of the cytoplasmic enzyme histone deacetylase 6 (HDAC6) leads to an increase in plasmid/microtubule interactions, increased rate of plasmid movement towards the nucleus, and increased transgene expression [83], the final phenomenon which has also been shown in our laboratory [84]. These are examples of modulating cell behavior to become more conducible to transfection, providing insight into mechanisms which can be exploited for successful gene delivery through enzyme inhibition.

While there exists a general understanding of the obstacles to efficacious gene delivery (as summarized above and in **Figure 1.1**), the molecules and mechanisms behind these barriers are very poorly understood. A more thorough understanding of the molecules responsible for these pathways that regulate gene delivery will lead to improvements in gene therapy and transient protein production. In the following chapters, the focus will be identification of exploitable enzyme targets for enhancing transgene expression and mechanistic evaluation of these targets' effects on transgene expression.

CHAPTER 2 - KINOME-LEVEL SCREENING IDENTIFIES INHIBITION OF POLO-LIKE KINASE-1 (PLK1) AS A TARGET FOR ENHANCING NON-VIRAL TRANSGENE EXPRESSION

2.1 INTRODUCTION

While the physical barriers discussed in chapter 1 formidably combat successful transfection, there also exist biochemical defenses that reduce promiscuity of cells to foreign DNA. For example, Toll-Like Receptor 9 (TLR9) of immune cells provide defense against bacteria and viruses by binding unmethylated cytosine-guanine (CpG) base pairs on foreign DNA (host CpGs are methylated and do not activate TLR9) [85, 86]. Upon TLR9 binding, a signal is transduced by means of several kinases (IRAK-1, IRAK-4, TAK1, IKK, and MAPK) which subsequently activates a number of transcription factors (NF-κB, AP-1, and IRF7), leading to expression of interleukins and interferons, inducing an immune response [87]. Activation of TLR9 has been shown to reduce plasmid transgene expression [88], an effect that can be partially obviated by design of plasmids lacking CpGs [89].

The kinases involved in the TLR9 pathway are just one example of greater than 500 kinases in the human kinome [90] that play key roles in intracellular processes, including endocytosis (PI3K [91], EGFR [92], AAK [93], mTOR [94]), cell cycle progression (CDK, PLK, Aurora)[95], and gene transcription (JAK/STAT [96] and JNK[97]) among many others. Due to the prominent role of kinases in mammalian processes, it is very likely that kinases are directly or indirectly involved in gene delivery, including the barriers discussed in chapter 1. There have already been demonstrated cases of kinase inhibition directly affecting gene delivery. For example, ur Rehman et al. showed that inhibition of Protein Kinase A (PKA) enhances gene delivery 2-3 fold by promoting lipoplex and polyplex

uptake through the generally more efficient caveolae-mediated endocytic route from the less efficient clathrin-mediated endocytic route [98]. Inhibition of Rho kinase by Y-27632 also increases lentiviral transduction by 20% in keratinocytes[99]. In contrast, inhibition of PI3K has been shown to reduce adenoviral transduction, since PI3K plays a key role in α integrin-associated endocytosis of viruses [91]. Adaptor-associated protein kinase 1 (AAK1) has been demonstrated to play a regulatory role in clathrin-mediated endocytosis. Through phosphorylation of the adaptor protein 2 (AP2) complex, which along with clathrin complexes forms the major protein coat around endocytic vesicles, AAK1 has an inhibitory effect on clathrin-mediated transferrin uptake [93]. Additionally, kinases involved in the mTOR pathway have been demonstrated to affect microtubule trafficking of caveolin-1 [94], a key component in the formation of cell membrane caveolae for caveolae-mediated endocytosis.

Given these examples of kinases demonstrated to affect transgene expression or endocytic processes that are likely involved in gene delivery, there exists some evidence to indicate that inhibition or activation of other kinases has the potential to either increase or decrease the efficacy of transgene expression. The experiments carried out in chapter 2 involve a kinome-level screen of small molecule inhibitors, with an output of normalized transgene expression observed with inhibition of many kinases. Many kinase targets were identified that enhance polymer-mediated transgene expression when inhibited; most prominently, the cell cycle regulatory protein polo-like kinase 1 (PLK1).

2.2 METHODS

2.2.1 Cell Culture

PC3-PSMA prostate cancer cells [100], derived from PC3 cells, were kindly provided by Michel Sadelain, MD, PhD, Memorial Sloan–Kettering Cancer Center (New York, NY). MB49 cells were kindly provided by Dr. Christina Voelkel-Johnson (Medical University of South Carolina) as part of an existing collaboration. PC3-PSMA cells were cultured in RPMI 1640 Medium (Hyclone®), containing 10% fetal bovine serum (Hyclone®) and a Penicillin (100 units/mL) – Streptomycin (100 µg/mL) antibiotic combination (MP Biomedicals, LLC). MB49 cells were maintained in Dulbeccos Modifed Eagle's Medium (Life Technologies) with the same serum and antibiotic content. Cells were grown in an incubator maintained at 37^{o}C and 5% CO_2.

2.2.2. Polymers

The 1,4C-1,4bis polymer was synthesized by mixing the monomers 1,4-cyclohexane dimethanoldiglycidyl ether (1,4C, Sigma) and 1,4-bis(3-aminopropyl)-piperazine (1,4Bis, Sigma) at a 1:1 molar ratio as described previously [30]. 25 kDa branched polyethyleneimine (PEI) was purchased from Sigma. Polymers were solubilized in 1X phosphate buffered saline (1X PBS, 10 mM PO_4^-, 137 mM NaCl, 2.7 mM KCl) following 16 hours of polymerization, and the pH was adjusted to 7.4.

2.2.3 Parallel Screening of Small Molecule Kinase Inhibitors

A library of kinase inhibitors pre-dissolved in DMSO at 10 mM was purchased from Selleck Chem (Cat# L1200, Houston, TX). A complete list of the kinase inhibitors and their known kinase targets can be found in **Appendix I**. PC3-PSMA cells were seeded

in 96 well plates (15,000 cells/well) and incubated overnight (~18 hrs) at 37^{o}C in serum-containing RPMI media (SCM). Polyplexes were prepared by mixing the polymer 1,4C-1,4Bis [30] with pGL3.0 plasmid DNA (Promega; luciferase expression plasmid with an SV40 promoter) at a 10:1 mass ratio and incubating the solution at room temperature for 20 minutes. SCM media was then removed from cells and replaced with SFM media. Polyplexes (60 ng plasmid DNA/well) and kinase inhibitors (final concentration of 10 x IC_{50} with 0.5% DMSO) were simultaneously added to each well using a Biomek NXP laboratory automated liquid handling station (Beckman-Coulter). Cells were incubated with polyplexes and inhibitors for 6 hours at 37^{o}C. The media was then changed to SCM (with a unique kinase inhibitor in each well) and the cells were incubated at 37^{o}C for an additional 48 hours to allow for transgene (luciferase) expression.

2.2.4 Dose Response Optimization of Kinase Inhibitor Leads

Small molecule PLK1 inhibitors (drugs) BI 2536, BI 6727, HMN-214, and ON01910 used for dose response optimization studies were all purchased from Selleck Chemicals, and stored at -80^{o}C. Optimization experiments with inhibitor leads were carried out in a similar fashion to screening experiments, but in 24 well plates with 200 ng pGL3.0 or pEGFP-C1 (Clontech; an EGFP expression plasmid with a CMV promoter) plasmid DNA/well, at various concentrations of each inhibitor with various polymers (10:1 w/w 1,4C-1,4Bis or 1:1 w/w PEI) and cell lines (PC3-PSMA or MB49, both seeded at 50,000 cells/well).

2.2.5 Determination of Cell Viability Using MTT Assay

Cell proliferation in case of different treatment conditions, relative to untreated control cells (treated as 100% viable, or a live control), was quantified using 3-(4,5-

Dimethylthiazol-2-yl)-2,5-diphenyltetrazolium bromide (MTT), a yellow colored reagent which is converted to formazan (a purple dye) by living cells. For screening experiments, transfections were carried out in 96-well cell culture plates, seeding 15,000 cells. Following 48 hours of transfection, ten microliters of MTT reagent was added to the cells and incubated at 37^{o}C for 2-4 hours, and the cells were then lysed by adding 20 microliters of MTT detergent and incubated for an additional 2 hours at room temperature. Inhibitor dose-optimization transfections were carried out in 24-well plates, seeding 50,000 cells. After 48 hours, 20 microliters MTT reagent was added, followed by 100 microliters of MTT detergent for lysis for 2 hours.

In both cases, the concentration of formazan was then determined by measuring the absorbance of each well at 570 nm (A_{570}). Cell proliferation (PRO) was calculated by dividing the A_{570} of each sample by the A_{570} of the live cell control (no inhibitor or polyplex added), after subtracting blank absorbance.

2.2.6 Quantification of Luciferase Expression

Luciferase expression was quantified using the Luciferase Assay Kit from Promega (Madison, WI). Media was removed from the plates and cells were washed once with PBS before adding cell culture lysis reagent (Promega) to each well and incubating the plates at 37^{o}C for 20 minutes. Cell lysate (15 μL) was then mixed with luciferin solution (30 μL) and luminescence (LUM) was immediately measured using a Synergy 2 plate reader (Biotek, Winooski, VT). Luminescence units accounting for changes in proliferation (LUV) were calculated by dividing luminescence values (LUM) by relative cell proliferation (PRO). The LUV values of each sample were then divided by the LUV value of the control sample (no drug) to provide the RLUV values shown in each figure.

Therefore, the RLUV values presented here account for changes in cell density (e.g. a condition with luminescence similar to the control but with 50% relative cell proliferation will be multiplied by a factor of two) and illustrate the degree of enhancement for each condition relative to the control.

2.2.7 Quantification of EGFP Expression

At 48 hours post-transfection, cells were washed with 1X PBS, trypsinized, and pelleted via centrifugation at 500 X g for 5 minutes. Pellets were resuspended in 1X PBS, and flow cytometry analysis, carried out using a FACSCalibur (Benton Dickinson) machine, was used to quantify intracellular EGFP fluorescence, as detected by the FL1 emission filter. PMT voltage settings were adjusted based on live cell controls. Fluorescence gating was performed such that control samples (at each drug concentration, lacking polyplex treatment) showed 0.1% fluorescence-positive cells. Side and forward scatter plots for the live cell control were also used for live/dead gating to ensure that only live cells were included in the final flow cytometry analyses. Calculations for fluorescence intensity per cell involved subtraction of the drug only conditions (no transfection) arithmetic average cell fluorescence from the transfected counterpart to avoid including drug background fluorescence or autofluorescence in reported values. In PC3-PSMA cells, all experiments involving the BI 2536 inhibitor were carried out three times. For all other conditions in PC3-PSMA and MB49 cells, at least two independent experiments (in some cases three) were carried out.

2.2.8 Production and Evaluation of Lentiviral Particles for PLK1 Knockdown

Plasmids expressing shRNA for knocking down PLK1 (total=20) were selected from the shRNA collection library (The RNA Consortium (TRC)) in Dr. Joshua LaBaer's

laboratory at The Biodesign Institute, Arizona State University. From these 20 clones, 4 (TRCN0000006246-6249) were selected based on target knockdown efficiency reported in previous publications [101-104]. cDNA was produced (Qiagen Maxiprep kit), and lentiviral particles were produced by transfecting LentiX-293T cells (Clontech) with either PLK1 or scramble control-shRNA and packaging plasmids using established SOPs [105]. After finalizing viral production, the resulting virus was used to infect PC3-PSMA cells.

To evaluate the silencing of PLK1 using the lentiviral particles, immunoblotting experiments were carried out on PC3-PSMA cell lysates after cells were infected with either a scramble control or each lentiviral clone for PLK1 knockdown (total=4). The GAPDH (loading control) and PLK1 antibodies were purchased from Cell Signaling and used at a working dilution of 1:1000. Following transfer, membranes were blocked with 5% milk in TBS-Tween (TBS-T, 0.2% tween), and incubated in primary antibody overnight at 4^{o}C. Membranes were then washed with TBS-T, and incubated with an HRP-conjugated secondary antibody (1:1000 dilution) for one hour at room temperature. Following additional washes, membranes were treated with SuperSignal West Femto Chemiluminescent substrate (Thermo) for antibody detection. Based on literature and our own results, it was determined that the virus correspondent to clone PLK1-shRNA 6247 would be used for further experiments. This virus successfully knocked down PLK1 in PC3-PSMA cells and affected cell growth.

2.2.9 Combined PLK1 Silencing and Transgene (pGL3 Plasmid) Delivery to PC3-PSMA Cells

PC3-PSMA cells were infected with either PLK1 or a scramble control lentivirus. In brief, 12,500 cells were plated in a 24 well plate, and on the following day, polybrene

(8 μg/mL) was added, followed by lentivirus (200 μl) or no further treatment (i.e. equivalent volume media). Plates were centrifuged for 30 minutes at 2250 rpm and incubated at 37ºC and 5% CO_2. Following 48 hours, transfection experiments and luminescence-quantifying assays were carried out as previously described. Experiments were carried out using 1,4C-1,4bis and PEI as polymer carriers at polymer to DNA weight ratios of 10:1 and 1:1, respectively.

2.2.10 Cell Cycle Analysis

Propidium Iodide (PI) staining was carried out in order to determine relative cell cycle proportions of the PC3-PSMA cell population in the presence and absence of PLK1 inhibitors, BI 2536 and HMN 214. Briefly, 250,000 PC3-PSMA cells were plated per well in a 6 well plate and allowed to attach and grow overnight. Cell culture media was removed and replenished with fresh SCM containing drug or vehicle control. After 48 hours, cells were washed with 1X PBS harvested via trypsinization, and resuspended in a small amount of 1X PBS. Pure ice-cold ethanol was added dropwise to the PBS cell suspension, resulting in a final EtOH concentration of 70%, at which point, cells were stored at 4ºC for 1 hour to allow for fixation. Cells were then washed with 1X PBS/2% FBS/0.001% Triton X, followed by a wash with 1X PBS/2% FBS. Cells were then incubated with a PI (Sigma) staining solution prepared in 1X PBS (5% FBS, 50 μg/mL PI, 100 μg/mL RNase A). Cells were then analyzed in a FACS Attune® acoustic focusing flow cytometer, with PI signal detection through the B3 emission filter. Live/Dead gating was carried out using a side/forward scatter dot plot, and only live cells were included in final analysis. Cell doublets were gated out of analysis, as determined by high fluorescent width (B3-W) values, indicative of long detector residence time. Cell cycle percentages given are

representative of percentage of cells falling in the subG1 (<2N DNA content; typically apoptotic fraction), G0/G1 (2N DNA content), S (between 2N and 4N DNA content), G2/M cycles (4N DNA content). A small portion of the cell population shows fluorescence greater than that represented by 4N DNA content. Some of these cells may actually have greater than 4N DNA content, while a proportion is likely cell doublets that are not eliminated by gating.

2.2.11 Intracellular Trafficking of Polymer-Plasmid DNA Polyplexes

The *Label* IT® fluorescein-conjugated plasmid from Mirus was used to monitor plasmid DNA intracellular trafficking. PC3-PSMA prostate cancer cells were plated in 24 well plates at a density of 50,000 cells per well on top of coverslips, and allowed to attach overnight. On the following day, cells were incubated with 10 μg/mL DAPI and allowed to stain overnight at 37^{o}C. The following day, several washes with 1X PBS were carried out in order to remove residual DAPI, thus avoiding false nuclear detection by staining the plasmid DNA. Serum-free media containing the drug or 0.2% DMSO control was added to the cells while polyplexes were formed by mixing PEI with 2 μg of fluorescein-labeled plasmid DNA at a 1:4 polymer to DNA mass ratio. Polyplexes were added to the cells and allowed to be internalized for 6 hours after which, cells were replenished with serum-containing media containing drug or DMSO. Following 48 hours of transfection, cells were washed twice with 1X PBS, and fixed with 2% formaldehyde for 20 minutes. Cells were then washed 5 times with 1X PBS, and mounted using a 90% glycerol solution containing n-propyl gallate. Confocal microscopy was carried out with a Nikon C2 Confocal equipped with a 60X water immersion objective, which was utilized to determine polyplex trafficking relative to the nucleus. Laser excitation of 488 nm was used and emission at

525 nm was captured for fluorescein detection. Z-stack images were taken with a step size of 0.330 μm, with the images displayed representing a maximum projection signal through the z-axis, unless otherwise noted.

2.3 RESULTS

2.3.1 Kinase Inhibitor Screen

A library of 182 kinase inhibitors was screened in order to identify leads that enhance polymer-mediated transgene (luciferase) expression in PC3-PSMA prostate cancer cells (complete list of kinase inhibitors tested in **Appendix I** [106]). Fifteen different inhibitors enhanced luciferase expression by a factor of 4-fold or greater relative to the vehicle control (1,4C-1,4Bis polymer [30] complexed with pGL3.0 plasmid DNA in 0.5% DMSO); a concentration of 10 times the reported IC_{50} value for each inhibitor was employed in the screen (**Table 2.1** for 15 inhibitor leads, **Appendix I** [106] for a complete list of screening results). Luminescence values were normalized to total protein (eg. luminescence/mg protein) to account for any differences in cell plating, and further normalized to viability, yielding relative luminescence units normalized to viability (RLUV in **Table 2.1**). Interestingly, some inhibitors, including two PI3K inhibitors (TGX-221 and AS252424), two CDK inhibitors (AZD5438 and Flavopiridol HCl), and a single JAK inhibitor (LY2784544), decreased luciferase expression to less than 50% of the control in cells.

Since many kinase targets were represented by multiple small molecule inhibitors, the data were organized by target with an average RLUV represented for each target

(**Figure 2.1** [106]**).** The clear top screen identified target for enhancing transgene expression is polo-like kinase 1 (PLK1), a cell cycle regulatory kinase, with expression strongly enhanced at 9.5 ± 3.7 fold relative to the vehicle control, with the top four individual inhibitors all targeting PLK1 (**Table 2.1**). These four PLK1 inhibitors constitute four of five total PLK1 inhibitors tested, with the fifth one also performing well (ON-01910, 3.2 ± 1.5 RLUV).

Table 2.1 – Enhancement of luciferase transgene expression (RLUV) by the 15 most effective small-molecule kinase inhibitors identified from the screen

Inhibitor	Kinase Target(s)	RLUV
BI 6727	PLK1	12.4 ± 13.8
BI 2536	PLK1	12.3 ± 5.3
GSK 461364	PLK1	9.9 ± 4.8
HMN-214	PLK1	9.5 ± 8.3
SKI-606	Src/Abl	6.6 ± 11.0
AG-490	EGFR/JAK/ErbB2	6.4 ± 10.7
PD0332991	CDK 4,6/Cyclin D1,2	6.1 ± 5.6
SNS-314	Auroras A, B, C	6.0 ± 6.1
Imatinib	Abl/c-Kit/PDFGR	5.3 ± 4.7
Vinorelbine	p38 MAPK	4.9 ± 2.5
VX-702	p38 MAPK	4.8 ± 4.1
PHA-680632	Auroras A, B, C	4.4 ± 5.5
KW 2449	FLT-3/Abl/Aurora A	4.4 ± 4.1
NVP-ADW742	IGF-1R	4.4 ± 5.9
SNS-032	CDK 2, 7, 9	4.1 ± 2.4

In addition to PLK1 inhibitors, several other inhibitors for kinases involved in the cell cycle (CDK, Cyclin, p38 MAPK, and Aurora) also showed 2-fold enhancement or higher. These include PD0332991 (CDK/Cyclin inhibitor, RLUV = 6.1 ± 5.6), SNS-314 (Aurora inhibitor, RLUV = 6.0 ± 6.1). Additionally, an inhibitor of p38 MAPK, involved in stress response, enhanced transgene expression drastically (Vinorelbine, RLUV = 4.9 ± 2.5). Inhibition of the cell cycle kinases reduced cell proliferation by at least 20% (Aurora

kinase) relative to the control, while some PLK1 inhibitors decreased proliferation by up to 36% (data not shown).

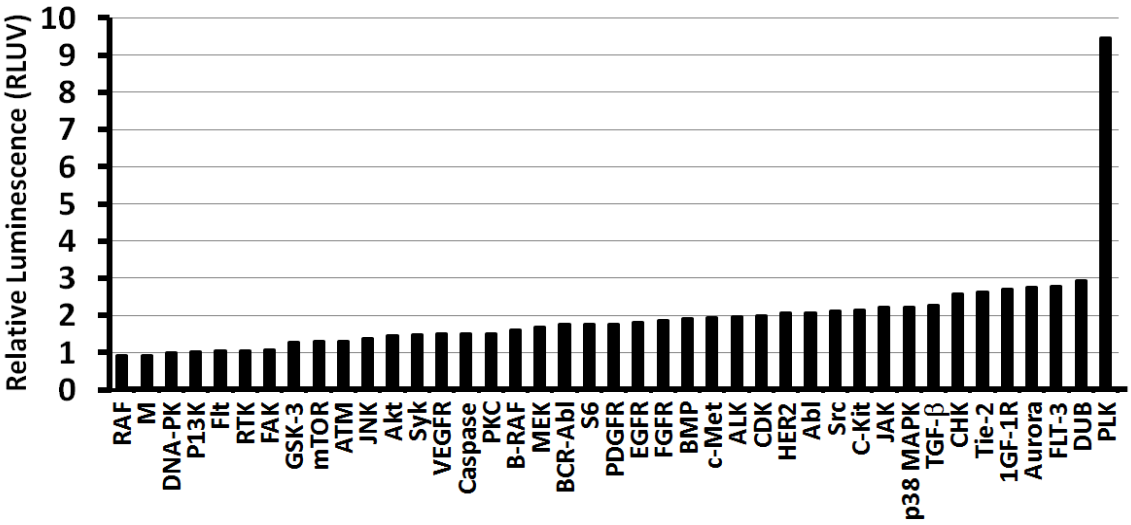

Figure 2.1 Identification of kinase targets that influence transgene expression. The enhancement values of individual inhibitors with the same kinase target were pooled together to prepare this figure. The y-axis shows enhancement relative to the polyplex control (RLUV = 1), while the x-axis indicates the kinase enzyme targeted by the inhibitor(s)

In addition to cell cycle kinases, 4 out of the 9 JAK inhibitors tested showed greater than 2.4-fold enhancement (AZ960, AZD1480, AT9283, and AG-490), with the JAK2 inhibitor AG-490 (IC_{50} = 10 μM) showing the highest enhancement of 6.4-fold relative to the polyplex control. Interestingly, AG-490 also inhibits the membrane-bound growth factor receptors EGFR (IC_{50} = 0.1 μM) and HER2 (IC_{50} = 13.5 μM)[107]. Several other growth factor receptor inhibitors also showed significant enhancement of luciferase expression compared to the polyplex control, including two additional EGFR inhibitors, CI-1033 and Neratinib, which showed 2.7 and 3.8-fold enhancement, respectively. Several different PDGFR inhibitors also enhanced luciferase expression (AP24534, Crenolanib, TSU-68, Masitinib showed 2.1-2.3 fold enhancement), while Imatinib (aka Gleevec)

demonstrated the strongest enhancement (5.3-fold). It is important to note that multiple PDGFR inhibitors also inhibit FGFR (AP24534, TSU-68, and Masitinib) and VEGFR (AP24534 and TSU-68). Three VEGFR-specific inhibitors also showed 2.3-2.6 fold enhancement (Axitinib, MGCD-265, and Vatalanib). Finally, the IGF-1R inhibitor NVP-ADW742 and the TGF-β inhibitor SB525334 exhibited 4.4- and 2.3-fold enhancement of luciferase expression, respectively. While these results suggest that growth factor receptor inhibition enhances transgene expression, several other growth factor receptor inhibitors showed no significant enhancement of luciferase expression (RLUV $\leq$ 1.0).

While this screen revealed a number of kinase targets for enhancing polymer-mediated transgene expression, it is important to point out that the kinases covered constitute less than 10% of the 518 known human kinases. Thus, this screen is not exhaustive, and there are likely many other kinase targets that we have not identified. Nonetheless, the screen revealed several kinase targets for enhancing transgene expression, mainly in the classes of cell cycle, signal transduction, and growth factor receptor kinases. The most promising target, PLK1, was selected for further investigation.

2.3.2 Dose-Optimization of Lead Inhibitors – PLK1 and JAK2 (Luciferase Expression)

Two of the most effective PLK1 inhibitors were evaluated at various concentrations in order to further investigate the effects of PLK1 inhibition on transgene (luciferase) expression in the original screening cell line (PC3-PSMA) as well as a murine bladder cancer cell line (MB49). HMN-214 consistently showed high enhancement of luciferase expression relative to vehicle control with the 1,4C-1,4Bis polymer (11-fold) and PEI (37-fold) at an optimum concentration of 3.3 μM in PC3-PSMA cells (**Figure 2.2**). HMN-214 also demonstrated greater enhancement with PEI than 1,4C-1,4Bis in MB49 cells, but to a

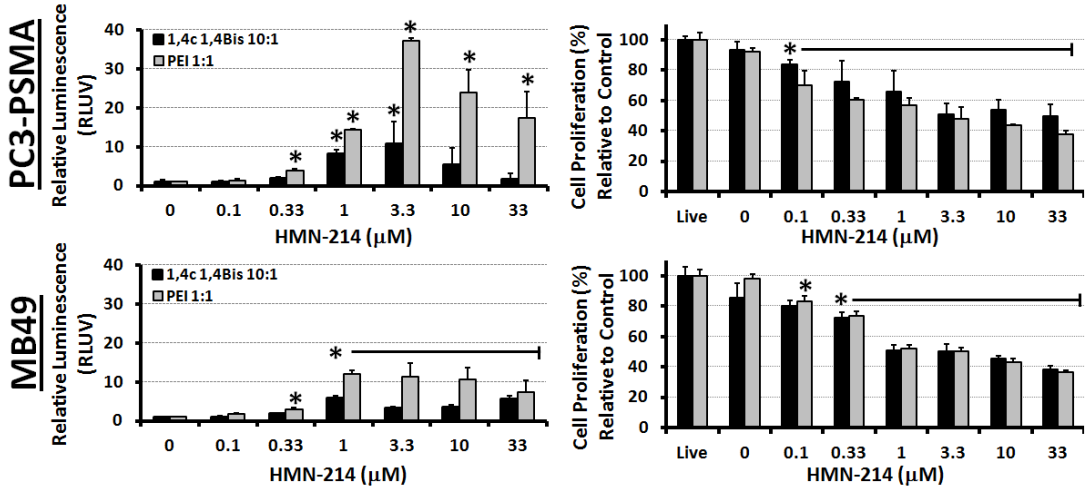

Figure 2.2 Dose-dependent enhancement of luciferase transgene expression by the PLK1 inhibitor HMN-214 in PC3-PSMA human prostate cancer and MB49 murine bladder cancer cells following delivery of pGL3.0 plasmid DNA using PEI and 1,4C-1,4Bis polymers. Relative enhancement of luciferase expression (RLUV) compared to the polyplex control is shown in the left panels, while effects of the drug on cell proliferation are shown in the panels on the right side. Asterisks (*) indicate statistically significant difference (student's T-test) from the corresponding polyplex control (n = 3 independent experiments; $p < 0.05$)

lesser extent (6 and 12-fold enhancement with 1,4C-1,4Bis and PEI, respectively) at an optimal concentration of 1 μM. As expected for PLK1 inhibition, HMN-214 also significantly reduced cell proliferation, with the lowest viabilities (40-50%) at concentrations above 3.3 μM. Interestingly, a sharp drop in proliferation was observed in MB49 cells at the same HMN-214 concentration which maximally enhances transgene expression (1 μM). This anti-proliferative activity of the drug can be useful in cancer gene therapy applications.

The dose optimization of another effective PLK1 inhibitor, BI 2536, is shown in **Figure 2.3**. BI 2536 increased luciferase expression 3-6 fold at concentrations of 10 and 100 nM in PC3-PSMA and MB49 cell lines, respectively. While the optimal concentration for enhancing luciferase expression differs by a factor of 10 between the two assayed cell lines, it is interesting to note that the optimal concentration in both cell lines coincides with the point at which cell proliferation is reduced by 40% **(Figure 2.3** [106]**)**, suggesting that inhibition of cell division by the drug is necessary for the enhancement of gene delivery.

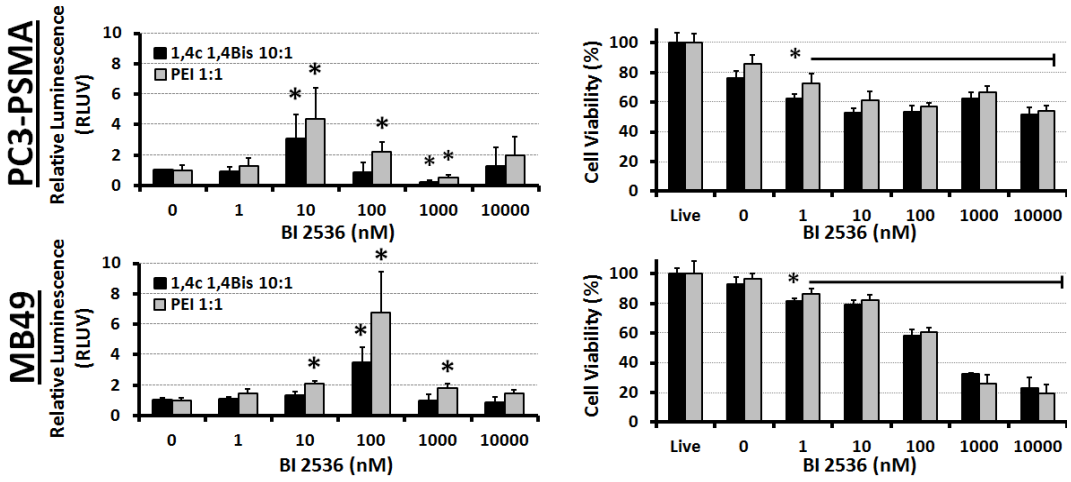

Figure 2.3 Dose-dependent enhancement of luciferase transgene expression by the PLK1 inhibitor BI 2536 in PC3-PSMA human prostate cancer and MB49 murine bladder cancer cells following delivery of pGL3.0 plasmid DNA using PEI and 1,4C-1,4Bis polymers. Relative enhancement of luciferase expression (RLUV) compared to the polyplex control is shown in the left panels, while effects of the drug on cell proliferation are shown in the panels on the right side. Asterisks (*) indicate p-values <0.05, which show statistically significant enhancement relative to vehicle control (Student's t-test)

Concentrations of BI 2536 above 1 μM (1000 nM) drastically reduced MB49 cell viability to approximately 20%. Additionally, a lead inhibitor targeting another cell-cycle regulatory kinase, Aurora kinase, was dose-optimized for transgene expression (**Appendix I, Figure A1**).

Another interesting target identified in the kinase inhibitor screen is the Janus-Kinase Signal Transducer and Activator of Transcription (JAK-STAT pathway). Although

only one inhibitor from this group, AG-490, appeared in the top 15 (**Table 2.1**), five of the nine tested inhibitors showed greater than 2-fold enhancement in transgene expression (**Table 2.2**). However, four of these five inhibitors possess known inhibitory activity against non-JAK targets, while TG101209, the mild enhancer of transgene expression of this group, is a JAK2-specific inhibitor. Each of these four non-specific JAK inhibitors in **Table 2.2** also inhibit a growth factor receptor or the cell cycle regulating Aurora kinase, both sets of kinases which were also identified as leads for enhancing transgene expression. Due to the difficulty of attributing the effects of these inhibitors with one target, each possessing multiple kinase inhibition activities, a dose-response set of transfections was carried out with the JAK2-specific inhibitor TG101209 (**Figure 2.4**). It is important to note that the plasmid used for this experiment is the pGL4.50 plasmid (Promega), which is driven by the CMV promoter as opposed to the SV40 promoter present on the pGL3 plasmid used for the initial screening. Using 1,4C-1,4Bis as the plasmid carrier, RLUV values reached 6-fold enhancement relative to treatment with the polyplex vehicle control, while moderate enhancement was observed with PEI as the delivery vector. This observation further evidences JAK-STAT as a target for enhancing transgene expression.

The JAK-STAT pathway is a signal transduction pathway, which translates signals from the extracellular environment through cytokine binding to receptors, into a

Table 2.2 – Lead JAK inhibitors identified in screening and their targets

Inhibitor	Target(s)	RLUV
AZD1480	JAK2-STAT3-FGFR	2.65 ± 2.99
AZ 960	JAK2, Aurora A	2.37 ± 2.24
AT9283	JAK2/3 and Aurora	3.24 ± 1.35
AG-490	EGFR/JAK2/ErbB2	6.43 ± 10.66
TG101209	JAK2	2.09 ± 2.00

transcriptional response at the nuclear level. It is not currently clear how inhibiting this pathway enhances transgene expression.

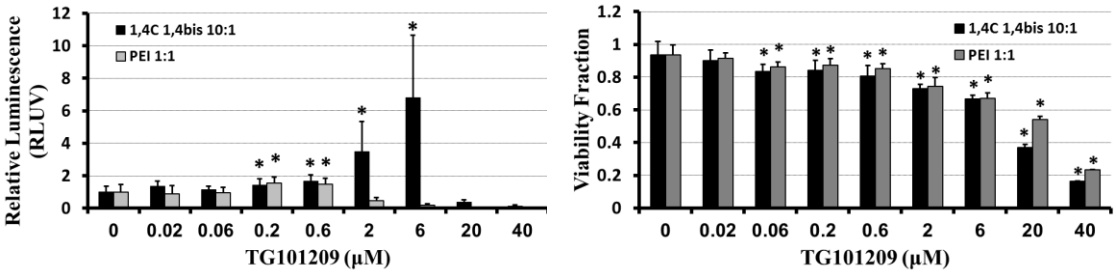

Figure 2.4 Dose-dependent enhancement of luciferase transgene expression by the JAK2-specific inhibitor TG101209 in PC3-PSMA human prostate cancer cells following delivery of pGL4.5 plasmid DNA using PEI and 1,4C-1,4Bis polymers. Relative enhancement of luciferase expression (RLUV) compared to the polyplex control is shown in the left panel, while effects of the drug on cell proliferation are shown in the panel on the right side. Asterisks (*) indicate p-values < 0.05, which show statistically significant enhancement relative to vehicle control (Student's t-test)

2.3.3 Dose-Optimization of Lead PLK1 Inhibitors – GFP Expression

The previous luciferase-plasmid observations were expanded by testing the effects of the PLK1 inhibitors on expression of a GFP-expressing plasmid driven by a different promoter (CMV as opposed to SV40). **Table 2.3** [106] shows the fold increase (FI) of EGFP expression per cell (Fluor/cell) and of percentage of cells expressing EGFP (EGFP+%), quantified by flow cytometry, for the optimum concentration of each drug. Both BI 2536 and HMN-214 showed consistently strong enhancement of transgene expression. BI 2536 strongly enhanced the fluorescence per cell with the 1,4C-1,4Bis polymer (15.8±4.2), but showed a more modest effect with PEI (3.6±1.6). The same phenomenon was also observed with BI 2536 in MB49 cells, where enhancement was strong with 1,4C-1,4Bis (9.7±3.2), but not with PEI (0.4±1.7). In contrast, HMN-214 showed the opposite effect in PC3-PSMA cells, with higher enhancement of transgene

expression with PEI than 1,4C-1,4Bis polymers. It is possible that these drugs differentially affect the ability of different polymer carriers to enter cells, perhaps as a function of N to P (nitrogen to phosphate) ratio. It is worth noting that BI 6727 also showed significant enhancement of EGFP and luciferase expression, but this effect was inconsistent (hence the large standard deviation). The effects of ON01910 were also somewhat inconsistent (32.3±17.0) and sharply decreased cell viability. Taken together, it can be seen that inhibition of PLK1 using different small molecules increases GFP expression across the cell population, and also increases fluorescence / cell in cells that express the protein.

Representative fluorescence microscopy images for PC3-PSMA cells treated with each of the four PLK1 inhibitors and 1,4C:1,4Bis-pEGFP polyplexes are shown in **Figure 2.5** [106]. Both BI 2536 and HMN-214 exhibit moderate enhancement of EGFP expression in these cells. Interestingly, the baseline EGFP expression using 1:1 PEI was low enough that enhancement in transfection was undetectable using the flow cytometry assay, but results are shown in **Table 2.3**. Visually, cell fluorescence was almost non-existent with

Table 2.3 - Fold increase (FI) of polymer-mediated EGFP Expression by PLK1 inhibitors identified as leads from the screen

PC3-PSMA Cells				
Polymer	1,4C-1,4Bis		PEI	
PLK1 Inhibitor	FI %EGFP+	FI Fluor/Cell	FI %EGFP+	FI Fluor/Cell
BI 2536 (25 nM)	5.1±1.0*	15.8±4.2*	3.6±1.6*	3.4±1.1*
BI 6727 (100 nM)	4.9±4.0	45.8±45.2		
HMN-214 (3.3 μM)	4.3±0.5*	5.6±0.7*	6.7±4.0	15.2±12.8
ON01910 (100 nM)	6.3±3.3	32.3±17.0		
MB49 Cells				
Polymer	1,4C-1,4Bis		PEI	
PLK1 Inhibitor	FI %EGFP+	FI Fluor/Cell	FI %EGFP+	FI Fluor/Cell
BI 2536 (100 nM)	2.5±0.3*	9.7±3.2*	0.5±0.2	0.4±1.7
HMN-214 (3.3 μM)	1.8±0.4*	9.8±2.3*		

or without drug when PEI was used as the vehicle for pEGFP delivery. It is important to note that optimal weight ratios of 1:1 PEI to plasmid DNA and 10:1 1,4C-1,4bis to plasmid were employed in these studies.

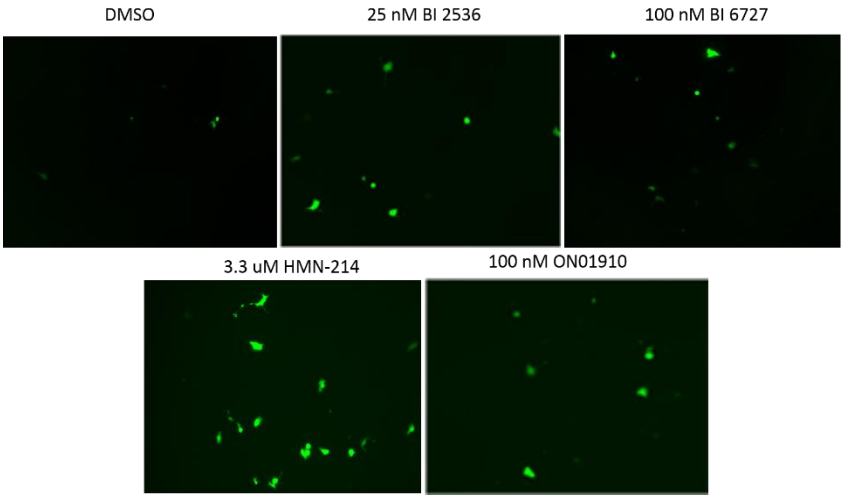

Figure 2.5 Representative fluorescence microscopy images of PC3-PSMA cells transfected with polyplexes formed with a 10:1 mass ratio of 1,4C-1,4Bis : pEGFP DNA, in the presence of no drug (DMSO) or with PLK1 inhibitors, BI 2536, BI 6727, HMN-214, ON01910. Images were obtained using a Zeiss inverted fluorescence microscope 48 hours post-transfection.

Taken together, the above results with two different reporter genes (firefly luciferase and EGFP), two different cationic polymers, and treatment with several PLK1 inhibitors, PLK1 as a target for enhancement of polymer-mediated transgene expression is likely a generalizable phenomenon.

2.3.4 Effects of PLK1 Silencing on Transgene Expression

Previous results clearly showed that multiple small-molecule inhibitors of PLK1 enhanced the delivery of multiple transgenes with two cationic polymers in different cell

lines. We therefore investigated if PLK1 silencing / knockdown using a lentiviral vector could enhance transgene expression in cells. Viruses with four different shRNA constructs were designed and investigated for PLK1 knockdown in PC3-PSMA cells. The efficacy of each construct was tested by immunoblotting cell lysates in order to determine PLK1 expression levels (not shown). Based on PLK1 knockdown efficacy, as determined by Western blot against two scramble control viruses (**Figure 2.6 left** [106]), PLK1 silencing using the virus expressing PLK1 shRNA 6247 (denoted "PLK1 KO") clearly reduced PLK1 expression, as reported previously [101]. We therefore chose this virus for knocking down PLK1 in our subsequent experiments.

PLK1 knockdown led to a modest increase in 1,4C-1,4Bis mediated transgene expression, (**Figure 2.6 right** [106]) although interestingly this phenomenon was not observed when using PEI as the delivery vector (data not shown). Surprisingly, the

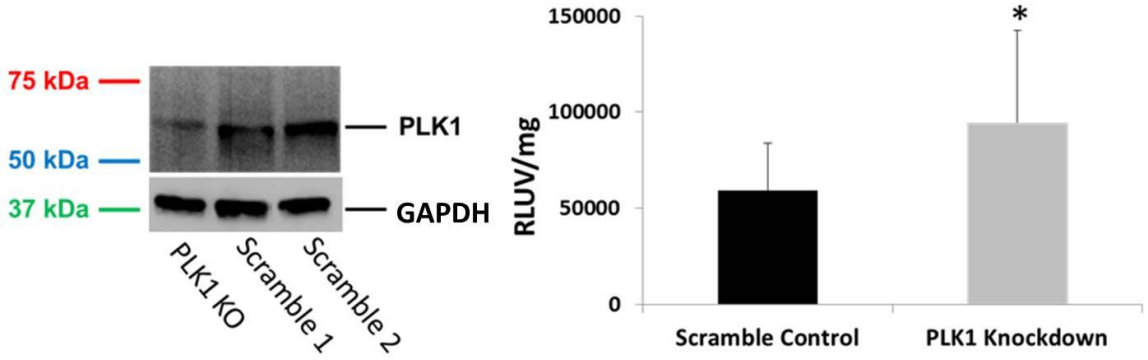

Figure 2.6 Left – PC3-PSMA cells were infected with a lentivirus expressing scrambled sequence shRNA or lentivirus expressing shRNA construct 6247 against the mRNA of PLK1 (denoted PLK1 KO). Cell lysates, prepared 72 hours after infection, were immunoblotted using a PLK1 antibody probe. Right – Polymer-mediated transfections with polyplexes formed at a 10:1 1,4C-1,4bis : pGL3 plasmid weight ratio, in PC3-PSMA cells, beginning 48 hours after infection with the lentivirus, and proceeding for 48 additional hours to allow for determination of luciferase expression. Transgene expression is reported in relative luminescence units normalized to protein content, and normalized to cell viability (RLUV / mg). * p-value =0.02, Student's T-test, compared to scrambled control

scramble control virus increased transgene expression relative to treatment without any virus when using 1,4C-1,4bis as the polymer carrier (data not shown). Given that viruses have evolved to be extremely efficient gene delivery vehicles, in part due to their enhanced ability to enter target cell nuclei, it is possible that both scramble control and anti-PLK1 shRNA expressing viruses were able to assist the plasmid in overcoming particular gene delivery barriers faced by polymer-mediated plasmid DNA delivery. This could be due to direct virus-plasmid or virus-polymer binding [108, 109], or indirectly by viral-induced interruption of the target cell's natural defense(s) against foreign DNA. It is possible that the virus itself was able to assist the plasmid in circumventing particular gene delivery barriers overcome by PLK1 silencing, thus dampening the increase in observed transgene expression enhancement using our method of PLK1 silencing. Interestingly, PEI-mediated gene delivery did not significantly increase in the presence of either virus (data not shown) suggesting that PEI and the lentiviral vectors used may assist foreign DNA in overcoming similar gene delivery barriers. However, silencing of PLK1 resulted in enhancement of transgene expression with 1,4C-1,4Bis, further providing evidence of PLK1 as a transgene expression enhancement target.

2.3.5 Effect of PLK1 Inhibitors on Cell Cycle Distribution

PLK1 plays a significant role in cell cycle regulation, mainly in promoting cell entry into mitosis. PLK1 localizes the two protein components of the mitosis promoting factor (cyclin B1 and CDC2) to the nucleus and phosphorylates the former [110], in addition to phosphorylating CDC25 [111], a phosphatase which also promotes the activity of the mitosis promoting factor Given the established role of PLK1 in cell cycle regulation, the effects of HMN-214 and BI 2536 on PC3-PSMA cell cycle progression were

Table 2.4 - Quantification of PC3-PSMA cell cycle phase in absence and presence of small molecule PLK1 inhibitors based on (N=3)

Cell Cycle Phase	Vehicle Control	25 nM BI 2536	3.3 µM HMN-214
Sub-G0/G1	0.8±0.3%	2.0±1.0%	1.8±0.1%
G0/G1	63.1±7.6%	3.6±0.6%	1.7±0.4%
S	9.6±2.3%	7.2±4.7%	2.9±1.2%
G2/M	26.6±7.0%	87.1±5.0%	93.6±1.6%

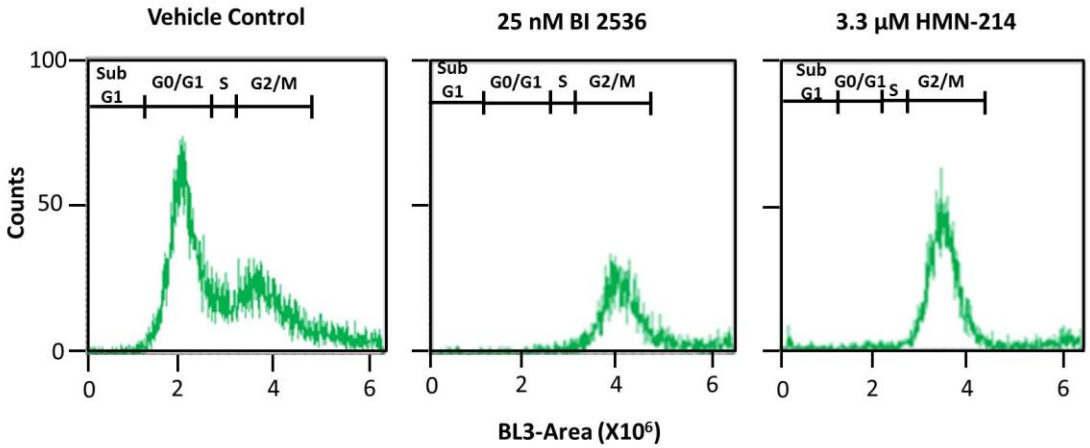

Figure 2.7 Cell cycle analysis of PC3-PSMA cells treated with vehicle control (DMSO), 25 nM BI 2536, or 3.3 µM HMN-214 using flow cytometry and staining with propidium iodide (PI). Results from one representative experiment out of N = 3 independent experiments are shown. The y-axis (counts) indicates the number of cells with the specific fluorescence intensity shown on the x-axis (BL3-A)

investigated. Nuclear DNA was stained with propidium iodide (PI) in order to determine the amount of DNA using flow cytometry, which allowed for elucidation of the fractions of the cell population in different stages of the cell cycle phase. In all cases, drugs or equivalent volume DMSO (vehicle control) were added to cells, in the *absence* of polyplexes. **Figure 2.7** and **Table 2.4** [106] indicate that vehicle control (i.e. DMSO)-treated cells were mostly in the G_0/G_1 phase (63.1 ± 7.6%), with a small fraction of the cells in the S (9.6 ± 2.3%) phase, and approximately a quarter of the cell population (26.6 ±7.0%) in the G2 or M phases of the cell cycle. However, inhibition of PLK1 with 3.3 µM HMN-214 almost completely arrested cells in the G_2/M phase (93.6 ± 1.6%), while PLK1

inhibition with 25 nM BI 2536 also resulted in strong accumulation of the cell population (87.1 ± 5.0%) in the G2/M phase of the cell cycle. These results are consistent with the known PLK1 inhibition activity of the drugs in other cell lines [112, 113].

2.3.6 Effect of PLK1 Inhibitors on Intracellular Trafficking of Plasmid DNA

Intracellular transport/trafficking of plasmid DNA has been demonstrated to significantly influence transgene expression in cells [49, 83, 84, 114-118]. In order to determine if trafficking of plasmid is altered in our system with PLK1 inhibition, a fluorescently-tagged plasmid was complexed with PEI, delivered to PC3-PSMA cells and imaged via confocal microscopy 48 hours later. The distribution of delivered plasmid for each inhibitor treatment case is shown in **Figure 2.8** [106]. In the absence of BI 2536 (**Figure 2.8A**), plasmid DNA is localized at the Perinuclear Recycling Compartment (PNRC, white arrows) which is consistent with previous observations of polyplex and nanoparticle transport in these cells [84, 119]. In contrast, treatment with BI 2536 (**Figure 2.8B**) disrupts PNRC localization and disperses plasmid DNA throughout the cytoplasm (red arrows). Images of BI 2536 treated cells (**Figure 2.8B**) and cells simultaneously treated with DMSO vehicle control (**Figure 2.8A**) were acquired 48 hours following transfection, corresponding temporally to the transgene expression data above. Treatment of cells with HMN-214 (3.3 μM), however, resulted in significant detachment and difficulty in imaging beyond 24 hours; thus cells treated with HMN-214 (**Figure 2.8D**) and vehicle control (**Figure 2.8C**) were imaged 24 hours following transfection. Even though images displayed for HMN-214 treated cells represent a time 24 hours prior to optimal transgene expression, it is still clear that HMN-214 treatment alters intracellular trafficking of the delivered plasmid **(Figure 2.8D**), resulting in a similar release from the PNRC as

observed with BI 2536 treatment (red arrows). Both drugs appear to disrupt sequestration of the plasmid at the PNRC, and favor the distribution of the plasmid throughout the cytoplasm.

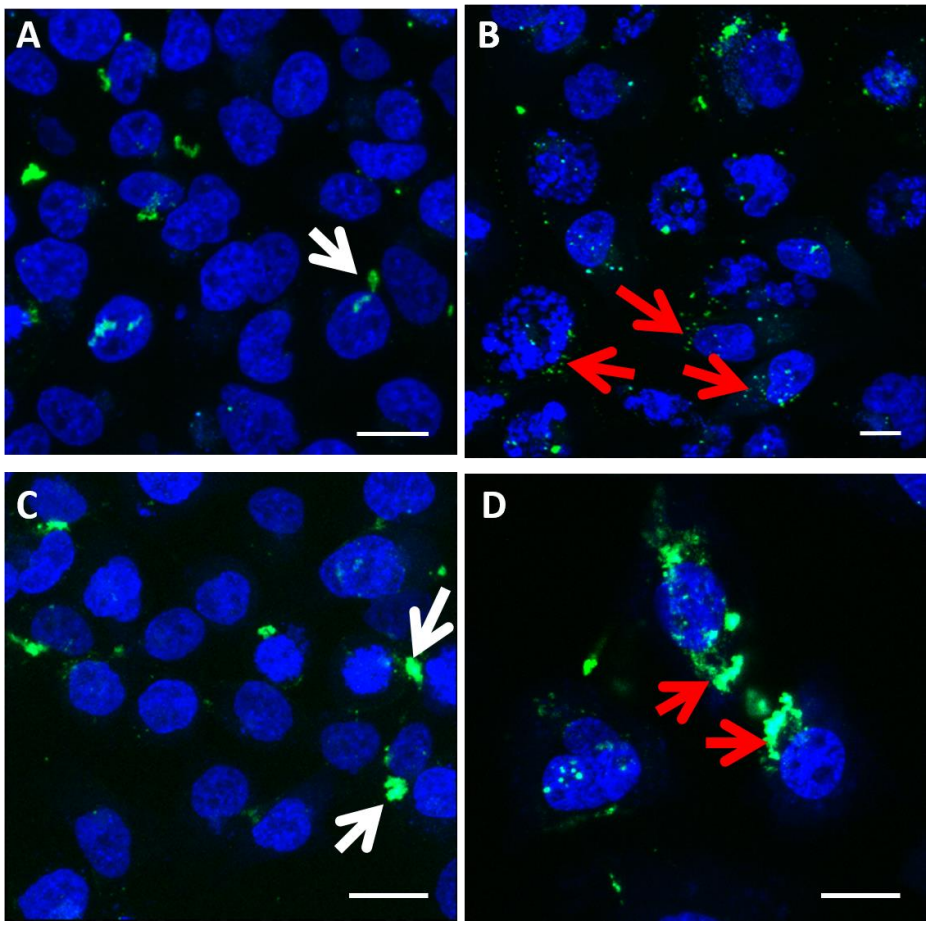

Figure 2.8 Intracellular trafficking of plasmid DNA in presence and absence of PLK1 inhibitors. PC3-PSMA cells were transfected with polyplexes of PEI:fluorescein (green)-labeled plasmid DNA at a weight ratio of 1:4. Cells treated with A) vehicle control (DMSO) and B) 25 nM BI 2536 are shown 48 hours after co-treatment with polyplexes. Cells treated with C) vehicle control (DMSO) and D) HMN-214 are shown 24 hours after co-treatment with polyplexes. Scale bar = 20 μm. Blue signal indicates DAPI-stained nuclei, and white arrows indicate sequestration of plasmid DNA in the perinuclear recycling compartment (PNRC). Red arrows indicate altered plasmid DNA localization following treatment with PLK1 inhibitors. Images are representative of three independent experiments (N=3)

2.4 DISCUSSION AND CONCLUSIONS

These experiments discussed above have led to the identification of several kinase targets for enhancing polymer-mediated transgene expression, but most prominently, PLK1. The results clearly show that the kinase inhibitors HMN-214 and BI 2536 significantly enhance transgene expression using different carriers, plasmids, and target cell lines. When coupling these findings with the application of PLK1 silencing, PLK1 has been strongly established as a target for transgene expression enhancement. Excitingly, our and expression in cancer cell lines. These results are significant since Polo-like kinases are an emerging target for anti-cancer therapies, and the PLK1 inhibitor BI 2536 is currently in clinical trials for cancer treatments [120, 121], presenting an exciting future opportunity to interface this newly found gene therapeutic ability and existing chemotherapeutic strategy of PLK1 inhibition for synergistic treatments.

The exact mechanism by which PLK1 enhances transgene expression is not clear, but it is very likely related to the accumulation of cells in the G_2/M phase of the cell cycle. It is generally accepted that dividing cells, especially cells that are at or near the G2/M transition, are more amenable to transgene expression [81, 122], and many targets identified in the kinase screen for enhancing transgene expression (including many of those targeted by the top 15 inhibitors in **Table 2.1**) are regarded as cell cycle kinases. The most common explanation for enhancement of transgene expression just prior to mitosis (i.e. G2/M transition) is the increased permeability of the nuclear membrane prior to nuclear envelope breakdown. However, preliminary qPCR experiments were carried out to detect plasmid levels in extracted nuclei, and no increase was detected with PLK1 inhibition in our system (data not shown). Another model that has been proposed is increased protein

production associated with the increase in cell diameter which commonly occurs with G2/M arrest [82]. Additionally, inhibition of the cell cycle related kinases polo-like kinase 3 and MEK1 have been identified through a silencing-screening approach to affect endocytosis, particularly re-directing transferrin-containing endosomes to the plasma membrane [123], illuminating the possibility that cell cycle kinases can affect trafficking of endosomally trafficked transgene cargo.

The experiments carried out in chapter 2 were motivated by a curiosity to understand what kinase targets regulate transgene expression and how they do so. While a complete mechanistic explanation of how PLK1 inhibition enhances transgene expression was not obtained, clearly cytoplasmic trafficking of transgene cargo was altered, which could very well play a role in the observed enhancement. Gene delivery obstacles such as cellular uptake, endosomal escape, cytoplasmic trafficking, and nuclear entry are commonly acknowledged and studied. However, factors that may regulate transgene expression *after* the transgene has entered the nucleus are rarely addressed. In the next chapter, inhibition a nuclear histone deacetylase and resulting enhancement in plasmid transgene expression will be discussed.

CHAPTER 3 - INHIBITION OF NUCLEAR HISTONE DEACETYLASE FOR ENHANCEMENT OF TRANSGENE EXPRESSION IN CANCER CELLS

3.1 INTRODUCTION

The chromosomal DNA inside of a single human cell would extend to nearly two meters in length if stretched out [124], a certainly infeasible method for storing DNA inside of a cell nucleus. However, this immense amount of DNA is wrapped up in a mixture of RNA and proteins called histones in a surprisingly organized and regulated structure referred to as chromatin. The sub-structure of chromatin is organized into octameric histone/DNA structures, nucleosomes (**Figure 3.1A**), consisting of duplicates of four core histone molecules; H2A, H2B, H3, and H4, as well as a linker histone H1 which binds DNA on both ends of the nucleosome [125], and assists in condensing chromatin into chromosomes during mitosis [126].

Histones which act as a condensing factor for chromosomal DNA can actually *decrease* gene expression through tight binding, preventing DNA accessibility to transcriptional machinery. The extent to which DNA and histones interact and, by extension, local gene expression, is regulated by a number of posttranslational modifications to histones, including phosphorylation, methylation, acetylation (**Figure 3.1**), among others. These modifications are carried out by a number of enzymes [127] [128] [129] [130], which will be discussed in more detail in Chapter 4. These modifications can be classified as "epigenetic", meaning they induce changes in gene expression without changing the sequence of the gene itself.

Two examples of epigenetic modifying enzymes are histone acetyltransferases (HATs) and histone deacetylases (HDACs) (**Figure 3.1B)**, which have opposing effects on

chromatin structure and local gene expression. HATs use acetyl CoA to acetylate and neutralize the charge of ε-amino groups on lysine residues, thereby releasing DNA for transcription. In contrast, histone acetylation may be reversed by HDACs, which remove acetyl groups to restore the positive charge and DNA binding activity of histones [131, 132]. HATs and HDACs are generally non-specific [133], but HDACs have been shown to form complexes with other proteins that target deacetylase activity to specific DNA sequences, for example a DNA sequence that binds the zinc finger motif of a complex containing HDAC2 [134, 135].

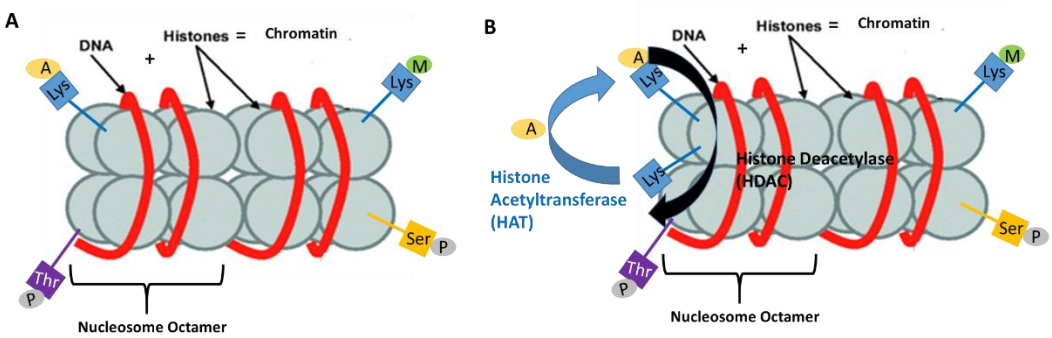

Figure 3.1 A) Chromosomal DNA is organized in the nuclei of mammalian cells by winding around core histone proteins. Structures containing two copies each of four core histones (octamer) combined with interacting DNA is referred to as a nucleosome. Histones contain amino acid groups which can be (de)phosphorylated, (de)acetylated, and (de)methylated (among other modifications), which result in reorganiziation of chromosomal structure and consequently, local gene expression. B) Experiments in chapter 3 focus on inhibiting histone deacetylase (HDAC) 1 and 3. While inhibition of HDAC enzymes is known to enhance local gene expression through minimizing local histone-chromsomal DNA interactions, this will be applied to enhance *transgene* (plasmid) expression. Histone acteyltransferaes (HATs) carry out the opposite process of HDACs, adding acetyl groups to histone lysines and increasing local gene expression (image modified from dev.biologists.org)

The name "HDAC" can be slightly misleading, as these enzymes also have the ability to remove acetyl groups from non-histone proteins, such as NF-κB and other

transcription factors [136, 137]. Consequently, aberrations in HAT/HDAC activity have been implicated in several neurodegenerative diseases [138] and cancer [139].

Interestingly, in addition to chromosomal DNA, histone acetylation can affect expression of exogenous or invading DNA. For example, Bishop et al demonstrated that viral DNA, which efficiently enters the nucleus is bound and silenced by histones, with expression eventually restored by inhibition of HDAC using trichostatin A [140, 141]. Also, bacterial plasmid DNA has been shown to bind histones and form nucleosomes in cell free assays [142], with evidence also pointing to nucleosome formation of local histones with exogenous plasmid DNA *in vitro* [143]. Applications of histone-DNA binding have actually been directly applied to gene delivery, using cationic histone tail sequences to carry out non-viral gene delivery [144, 145], a process referred to as "histonefection". Given the existing evidence exogenous DNA/local histone binding, it was hypothesized that HDAC inhibition could potentially enhance non-viral polymer-mediated transgene expression, the focus of the remainder of chapter 3.

Previously work by Rege et al indicated that inhibition of the cytoplasmic HDAC6 with tubacin increases polymer-mediated transgene expression likely by influencing intracellular plasmid trafficking on stabilized microtubules [84]. In the experiments highlighted in chapter 3, the effects of Entinostat, a selective inhibitor of class 1 HDACs 1 and 3 [146] on polymer-mediated transgene expression are studied in cancer cell lines. It is hypothesized that inhibition of nuclear HDACs 1 and 3 (the latter which also has cytoplasmic activity) will enhance polymer-mediated transgene expression due to increased plasmid DNA availability to transcriptional machinery brought about by histone acetylation

3.2 METHODS

3.2.1 Polymer Synthesis

The 1,4C-1,4Bis and PA8 polymers were synthesized using methods similar to our previously published protocols [29, 30, 147]. Briefly, the epoxide groups of diglycidyl ether (DGE) monomers 1,4 cyclohexanedimethanol DGE or ethylene glycol DGE, respectively, were reacted with polyamine monomers 1,4 bis(3-aminopropyl)piperazine and paromomycin, respectively, resulting in the formation of cationic polymers with molecular weights (MWs) > 5,000 g/mol. Branched polyethyleneimine (PEI, MW = 25,000 g/mol) was purchased from Sigma (St. Louis, MO), and fresh stocks (50 ng/μL in HEPES buffer, pH 7.4) were prepared before every experiment in order to obviate any effects due to storage. Monomer structures used to synthesize 1,4C-1,4Bis and PA8 are shown in **Appendix III, Figures A2 and A3**.

3.2.2 Transfections in the Presence of Entinostat

Entinostat was kindly provided by Syndax Pharmaceuticals of Waltham, MA through an agreement with the Cancer Therapeutics Evaluation Program (CTEP) at NIH. Stocks were prepared in DMSO at concentrations ranging from 60 μM–20 mM and frozen at -80^{o}C until needed. Human prostate (PC3 and PC3-PSMA) and murine bladder (MB49) cancer cells were seeded onto 24-well plates at a density of 50,000 cells per well with 500 μL RPMI (PC3 and PC3-PSMA) or DMEM (MB49) containing 10% heat-inactivated fetal bovine serum (FBS), 100 units/mL penicillin, and 100 μg/mL streptomycin. All cell lines were incubated overnight (~18-20 hrs) at 37^{o}C, and the serum-containing media (SCM) was replaced with serum-free media (SFM) immediately prior to transfection Polyplexes

were prepared by incubating cationic polymers (1,4C-1,4Bis, PEI, or PA8) with pGL3-Control (luciferase reporter gene, Promega, Madison, WI) or pEGFP-C1 (enhanced green fluorescent protein or EGFP reporter gene, Clontech, Mountain View, CA) plasmid DNA. The concentration of plasmid DNA was kept constant at 200 ng/well, while the polymer:pDNA mass ratio varied for each polymer (PEI = 1:1, 1,4C-1,4bis = 10:1, PA8 = 50:1), depending on their previously determined optimal concentrations [29]. Polyplexes and different doses (0, 0.33, 1, 3.3, 10, 33, and 100 μM) of the HDAC inhibitor Entinostat were simultaneously added to the cells; a constant DMSO (for solubilizing the drug) concentration of 0.5% (v/v) was employed in all cases. Following six hours of incubation at 37^{o}C with the polyplex and drug, serum-free media was exchanged with serum-containing media containing corresponding Entinostat concentrations. The cells were then incubated at 37^{o}C for an additional 48 hours to allow for transgene expression. Transfections with 0 μM Entinostat with or without 0.5% DMSO were also performed as controls, and 0.5% DMSO was found to not have any significant effects on transgene expression efficacy (data not shown).

3.2.3 Luminescence Assay and Fluorescence Microscopy

Luciferase assay was carried out in a similar manner as was done for the kinase screening in chapter 2. Following transfections with the pEGFP-C1 plasmid, cells were examined with a Zeiss fluorescence microscope to visualize EGFP expression. All images were acquired within areas of 90-100% confluence near the center of each well.

3.2.4 Quantification of DNase Accessibility and Plasmid DNA in Target Cell Nuclear Fraction

The relative presence and availability of plasmid DNA in the nuclear fraction of cells following Entinostat treatment was measured and quantified using methods described below.

3.2.4A Genomic DNA Extraction -

Genomic DNA (gDNA) was extracted from PC3-PSMA cells to test primer specificity against pGL3 plasmid DNA, in the presence of target cell genomic DNA. Extraction was carried out using a phenol:chloroform:isoamyl alcohol (iaa) technique. Briefly, cells were trypsinized, washed and lysed. Cell content was then isolated via extraction with a 25:24:1 phenol-chloroform-iaa buffer (Sigma). A second extraction was carried out with chloroform, and trace amounts of chloroform were subsequently evaporated at 55ºC. DNA was precipitated overnight using a sodium acetate/EtOH mixture, and resuspended in TE buffer (10 mM Tris-HCl pH 8.0, 1 mM EDTA).

All primers, designed against the promoter or luciferase (*luc*+) gene region of the pGL3 plasmid, were purchased from Integrated DNA Technologies (Coralville, IA). The sequences of the forward and reverse primers for the four regions on the plasmid, denoted 1-4, are as follows (5'-3'):

Forward 1 – GGTACCGAGCTCTTACGCGTGC

Reverse 1 – CGGGATGGGCGGAGTTAGGG

Forward 2 – CAGAAGTAGTGAGGAGGCTTTTTTGGAC

Reverse 2 – TATGTTTTTGGCGTCTTCCATGGTGGC

Forward 3 – GCTTTTACAGATGCACATATCGAGGTGG

Reverse 3 – GTATTCAGCCCATATCGTTTCATAGCTTC

Forward 4 – CGAAATGTCCGTTCGGTTGGCAGAAG

Reverse 4 – GCATAAAGAATTGAAGAGAGTTTTCACTGCATAC.

Region 1 mostly consists of the upstream portion of the SV40 promoter, region 2 bridges the promoter region as well as the upstream region of the *luc+* gene, covering portions of both, and regions 3 and 4 are located entirely on the *luc+* gene. Endpoint PCR was carried out against both the pure pGL3 plasmid template as well as against PC3-PSMA gDNA using all pGL3 primer pairs. Agarose gel electrophoresis analyses were carried out on PCR products in order to validate the efficacy and specificity of the pGL3 primers.

3.2.4B Nucleosomal DNA Purification -

PC3-PSMA and PC3 cell nuclei were extracted using the EZ Nucleosomal DNA Prep Kit (Zymo), and purified nuclear DNA was treated with DNase following 48 hours of transfection (process summarized in **Figure 3.1**. Transfections were carried out with the pGL3 plasmid complexed with 1,4C-1,4Bis polymer, in the presence or absence of 33 μM Entinostat, as described above. Isolated nuclei were then either treated with Atlantis dsDNase (0.4 Units/100 μL, per kit instructions, resulting in cut DNA), or equivalent volume 1X PBS (resulting in uncut DNA). Nucleosomal DNA (cut and uncut) were then isolated using spin columns, supplied with the EZ Nucleosomal DNA Prep kit. The spin columns efficiently (70-90%) capture DNA 75 bp to 10 kb, which is a relevant size range for the pGL3 plasmid.

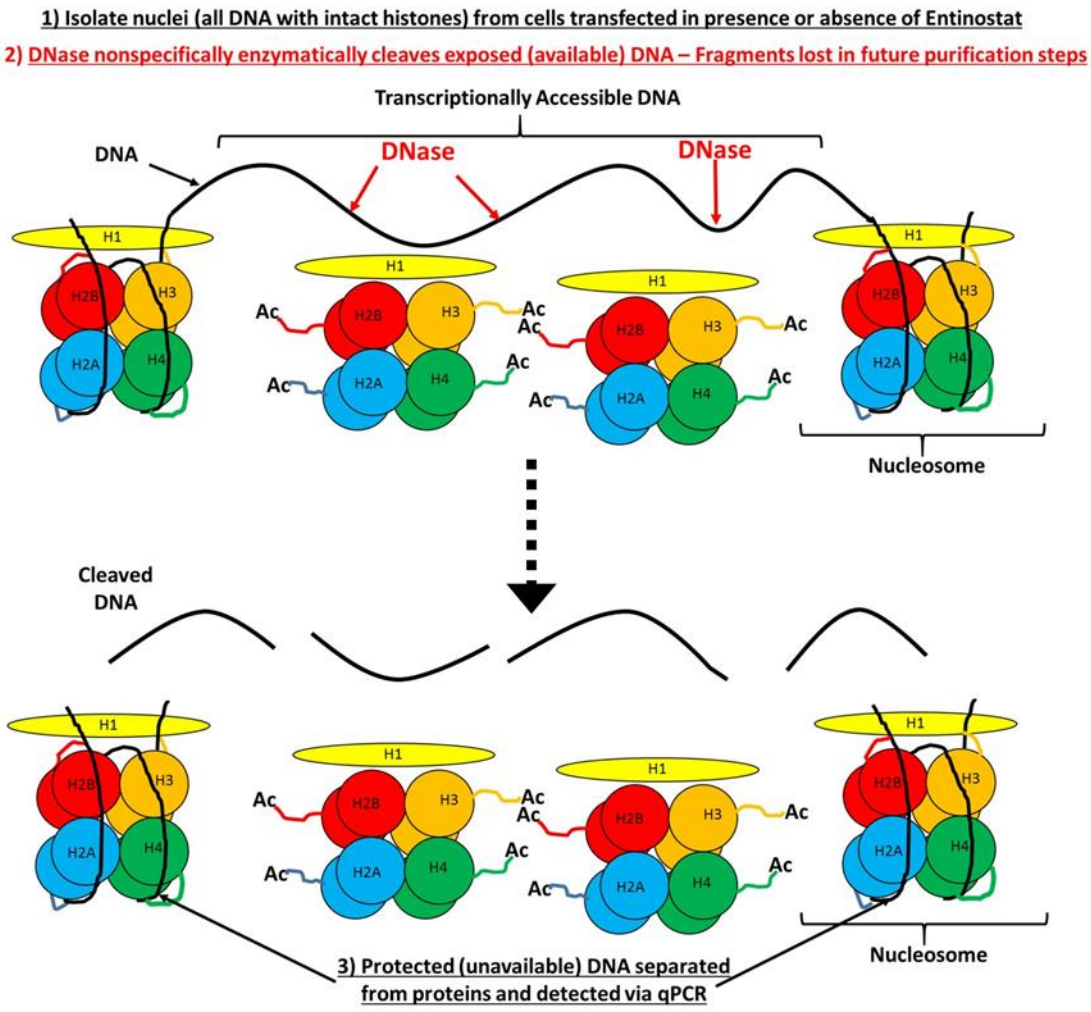

Figure 3.1 Illustration of the process of nucleosomal DNA purification for normalized DNase accessibility and plasmid nuclear presence quantification

3.2.4C qPCR Experiments and Analysis -

Quantitative PCR (qPCR) experiments were carried out on DNA isolated from the nuclear fraction of PC3-PSMA or PC3 cells (above), using the primers described above. Detection of fluorescence accumulated by amplified, double stranded DNA was carried out using SYBR® Green Master Mix (Life Technologies). PCR reactions (15 µL volumes) were prepared in triplicate for each independent experiment as follows: 2 µL template DNA

(1/75 total cellular nucleosomal DNA extraction, or roughly $3.8X10^4$ nuclei for vehicle-control treated PC3-PSMA cells and $1.0X10^4$ nuclei for Entinostat-treated PC3-PSMA cells; PC3 cell counts were not quantified), 7.5 μL 2X SYBR Green Master Mix, 1.5 μL forward primer (0.57 pmol), 1.5 μL reverse primer (0.57 pmol), and 2.5 μL ddH_2O. Reactions were carried out in opaque white 96-well plates (Roche 04 729 692 001), and thermal cycling was conducted in a Light Cycler® 480 PCR instrument (Roche). A pre-incubation step was carried out for 5 min. at 95ºC. Next, 45 amplification cycles were run: denaturation at 95ºC for 10 sec., annealing at 58ºC for 10 sec., extension at 72ºC for 10 sec. Fluorescence was recorded after each extension step. Melting analysis (95ºC for 60 sec., 40ºC for 120 sec., 95ºC at 0.19ºC (sec^{-1}) with fluorescence readings at 3(sec^{-1})) of reactions with and without DNA templates confirmed that 95-100% of the fluorescence signal was associated with PCR amplicons rather than primer dimers. The Roche Light Cycler® 480 software was used for subsequent calculations of DNase accessibility and relative plasmid content in the nuclear fraction.

C_p values (maximum y-value of the second derivative of fluorescence = y / cycle number = x) for cells treated with Entinostat (E) or 0.2% DMSO (D) were used in DNase accessibility calculations. Calculations were performed separately for every PCR-amplified region (**Figure 3.5**). C_p (crossing point) values indicate the PCR cycle number at which fluorescence due to amplification exceeds background fluorescence; thus, a lower C_p value indicates a greater amount of target DNA template since fewer numbers of cycles are required to produce a detectable fluorescence signal. The effect of DNase treatment on the purified nuclear DNA was quantified for cases with vehicle control (DMSO) and

Entinostat treatment, simply as the difference in C_p for DNA treated with DNase (C = cut) and without (UC = uncut):

$$\text{DMSO: } \Delta C_{P,D} = C_{P,D,C} - C_{P,D,UC}$$

$$\text{Entinostat: } \Delta C_{P,E} = C_{P,E,C} - C_{P,E,UC}$$

where each delta value represents the difference in intact DNA before and after DNase treatment. A larger delta value indicates greater sensitivity to DNase, and thus indicates greater accessibility. All delta values were normalized using the average DMSO control value to test the hypothesis that relative to the DMSO control, Entinostat treatment increases DNA accessibility:

$$\text{DMSO: } \Delta\Delta C_{P,D} = \Delta C_{P,D} - \Delta C_{P,D\_avg}$$

$$\text{Entinostat: } \Delta\Delta C_{P,E} = \Delta C_{P,E} - \Delta C_{P,D\_avg}$$

where $\Delta C_{P,D\_avg}$ is an average of $\Delta C_{P,D}$ across all replicates. DNase accessibility can be expressed as a fold-difference in the template DNA that remains after cutting by DNase for all samples, relative to the DMSO control

$$Normalized\ DNase\ Accessibility, DMSO = 2^{\Delta\Delta C_{P,D}}$$

$$Normalized\ DNase\ Accessibility, Entinostat = 2^{\Delta\Delta C_{P,E}}$$

"Normalized DNase accessibility, DMSO" has an average value close to 1, since it is normalized by its own average value (**Figure 3.5**). "Normalized DNase accessibility, Entinostat" values greater than 1 support the hypothesis that an increase in DNase accessibility is associated with Entinostat treatment, while other values reject the hypothesis (**Figure 3.5**).

Next, we used C_p values from the uncut DNA samples to compare the amount of plasmid DNA in the nuclear fraction of Entinostat-treated versus untreated (DMSO) cells. All values were normalized using the average C_p value for the DMSO control sample

$$\text{DMSO: } \Delta C_{P,D,UC} = C_{P,D\_avg,UC} - C_{P,D,UC}$$

$$\text{Entinostat: } \Delta C_{P,E,UC} = C_{P,D\_avg,UC} - C_{P,E,UC}$$

with fold-increase of plasmid in the nuclear fraction calculated as

$$Normalized\ Plasmid\ in\ Nuclear\ Fraction, DMSO = 2^{\Delta C_{P,D,UC}}$$

$$Normalized\ Plasmid\ in\ Nuclear\ Fraction, Entinostat = 2^{\Delta C_{P,E,UC}}$$

"Normalized plasmid in nuclear fraction, Entinostat" values greater than 1 support the hypothesis that greater plasmid uptake is associated with Entinostat treatment, while other values reject the hypothesis (**Fig**ure **3.6**).

3.3 RESULTS

3.3.1 Enhancement of Luciferase and EGFP Transgene Expression by Entinostat

The effects of Entinostat on transgene expression were evaluated in three cell lines: two human prostate cancer cell lines (PC3 and PC3-PSMA) and a murine bladder cancer cell line (MB49) (**Figure 3.2**) [148]. The left side of **Figure 3.2** represents enhancement in luciferase expression relative to polyplex + vehicle (DMSO) control for Entinostat dose responses using three different polymers to deliver the pGL3 plasmid, which encodes for the firefly luciferase gene, controlled by the SV40 promoter. Regardless of the polymer used, enhancement of transgene expression seems to be a generalizable phenomenon in all

three cell lines tested. However, there are notable differences between the evaluated systems. For instance, in PC3 cells, PEI mediated transfection was enhanced about 24-fold when treated with 33 μM Entinostat. However, PA8 and 1,4C-1,4Bis mediated delivery was enhanced to a much lesser extent. In PC3-PSMA cells, Entinostat again drastically enhanced PEI-mediated transfection levels, but PA8 transgene expression enhancement was greatly increased with Entinostatin this cell line when compared to PC3. Interestingly, in MB49 cells, Entinostat treatment similarly affected transfection with each of the three polymers tested. Taken together, these results point to HDAC 1/3 inhibition with Entinostat treatment as a reliable strategy for enhancing polymer-mediated transgene expression. However, polycations do affect the level to which enhancement may occur. It should be noted that in PC3 and PC3-PSMA cells, 1,4C-1,4Bis baseline transfection efficacy was 5-10 times lower than observed with PA8 or PEI as a delivery vehicle. However, in MB49 cells, basal levels of transgene expression were similar using all three polymer carriers. In addition to the pGL3 plasmid, transfection experiments were carried out using PEI-(pEGFP-C1) polyplexes (**Figure 3.2**, right side) in PC3 and PC3-PSMA cells. At Entinostat doses correlating to optimal enhancement in transgene expression observed with the pGL3 vector, clear visual enhancement in recombinant EGFP expression can be observed. Given that the pEGFP-C1 plasmid uses the CMV promoter to drive reporter expression, these results indicate that Entinostat can enhance polymer-mediated transgene expression with a variety of different polymers in multiple cancer cell lines, and is likely not promoter-specific.

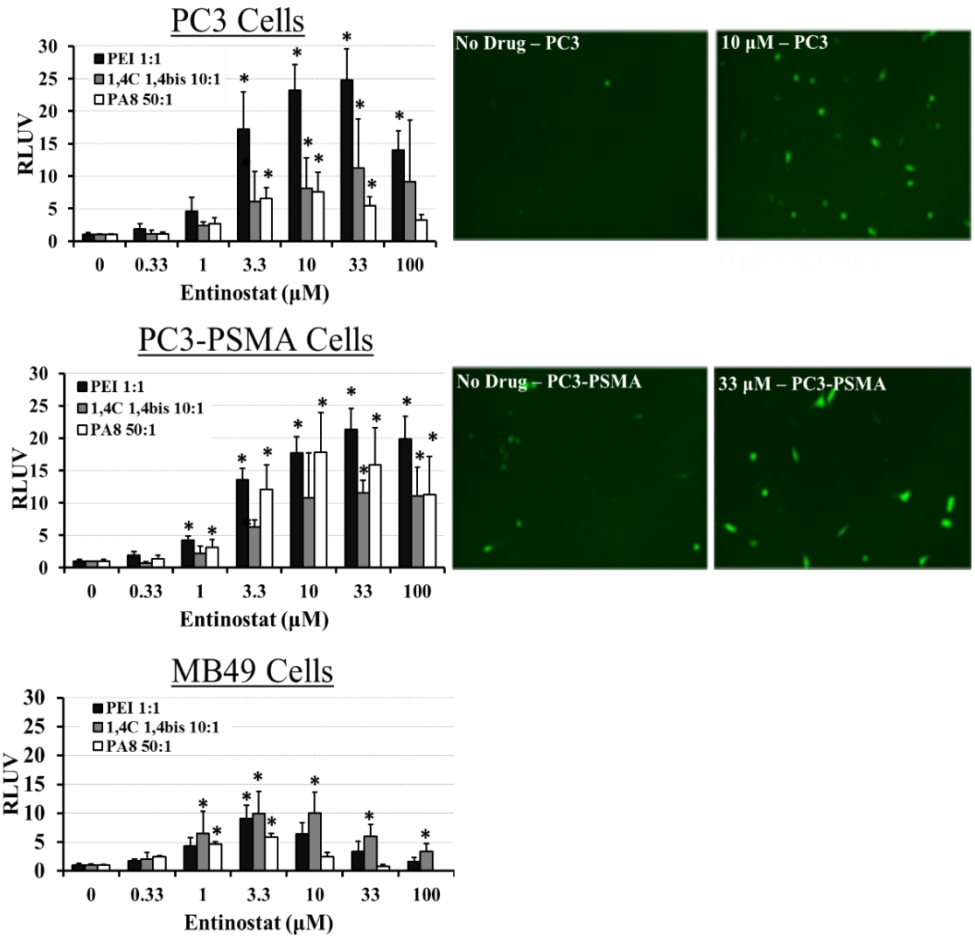

Figure 3.2 Left - Relative luciferase expression (pGL3 plasmid, SV40 promoter) in PC3 human prostate cancer, PC3-PSMA human prostate cancer, and MB49 murine bladder cancer cells. Asterisks (*) denote statistically significant ($p < 0.05$) enhancement of luciferase expression relative to the corresponding polyplex controls. Data shown indicate mean values ± one standard deviation. Right - Enhancement of EGFP expression by Entinostat at the indicated dose in PC3 and PC3-PSMA human prostate cancer cells post-transfection with PEI (polymer : plasmid DNA mass ratio of 1:1). These representative images are consistent with n

3.3.2 Enhancement of Transgene Expression Relative to Change in Global Protein Expression

Due to the effects of Entinostat on HDAC and, consequently, chromatin structure, it is possible that Entinostat treatment increases global protein production. This

necessitates an investigation into how increases in transgene expression might vary corresponding to any changes in global protein expression levels. Interestingly, the *total* protein content in PC3-PSMA cells transfected with 1,4C-1,4Bis:pGL3 polyplexes did not change significantly with optimal Entinostat treatment (33 μM) compared to DMSO (vehicle)-treated cells (i.e. absence of Entinostat) [148]. However, it is important to note that with fewer cells present following 33 μM Entinostat treatment, the total protein content *per cell* escalated as shown in **Figure 3.3**. This could be due to increased acetylation of chromatin or possibly reduced cell growth rate and a concomitant alteration in cell metabolism. However, the fold-increase in protein content per cell (approximately 2.8-fold) with 33 μM Entinostat treatment did not nearly account for the fold-enhancement in transgene expression observed per cell with inhibitor treatment (approximately 28-fold; cell counts, RLU values, and protein content in **Appendix II**) (**Figure 3.3**). This result indicates that mechanisms in addition to changes in total protein

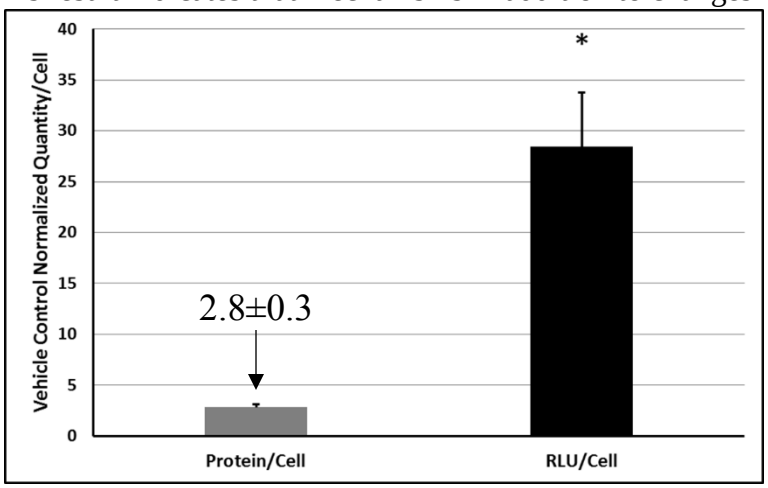

Figure 3.3 Effect of Entinostat on global protein expression (as measured via BCA assay) and transgene (luciferase) expression in PC3-PSMA cells transfected with 10:1 (w/w) 1,4C-1,4Bis pGL3 polyplexes in serum free-media i.e. SFM (n=3). The protein/cell and RLU/cell reported for Entinostat in this graph are normalized with those observed for the DMSO (i.e. vehicle control in absence of Entinostat). Data shown indicate mean values ± one standard deviation. Asterisks (*) denote significant increase in RLU/cell relative to protein/cell with 33 μM Entinostat treatment.

content are likely responsible for enhancement in transgene expression with 33 μM Entinostat treatment.

3.3.3 Effect of Entinostat Treatment on Cell Cycle Distribution

Given the known importance of cell cycle phase in transgene expression, we examined the effects of Entinostat on cell cycle progression in PC3-PSMA cells (**Figure 3.4 and Table 3.1**) [148]. The majority of the control cells (treated with only 0.5% DMSO) were found to be in the G_0/G_1 phase of the cell cycle (62%), while 28% of the cells were in the G_2/M phase and 10% were in the S phase. Treatment with 3.3 μM Entinostat resulted in significant accumulation (86%) of PC3-PSMA cells in the G_0/G_1 phase, with a concomitant decline in both S and G_2/M cells. Treatment with 33 μM Entinostat (the optimal tested dose for transgene expression in PC3-PSMA cells) showed no significant G_0/G_1 arrest, although a modest (6.2%) increase in the apoptotic cell population was observed. These results have some similarity to a previous study in which 1 μM Entinostat resulted in G_0/G_1 arrest of U397 human leukemic monocyte lymphoma cells, while a higher dose (5 μM) failed to induce G_0/G_1 arrest, but did lead to a significant increase in apoptotic cell population [149]. However, these results differ from a study in closely related PC-3 cells, in which, G_2/M arrest was reported with Entinostat treatment [150]. These cell cycle distribution results indicate that the observed increase in transgene expression observed with 33 μM Entinostat treatment is unlikely to be explained by cell cycle effects alone, but the G0/G1 arrest observed at 3.3 μM and the modest increase in apoptotic cells at 33 μM correlate with the observed decreases in cell viability at these concentrations, (64.6 ± 6.9 and 71.1 ± 6.0 % viability respectively) with PEI compared to PEI + 0.5% DMSO at 88.0 ± 6.5 % viability. While drug treatments prior to cell cycle staining were not accompanied

by polyplexes, viability experiments were not carried out in the absence of polyplexes, so the aforementioned statements regarding cell cycle and viability assume that PEI and Entinostat do not synergistically kill cells.

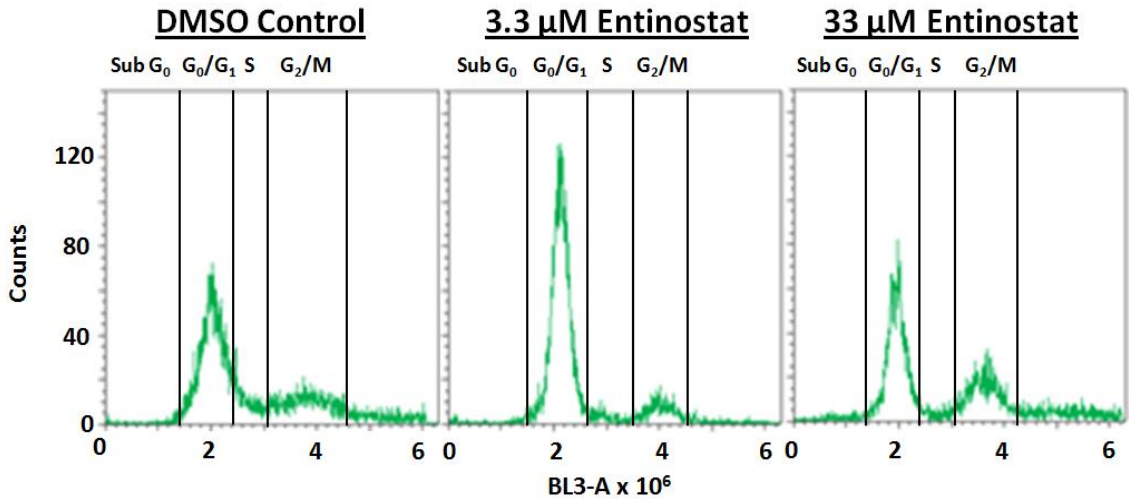

Figure 3.4 Cell cycle analysis of PC3-PSMA cells treated with 0.5% DMSO, 3.3 µM Entinostat, and 33 µM Entinostat (n = 3); results from one representative experiment are shown. The y-axis indicates the number of cells with the specific fluorescence intensity shown on the x-axis

Table 3.1 - Fractions of PC3-PSMA cells in each phase of the cell cycle following treatment with Entinostat. Asterisks (*) indicate significant change from vehicle control (DMSO control) treatment (Student's T-Test, p<0.05)

Cell Cycle Phase	Vehicle Control	3.3 µM Entinostat	33 µM Entinostat
Sub-G0/G1	0.7±0.4%	1.3±0.9%	6.2±1.3%*
G0/G1	61.9±7.8%	86.3±2.3%*	69.7±10.5%
S	9.9±2.7%	2.2±0.8%*	3.7±1.2%*
G2/M	27.6±7.3%	10.2±2.7%*	20.5±9.2%

3.3.4 DNase Accessibility with Entinostat Treatment

Positively charged deacetylated histones are tightly wrapped with negatively charged DNA, while acetylation of histones removes the positive charge, disrupts DNA-histone binding, and facilitates increased DNA availability for transcription. Given these

known mechanisms between histone (de)acetylation and chromosomal DNA, it was hypothesized that treatment of plasmid-transfected cells with Entinostat would, in part, increase transgene expression by reducing the binding of plasmid DNA to histones, thereby increasing the availability for transcription.

One way to indirectly measure the availability of a region of DNA is by treatment with DNase, which cuts "unprotected" or transcriptionally "accessible" DNA. This includes portions of the plasmid that do not interact with histones in the nucleus. Thus, determination of amount / extent of 'cut' portions, e.g. using qPCR, is an indication of how accessible the plasmid is for transcription inside host cell nuclei. This approach has been previously applied to elucidate the availability of promoter and other regions of chromosomal DNA [151-153]. In our case, we applied this same principle, but to exogenously delivered plasmid DNA, as opposed to host cell chromosomal DNA assayed in these previous investigations. As stated previously, evidence suggests that plasmids do form nucleosomes extracellularly and possibly *in vitro*, which motivated the use of this strategy for elucidation of DNase accessibility *in vitro*.

qPCR analyses were performed on purified PC3-PSMA nuclear DNA fractions with primer pairs amplifying different regions around the *luc+* and SV40 promoters gene on the pGL3 plasmid; control experiments with nuclei from untransfected cells were carried out in order to verify that the PCR signal was exclusively from pGL3 plasmid DNA. The regions amplified using qPCR include: a region on the SV40 promoter (primer pair 1), a region bridging the SV40 promoter and *luc+* gene (primer pair 2), and regions on the *luc+* gene (primer pairs 3 and 4) (**Figure 3.5**). Normalized DNase accessibility for each of the four explored regions in the promoter and gene area are shown in **Figure 3.5** [148].

The results are similar for each of the four regions assayed in that no statistically significant change in DNase accessibility was observed due to Entinostat treatment.

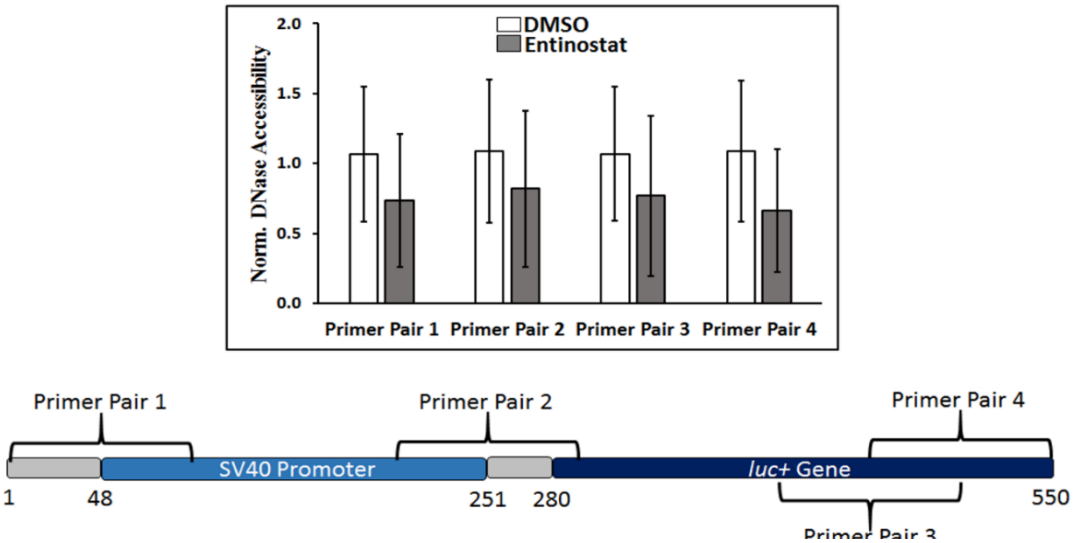

Figure 3.5 DNase accessibility data normalized to DMSO treatment (n = 3) in PC3-PSMA cells. The y-axis indicates fractional DNase accessibility relative to DMSO-treated cells. Data shown indicate mean values ± one standard deviation. For all four regions, as indicated by primer pairs 1-4 in the promoter/gene map, the difference in DNase accessibility between DNA harvested from DMSO and Entinostat (33 μM) treated cells was *not* found to be statistically significant ($p<0.05$ threshold, Student's t-test)

It is possible that plasmid DNA forms nucleosomes inside cells, and that Entinostat does not strongly influence the transcriptional availability in the *luc+* promoter/gene region in our particular system. It is also possible that nucleosomes did not form with the delivered plasmid, and the increase in transgene expression observed with Entinostat treatment is due to changes in chromosomal availability (discussed below). Additionally, there may be regions, upstream of the promoter or elsewhere on the promoter that were not included in the qPCR analyses, but may play a role in transcription factor binding.

3.3.5 Evaluation of Plasmid DNA Content in the Nucleus

While a change in DNase accessibility to exogenously delivered plasmid with Entinostat treatment was not detected, qPCR experiments revealed a very interesting result.

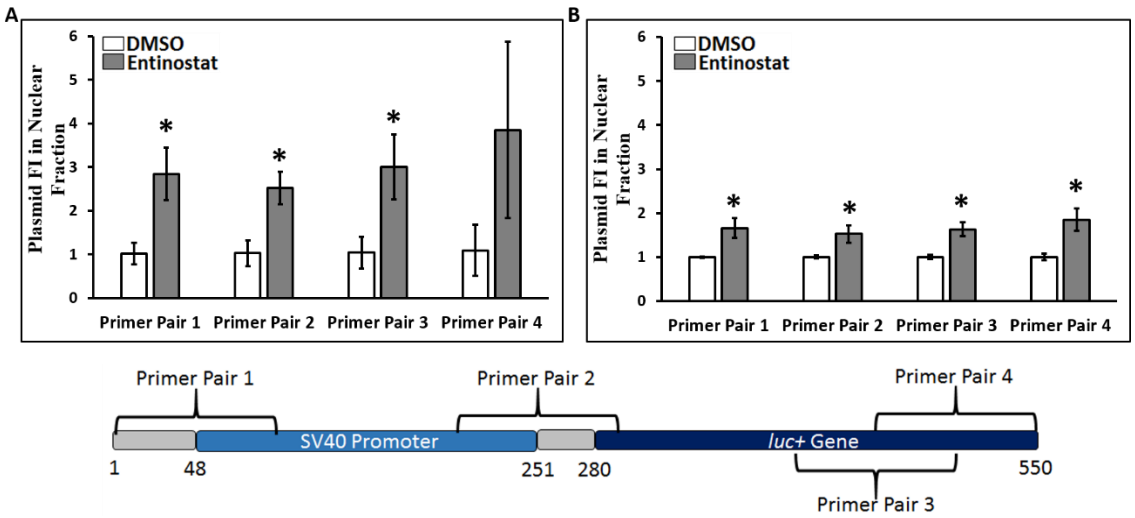

Figure 3.6 Normalized plasmid content in the nuclear fraction (FI = fold increase) indicating the relative amount of exogenously delivered plasmid DNA present in the nucleus following A) 33 μM Entinostat treatment in PC3-PSMA cells or B) 10 μM Entinostat treatment in PC3 cells. Data represented as mean ± one standard deviation. Asterisks (*) denote $p<0.05$ (Student's T-test) comparing pGL3 levels in nuclear fraction of Entinostat + polyplex treated cells relative to DMSO + polyplex treated cells. The base pairs are labeled such that position 1 is the first base pair amplified by our primers. The numbering system was defined for convenience, and is not relate to that provided by the vendor (Promega)

In two cancer cell lines, PC3-PSMA and PC3, Entinostat treatment at the optimal concentration for enhancing transgene expression increased detected intact (i.e. not treated with DNase) pGL3 in the nucleus (**Figure 3.6**) [148]. In PC3-PSMA cells treated with 33 μM Entinostat (**Figure 3.6A**), normalized plasmid in nuclear fraction values of 2.8 ± 0.6 and 2.5 ± 0.4 were observed with primer pair 1 and primer pair 2 for the plasmid in the nuclear fraction; both primer pairs amplify regions containing part of the SV40 promoter, with the latter including a portion of the *luc*+ gene. qPCR using primer pair 3 for amplification indicated the normalized plasmid levels to be 3.0 ± 0.7, while primer pair 4 yielded a value of 3.9 ± 2.0 compared to the control; both of these primer pairs amplify portions of the *luc*+ gene. In PC3 cells treated with 10 μM Entinostat, a modest increase in pGL3 in the nuclear fraction was observed (**Figure 3.6B**) [148]. As shown through PCR amplification of several portions close to / of the pGL3 SV40-*luc*+ region, the presence of

the exogenous plasmid DNA in the nucleus is significantly enhanced by Entinostat treatment in two different cell lines. These results indicate that the modest increase in plasmid present in cell nuclei (~3.1-fold in PC3-PSMA cells and ~1.7 in PC3 cells, from the average value for all primer pairs) likely contributes to the enhancement in transgene expression observed with Entinostat.

3.4 DISCUSSION AND CONCLUSIONS

The experiments carried out in chapter 3 have clearly identified inhibition of HDAC1/3 using the small molecule inhibitor Entinostat as a target for enhancing polymer-mediated plasmid transient expression in cancer cell lines. This phenomenon appears to be very general, as it was shown to be active in three cancer cell lines using three polycations delivery vehicles. Additionally, expression of a second plasmid driven by another promoter (CMV-EGFP) was shown to be improved with Entinostat treatment in two of the cancer cell lines. These results agree with previous findings that the pan-HDAC (HDAC 1, 3, 4, 6, and 10) inhibitor Trichostatin A significantly enhances expression from a variety of viral promoters, including the SV40 and CMV promoters used in this study [84, 154].

Treatment of PC3-PSMA cells with a low micromolar dose (3.3 μM) of Entinostat resulted in accumulation of cells in the G0/G1 phase, while addition of a higher dose (33 μM) yielded no significant alteration in cell cycle distribution. Given that both of these doses are correlated with high transgene expression, it is unlikely that the cell cycle plays a major role in the observed enhancement in transgene expression. It is interesting to note

that the optimum concentration of Entinostat observed in our experiments (3.3-33 μM) is much higher than the previously published submicromolar (< 1 μM) IC_{50} values for the anti-proliferative effects of Entinostat [149]. However, these concentrations are consistent with other studies showing enhancement of viral gene therapy at 3.3-10 μM [155, 156]. This optimum concentration range corresponds well with inhibition of HDAC 3 (IC_{50} = 8 μM) but is much higher than that required for inhibiting HDAC 1 (IC_{50} = 0.3 μM) [146], although IC_{50} values are often underestimated for *in vitro* applications, as they are often estimated in cell free assays. It is possible that inhibition of this second target at higher concentrations plays a role in the reversal of the cell cycle distribution. Given IC_{50} values, it appears that inhibition of HDAC3 may be at least partly responsible for the observed enhancement of transgene expression, although more studies are required to elucidate this.

DNase accessibility was not found to be altered by Entinostat treatment in these experiments. As addressed above, it is possible that the region(s) tested on the promoter and gene lie outside of an affected locus. It is also quite possible that Entinostat, by affecting chromatin structure of the target cell results in increased expression of a gene that itself directly or indirectly improves nuclear entry of our delivered plasmid. It is important to note DNase accessibility is not always positively correlated to high local gene expression. There is recent evidence that indicates a more complex relationship between these factors. For example, high rates of DNase I hypersensitivity were detected on cis-elements associated with low-expression genes in HeLa cells, suggesting DNase accessibility alone does not indicate high expression. Counter-intuitively, a *positive* correlation between *silenced* genes and chromatin relaxation was observed in one case [157]. To really understand if HDACs interact with delivered plasmids, more involved

assays, such as chromatin immunoprecipitation (ChIP) may be necessary (discussed in chapter 5). These experiments, however, did identify that Entinostat treatment improves nuclear entry of a delivered plasmid, or the gene delivery barrier that is generally considered the least efficient (or most difficult) for a transgene to overcome. The mechanism behind improved plasmid nuclear entry is not clear, but it is very likely an off-target effect, involving overexpression of a target cell gene through chromatin hyperacetylation, assisting in nuclear entry.

In chapters 2 and 3, certain kinase classes and HDAC1 (and/or HDAC3) have been identified as targets for enhancing transgene expression. Inhibition of PLK1 was clearly shown to affect trafficking of delivered plasmids in the cytosol, while the HDACs inhibited by Entinostat both have activity in the nucleus. The mechanism by which the signal transduction – transcription responsive JAK-STAT pathway enhances transgene expression is unknown. However, it is likely that all of these pathways act independently in certain facets of their functions, but may have overlapping functions as well. Experiments were carried out inhibiting the lead inhibitor of each of these three targets and in combination while delivering plasmid, ultimately observing how these inhibitors affect transgene expression individually and in combination (**Figure 3.7**) [106].

Simultaneous inhibition of PLK1 (H=HMN-214), histone deacetylase 1/3 (E = Entinostat), and JAK2-STAT (A=AG490) resulted in further enhancement of transgene expression relative to inhibition of each individual target. Each pairwise inhibition led to significant transgene expression enhancement compared to either individual component with at least one polymer, and the triple (HAE) combination significantly enhanced

expression relative to each dual-combination with 1,4C-1,4Bis as the carrier, and led to enhancement relative to all three single agent treatments with PEI as the gene carrier. These results demonstrate that inhibition of key intracellular kinase targets using small-molecule inhibitors can enhance transgene expression and potentially improve gene therapy efficacy. Interestingly, each of the three inhibitors tested have been shown to have anticancer activity, potentiating enzyme inhibition combinations for *cancer* gene therapeutic applications [158] [112, 159].

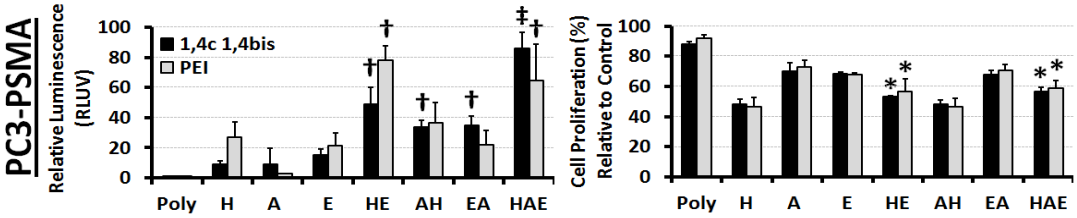

Figure 3.7 Effects of inhibitor drug combinations on relative luciferase expression (RLUV, left) and cell proliferation (right) in PC3-PSMA cells following transfections with 1,4C-1,4Bis and pGL3.0 plasmid DNA polyplexes. † indicates combinations with RLUV significantly higher than the corresponding individual treatments (e.g. HE compared to H or E), ‡ indicates triple combinations (HAE) with RLUV significantly higher than any pair-wise treatment (e.g. HAE compared to HE, AH, and EA). Asterisks indicate combination treatments containing HMN-214 with significant increases in proliferation compared to HMN-214 alone. In all cases, statistical significance was determined using the Student's t-test, and a p-value < 0.05 was considered significant. H = 3.3 μM HMN-214 (PLK1 inhibitor), A = 3.3 μM AG-490 (JAK/STAT/EGFR inhibitor), and E = 33 μM Entinostat (HDAC1 inhibitor, N = 3 independent experiments). Error bars indicate standard deviations

CHAPTER 4 – IDENTIFICATION OF EPIGENETIC ENZYMATIC TARGETS AFFECTING TRANSGENE EXPRESSION

4.1 INTRODUCTION

The studies discussed in chapter 2 were focused on phenomenological discovery of kinase targets for enhancing non-viral (polymer)-mediated transgene expression, as well as basic mechanistic evaluation of how inhibition of the lead kinase target (PLK1) enhances transgene expression. The kinase screening study was proposed based on the idea that several kinases have been established to play a role in transgene expression through affecting cargo endocytosis and trafficking, as well as many more which have potential, given their effects on known barriers of endocytosis and trafficking outside of the context of gene delivery (examples of both given in section 2.1). Experiments carried out in chapter 3 then focused on a downstream barrier to gene delivery, inhibiting an epigenetic modifying enzyme with known nuclear histone deacetylation activity. Given the lack of research efforts that have been focused on how events inside the nucleus affect transgene expression, the work carried out in chapter 4 focused on identification and mechanistic evaluation of epigenetic modifying enzymes for enhancing transgene expression.

Epigenetics is a vast field studying the effects on gene expression of factors that do not change the nucleic acid sequence of DNA. Different epigenetic states, resulting in expression activation or repression of particular genes are generally heritable, and can be activated by environmental changes [160]. Epigenetic modifications are involved in a number of cellular processes, such as development [161]**,** metabolic regulation [162], and

aging [163], and improper epigenetic regulation can lead to diseases such as cancer [164] and neurodegenerative disorders [165].

As discussed in chapter 3, chromosomal DNA is organized in a collective structure with histone proteins referred to as chromatin, and these DNA-histone interactions play a pivotal role in regulation of gene expression. In addition to DNA methyltransferases, which facilitate methylation of promoter DNA and generally have an inhibitory effect on gene expression [166], there are a number of enzymes which post-translationally functionalize histones, affecting chromatin structure and, ultimately, gene expression. A common theory used to describe the interplay between these enzymatic processes is the histone code theory, which classifies enzymes as writers (enzymes that carry out histone modifications), erasers (those that remove functional modifications), and readers (those that recognize the "epigenetic mark" of these modifications and recruit other proteins for chromatin remodeling) [167, 168]. These enzymes, which carry out modifications such as histone (de)acetylation, (de)phosphorylation, and (de)methylation mark histones for reader enzymes to enable a change in chromatin structure and gene expression; many of these marks and their effects on gene expression are well understood. The acetylation mark on many different lysine groups on core histones, as well as phosphorylation of histone H3 serine 10 are known to be activators of gene expression [165]. Histone methylation, on the other hand, can have activating or repressing effects on local gene expression; for instance, di- or tri- methylation of Histone H3 lysine 4 (H3K4me2 or H3K4me3, respectively) activates transcription, while trimethylation of H3K9 (H3K9me3) and H3K27me3 promote repression of transcription [165].

While many epigenetic modifications are well understood in the context of chromatin involving chromosomal DNA, a thorough understanding of how native gene expression machinery articulates with exogenously delivered DNA (eg. plasmid DNA), especially non-viral DNA, is severely lacking. However, the literature is not completely devoid of examples of epigenetic enzyme inhibition for enhancing non-viral transgene expression. The Pan-HDAC inhibitor sodium butyrate [169], and now the class I HDAC inhibitor Entinostat (chapter 3) have been demonstrated to enhance non-viral transient expression. Additionally, DNA methyltransferase inhibition with 5-Azacytidine has been shown to enhance transgene expression [170]. While these targets have been identified, there are likely many more to be discovered.

The major goal of this chapter is to identify epigenetic enzyme targets that can be inhibited (or conversely, overexpressed) to enhance transgene expression, and begin to understand why they do. Using a commercially available library consisting of 89 small molecule epigenetic enzyme inhibitors targeting writer, eraser, and reader enzymes of the epigenetic code, a screen has been carried out to determine the effects of inhibiting epigenetic modifiers on polymer-mediated transgene (plasmid) expression in two cell lines: UMUC3 bladder cancer cells, commonly used in modeling bladder malignancies and Chinese Hamster Ovary (CHO-K1) cells, a cell line commonly used in both stable and transient protein production biotechnology.

4.2 METHODS

4.2.1 Small Molecule Epigenetics Screening Library and Stock Solution Preparation

A library of 89 small molecule epigenetic enzyme inhibitors from Cayman Chemicals (Item number 11076, 10 mM in DMSO) was purchased. Based on a combination of published IC50 values and literature search for concentration ranges typically used, all inhibitors were categorized either as high dose candidates (screened at 500 nM, 5 μM, and 50 μM) or low dose candidates (screened at 50 nM, 500 nM, and 5 μM). Stock solutions were prepared in DMSO at 100X the highest concentration to be assayed (5 mM for high dose candidates, 0.5 mM for low dose candidates).

4.2.2 Epigenetic Inhibitor Transgene Expression Screen

On the evening prior to screening, 10,000 cells were plated per well in 96 well plates in RPMI 1640 media (10% fetal bovine serum and penicillin (100 units/mL) – streptomycin (100 μg/mL). On the following morning, neomycin resorcinol diglycidyl ether (N-RDGE) polymer solution [66] was prepared at 0.375 mg/mL in 1X PBS and filtered through a 0.2 μm regenerated cellulose syringe filter. pEF-Luc plasmid DNA was prepared at 15 ng/μL in EB buffer (Qiagen). In a sterile deep well 96-well block, small-molecule library inhibitors were added corresponding to experimental plate position. Cell-containing plates and the deep well inhibitor-containing block were then placed inside of a Biomek FXp liquid handing system (LHS) and, using an optimized protocol, serum-containing RPMI media was added to the 100X concentrated inhibitors, diluting them to the highest working concentration to be tested, and mixed using an orbital shaker. Old media was removed from cells and replenished with drug-containing media by the LHS. The LHS carried out 10X dilutions of the original inhibitor solution

to prepare media at the two lower working inhibitor concentrations to be tested. A reservoir of polymer-DNA complexes (polyplexes) was prepared manually in a laminar flow biohood at a 25:1 (w/w) ratio and allowed to form for 20 minutes at room temperature. Polyplexes containing 75 ng DNA/well were then distributed to all cells (10 μL/well) by the LHS, and transfection was allowed to proceed for 48 hours at 37°C/5% CO_2

4.2.3 Transgene Expression Quantification

48 hours after transfection, cells were assayed for transgene expression. Cell lysis was carried out using cell culture lysis reagent (Promega) and luminescence was detected using a Synergy 2 plate reader (Biotek, Winooski, VT). Protein content was assayed for each well using the BCA assay (ThermoFisher); to account for any well-to-well variation in cell plating, luminescence values were normalized to protein content. Additionally, MTT viability assays (ATCC) were carried out in parallel plates, and luminescence values were also normalized to viability. For dose-response optimization and combination transfections, protein content and viability were not assayed, thus luminescence values for these transfections are representative of total well luminescence.

4.2.4 Dose Response Optimization Transfections

Select lead inhibitors from the epigenetic screen were chosen for dose optimization with the pEF-Luc plasmid, driven by the EF1α promoter as well as the pGL3 plasmid, also expressing luciferase, but under control of the Simian Virus 40 (SV40) promoter. These transfection experiments were carried out by hand, using the same polymer and plasmid conditions as used in the screen. Inhibitors were purchased

from Cayman Chemical in solid form and dissolved in DMSO to 500x working concentration for each dose to be tested. Doses were chosen to test at and above (where possible) and below the optimal of three doses tested in the screen, based on screening results. Luciferase assay was employed in a similar manner as the screen, with the exception of viability and protein content normalization.

4.2.5 Plasmid Nuclear Localization

As in chapter 3, pGL3 transfections were carried out and 48 hours later, cell nuclei were isolated. Using the same primer pairs discussed for pGL3 detection in chapter 3, a qPCR routine was performed and relative nuclear plasmid levels were quantified.

4.3 RESULTS

4.3.1 Small Molecule Epigenetic Inhibitor Screening for Effects on Plasmid Expression

An epigenetics screening library, consisting of 89 small molecule inhibitors of many epigenetic effector enzymes, was screened for enhancement of transgene expression in CHO-K1 and UMUC3 cells. Each inhibitor was tested at three different concentrations, as described in section 4.2, with the dose yielding the greatest enhancement in transgene expression shown for CHO-K1 in **Figure 4.1A and 4.1B,** and for UMUC3 in **Figure 4.2A and 4.2B**. The actual doses with which these reported data correspond for each inhibitor can be found in **Appendix IV, Table A4**.

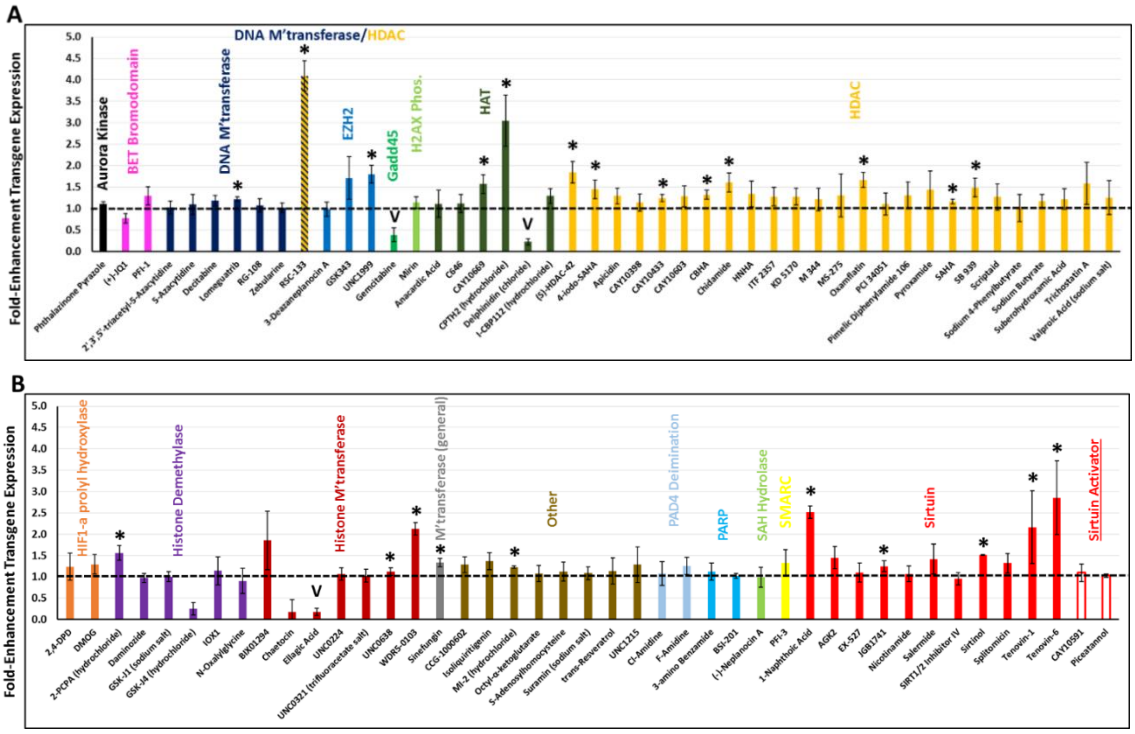

Figure 4.1 Epigenetics screening library inhibitors were assayed for enhancement of transgene expression in CHO-K1 cells. The concentration of each drug leading to the greatest enhancement in transgene expression is included. Polyplexes were formed by adding N-RDGE polymer to 75 ng EF-Luc plasmid DNA at a 25:1 (wt/wt) ratio. Inhibitors are organized by target, with targets organized alphabetically in figure A, continued in figure B. ***** = Student's T-test $p<0.05$ for enhancement in transgene expression; **v** = Student's T-test $p<0.05$ for reduction in transgene expression. Chaetocin and GSK-J4 were not considered statistically significant reducers of transgene expression because viability was very low for cells treated with these inhibitors

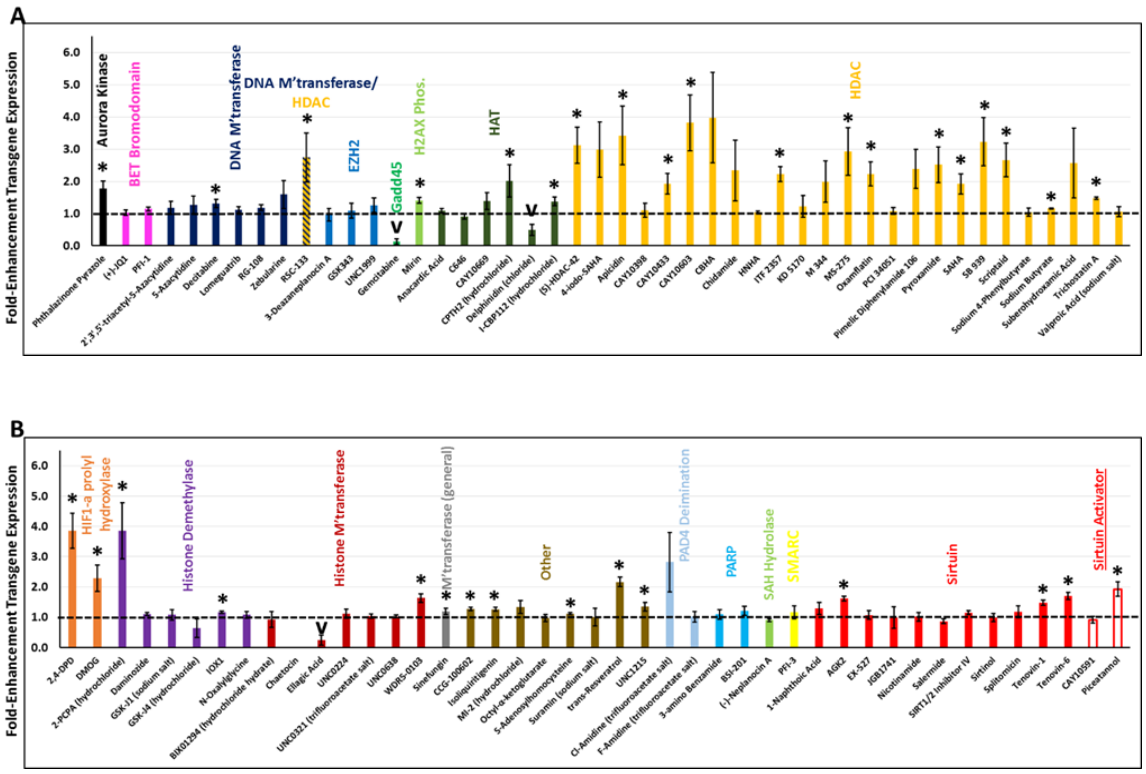

Figure 4.2 Epigenetics screening library inhibitors were assayed for enhancement of transgene expression in UMUC3 cells. The concentration of each drug leading to the greatest enhancement in transgene expression is included. Polyplexes were formed by adding N-RDGE polymer to 75 ng EF-Luc plasmid DNA at a 25:1 (wt/wt) ratio. Inhibitors are organized by target, with targets organized alphabetically in figure A, continued in figure B. ***** = Student's T-test $p<0.05$ for enhancement in transgene expression; **v** = Student's T-test $p<0.05$ for reduction in transgene expression. Chaetocin and GSK-J4 were not considered statistically significant reducers of transgene expression because viability was very low for cells treated with these inhibitors

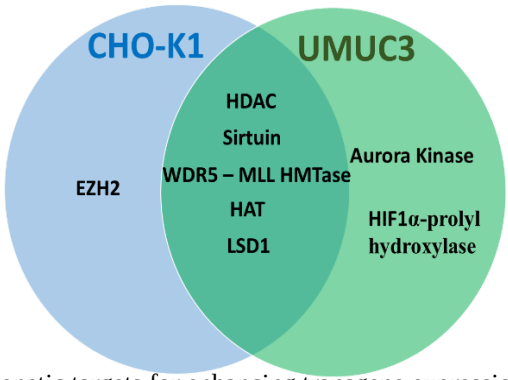

Figure 4.3 Identified epigenetic targets for enhancing transgene expression in the two cells lines included in the screen. Targets are defined as enzymes for which multiple small molecule inhibitors led to enhancement in transgene expression if multiple inhibitors were provided in the library. If only one inhibitor was provided for a target and it resulted in transgene expression enhancement, it is included here. The latter is the case for WDR5, LSD1, and Aurora kinase

The screening revealed inhibition of several enzyme candidates for enhancing polymer-mediated transgene expression in both CHO-K1 and UMUC3 cells, as well as some that show promise in only one cell line or the other (**Figure 4.3**). They are discussed subsequently by enzyme class.

4.3.1A Histone Deacetylase (HDACs, classes I and II) -

The HDAC family of enzymes was highly represented in the epigenetic screening library. HDACs catalyze the removal of acetyl groups from lysine residues of histones, generally leading to a decrease in local gene expression. HDAC inhibitors (HDACis) have been used extensively for treatment of diseases, especially cancer, in which aberrant expression of HDAC enzymes is common [171]. While HDACis have been used for altering endogenous gene expression, they have also been applied for the enhancement of transient gene expression, using a variety of gene delivery vehicles including baculovirus vector [172], cationic polymers [84, 148, 173], and calcium phosphate [169]. The screen in both CHO-K1 and UMUC3 cells identified several Class I/II HDACis as enhancers of transient transgene expression **(Figure 4.1A and 4.2A)**, in general leading to greater enhancement in UMUC3 cells than CHO-K1. (S)-HDAC-42 is a structurally optimized derivative of phenylbutyrate [174], which is a very weak HDACi. Vorinostat, also known as suberoylanilide hydroxamic acid (SAHA) and its more potent [175] hydrophobic derivative 4-iodo-SAHA both demonstrated enhancement in transgene expression. SAHA and 4-iodo-SAHA have been shown to inhibit HDAC1 and HDAC6, which are nuclear class I and cytoplasmic class II HDACs, respectively. Oxamflatin is a class I HDACi that belongs to the same biochemical class as SAHA [176]. CBHA is an inhibitor of HDAC1 and HDAC3 [177], while Chidamide inhibits these HDACs as well as HDACs 2

and 10, the latter which is a mostly cytoplasmic class II HDAC [178]. Finally, among inhibitors resulting in transgene enhancement in both cell line tested, SB939 is a pan-HDACi, inhibiting all HDAC enzymes with the exception of HDACs 6 and 7 [179].

Several Class I/II HDACis which were not found to consistently enhance transgene expression in CHO-K1 cells clearly improved expression in UMUC3 cells: apicidin, CAY10433, CAY10603, ITF2357, M 344, MS-275, pimelic diphenylamide 106, pyroxamide, scriptaid, suberohydroxamic acid (SBHA), and Trichostatin A. Interestingly among this group is CAY10603 which potently and exclusively inhibits HDAC6, a primarily cytoplasmic HDACi that is known to deacetylate tubulin, affecting intracellular trafficking. HDAC6is have previously been found to enhance transgene expression by modifying intracellular trafficking [84, 180].

Others have already demonstrated class I/II HDACis to enhance transgene expression in certain systems. Entinostat (MS-275), trichostatin A, sodium butyrate, and valproic acid are known enhancers of transgene expression, and we have previously demonstrated Entinostat's ability to enhance transgene expression in cancer cells [148]. It is important to note that due to constraints introduced by manufacturer-provided inhibitor concentrations in the screening library, valproic acid and sodium butyrate were tested well below their IC50 values in the above screen.

4.3.1B Sirtuins (HDACs, Class III) –

In addition to the classical HDAC classes I, II, and IV (those discussed above fall under class I and II), class III HDACs are a group of NAD+ dependent protein functionalizing enyzmes known as sirtuins. While several class I and II HDACis were

identified as enhancers of transgene expression, sirtuins were shown to be a potential target for transgene expression enhancement in both cell lines **(Figure 4.1B and 4.2B)**, although a more promising target in CHO-K1 than UMUC3 cells. Tenovin 1 and its improved analog Tenovin 6, both identified as enhancers of transgene expression in both cell lines, are inhibitors of sirtuins SIRT1 and SIRT2 [181], which are responsible for carrying out histone deacetylation on H3K9 and H4K16 (SIRT1) or just H4K16 (SIRT2) [182], in addition to many other non-histone protein targets. Tenovin 6 has been shown to have anti-cancer activity by attenuating the effects of SIRT1 overexpression common in cancers, through increased expression of death receptor 5 for apoptosis induction [183, 184] as well as interference with protective autophagy [185]. In addition to histone deacetylation and its downstream effects, SIRT1 regulates the activity of transcription factors such as p53 through direct deacetylation. Also identified as enhancers of transgene expression in CHO-K1 cells were sirtinol, a SIRT1/2 inhibitor [186] and its derivative naphthoic acid [187]. Also, JGB1741, an inhibitor of SIRT1 and weak inhibitor of SIRT2 led to moderate transgene expression enhancement. AGK2 a SIRT2 inhibitor enhanced transgene expression in both cell lines and salermide (SIRT1/2 inhibitor) also showed promise in enhancing transgene expression in CHO-K1 cells. In general, sirtuin inhibitors appear to be more promising for enhancing transgene expression in CHO-K1 cells than in UMUC3; interestingly, Piceatannol, which has been shown to *activate* SIRT1 expression in human monocytes [188], enhanced transgene expression in UMUC3, but not in CHO-K1 cells. This further indicates that the sirtuins may not be a strong inhibition target for enhancing transgene expression in UMUC3 cells.

4.3.1C Histone Acetyltransferase (HAT) -

HAT enzymes catalyze the addition of acetyl groups to the ε-amino groups of lysine residues present on core histones, carrying out the opposite activity of HDACs, with which they work to regulate gene transcription. Addition of these acetyl groups at nucleosomes lead to a general increase in chromatin accessibility [189], allowing interaction with necessary transcriptional machinery. The screen identified CPTH2 hydrochloride as a strong enhancer of transgene expression in both cell lines (**Figure 4.1A and 4.1B**). CPTH2 hydrochloride specifically inhibits the HAT enzyme Gcn5, which has known acetyltransferase activity at Histone H3K9 [190] and H3K14[191]. A similar protein with HAT activity, PCAF, was represented in the screening by the inhibitor CAY10669 which moderately enhanced transgene expression in CHO-K1 cells. In addition to the Gcn5/PCAF family of HATs, there were several inhibitors represented from the CBP/p300 family of HATs. Anacardic acid inhibits both PCAF and p300, while C646 inhibits p300 only; neither of these inhibitors enhanced transgene expression in either cell line. While the inhibitor of CBP, I-CBP 112 Hydrochloride, very moderately enhanced transgene expression in UMUC3 cells, delphinidin (chloride), a CBP/p300 HAT inhibitor, significantly *decreased* transgene expression in both cell lines, one of only three inhibitors in the library to do so. Taken together, while there are exceptions, inhibitors of HAT enzymes in the Gcn5/PCAF family appear to have the potential to enhance transgene expression while inhibitors of CBP/p300 HAT enzymes do not enhance transgene expression and, in one case, *decreases*, transgene expression, which is more in line with the function of HATs and chromosomal transcription regulation.

4.3.1D Histone Methyltransferase (HMT) -

Methylation of core histone tails by HMT enzymes plays a major role in the regulation of gene expression. Inhibitors of several HMT or HMT-complex associated enzymes were identified in the screen to affect transgene expression.

WDR5 is a WD-repeat family protein that is a non-catalytic subunit of trithorax (TRX) methyltransferase complexes, including the mixed myeloid leukemia (MLL) complex, catalyzing H3K4 methylation [192]. The small molecule inhibitor WDR5-0103, an inhibitor identified for enhancing transgene expression in both cell lines, has been demonstrated to bind with WDR5 and inhibit MLL methyltransferase activity *in vitro* [193]. Interestingly, the H3K4 methylation is a transcriptional activation mark, so it is assumed that there may be an off-target effect leading to enhanced transgene expression in both CHO-K1 and UMUC3 cells. WDR5 is overexpressed in bladder tissue, and is associated with poor prognosis [194], potentiating a synergistic gene therapeutic strategy involving the inhibition of this target. Another target that has been shown to bind with the MLL complex (Menin) is inhibited by MI-2 (under "other", **Figure 4.1B and 4.2B**); MI-2 demonstrated moderate enhancement in transgene expression. MI-2 has been found to reduce H3K4me3 and H3K79me2 in MLL leukemia cells [195].

G9a is a HMT that is capable of carrying out monomethyl and dimethyl histone transfer at H3K9; these are transcriptional activation or repression marks, respectively. BIX01294 hydrochloride and UNC0638 are G9a HMT inhibitors and both resulted in moderate transgene expression enhancement in CHO-K1 cells, while imposing no effect on UMUC3 cell transgene expression. Interestingly, other G9a inhibitors UNC0224,

UNC0321 trifluoroacetate salt, and UNC0638 did not show up in the screen as enhancers in either cell line.

Enhancer of Zeste Homolog 2 (EZH2) is a specific histone methyltransferase that functions as the catalytic unit of the polycomb repressive complex 2 (PRC2). Within the context of PRC2, EZH2 facilitates *tri*methylation of histone H3, lysine 27 (H3K27me3), generally resulting in transcriptional repression [196]. The EZH2 inhibitors GSK343 and UNC1999 displayed moderate promise as transgene expression enhancers in CHO-K1 cells, while they did not have this effect in UMUC3 cells.

Each of the HMT targets discussed so far in this subsection catalyze methylation at lysine sites on histone H3. Conversely, the enzyme coactivator-associated arginine methyltransferase 1 (CARM1) facilitates methylation at an arginine site (H3R17). Additionally, CARM1 methylates the p300/CBP HAT, contributing to gene activation activity of this HAT [197]. CARM1 was represented by a single inhibitor in the screen, Ellagic acid, which resulted in a drastic *decline* in transgene expression; this behavior is consistent with the known gene activation activity of CARM1.

4.3.1E Histone Demethylase -

Only one histone demethylase was detected as a promising target in the screen; lysine specific demethylase 1 (LSD1) is a demethylase that specifically removes methyl groups from lysines H3K4 and in some cases, H3K9. While only one inhibitor of LSD1, 2-PCPA hydrochloride, was available in the enzyme library, it led to transgene expression enhancement in both cell lines (**Figure 4.1B and 4.2B** under "histone demethylases"). Another LSD1 inhibitor was purchased from Cayman Chemicals to validate LSD1 as a target (**Figure 4.5**). Demethylation at H3K4 is a repression mark of

the histone code, and LSD1 participates as part of the CoREST complex with HDAC1/2 [198], linking demethylation and deacetylation. Additionally, LSD1 can demethylate H3K9, which can have either a repressive (H3K9me → H3K9) or enhancing (H3K9me2 → H3K9me) effect on transcription. Both of these lysine sites can also be trimethylated, but LSD1 is not capable of demethylating H3K4me3 or H3K9me3. Interestingly, IOX-1 and N-Oxalylglycine, which both inhibit jumonji domain histone demethylases, responsible for demethylating H3K9me3, did not show promise in enhancing transgene expression in the screen. This indicates that the extent of methylation at one or both of these sites may play a role in the ability to enhance transgene expression.

4.3.1F DNA (De)Methylation -

RSC-133 strongly enhanced transgene expression in both CHO-K1 and UMUC3 cells. RSC-133 is a unique inhibitor, in that it has been shown to inhibit both HDAC1 and DNA Methyltransferase 1 (DNMT1). Cytosine methylation at promoter sites, carried out by DNMT1 as well as deacetylation of histone lysines are generally repressive marks on gene expression, and a coordination between these two functionalities is well established. Specifically, methylated CpG sites recruit HDACs to repress transcription [199] and physical binding between these two enzymes has even been observed [200]. RSC-133 was found to be more efficient than individual DNMT or HDAC inhibitors in reprogramming human somatic cells into pluripotent stem cells [201], a process that is carried out by epigenetically forcing expression of several transcription factors. Therefore, it is conceivable that the strategy of simultaneously inhibiting class I HDACs and DNMT1 could synergistically enhance transgene expression in cases when promoter DNA methylation is high, if the same epigenetic mechanisms apply to both chromosomal

and transient transgene expression. Interestingly, synergistic enhancement in transgene expression with simultaneous inhibition of RSC-133 appeared to occur in CHO-K1 cells (**Figure 4.1A**), while it did not occur in UMUC3 (**Figure 4.2A**). In CHO-K1 cells, neither HDAC nor DNMT inhibitors drastically enhanced transgene expression, while simultaneous inhibition with RSC-133 greatly enhanced transgene expression. It is possible that the cytosine methylation levels of the EF1α promoter driving plasmid luciferase expression differs in the nuclei of these two cell lines, although this has not been tested.

Gemcitabine, an inhibitor of Growth arrest and DNA-damage-inducible protein a (Gadd45a) [202] drastically *reduced* transgene expression in both cell lines (**Figure. 4.1A and Figure 4.2A**). As discussed in chapter 1, Gadd45 is expressed in response to DNA damage, leading to G2/M arrest, and Kim et al produced a CHO cell line that inducibly over-expressed Gadd45, leading simultaneously to G2/M cell cycle arrest and enhanced PEI-mediated transgene expression [82]. The use of gemcitabine conversely *inhibits* this protein rather than increasing its expression. The observed decrease in transgene expression is in agreement with this study. Epigenetically, Gadd45 overexpression increases global DNA demethylation [203], a known activating mechanism for gene expression. The observed decrease in transgene expression may be attributable to increased plasmid promoter methylation, increased progression through the G2/M checkpoint (the opposite effect of transgene expression enhancers such as inhibitors of PLK1 and Aurora kinase discussed in chapter 1, which arrest cells in G2/M), or a combination of these effects.

Sinefungin is a nucleoside which is isolated from *Streptomyces griseolus* [204], and has known inhibitory activity against lysine methyltransferases [205], but also has shown activity against DNA methyltransferases [206]. Sinefungin (**Figure 4.1B and 4.2B** under "M'transferases (general)") led to moderate transgene expression enhancement in both cell lines. Despite the leads discussed in this section, the majority of DNA methyltransferase inhibitors included in the screen did not increase transgene expression, suggesting that this modification in isolation may not be a strong candidate for enhancing transient plasmid expression in the cell lines used.

4.3.1G Other Interesting Inhibitors –

Inhibitors of two other targets, hypoxia-inducible factor 1-alpha prolyl hydroxylase (HIF-PH) and aurora kinase A, surfaced as interesting candidates from the screening (**Figures 4.1A and 4.2A**). These targets differ from the above targets because they do not carry out functional histone addition or removals with well-characterized effects on transcriptional regulation. HIF1α is a transcription factor that is activated in the presence of hypoxia and other stresses, resulting in the expression of certain genes in response to these stresses; it is regulated by the oxygen-sensing enzyme, HIF-PH, which hydroxylates a proline residue, marking HIF1α for degradation. Inhibition of HIF-PH using 2,4-DPD and DMOG drastically enhanced transgene expression in UMUC3 cells, while it did not improve transfection in CHO-K1 cells. Because HIF-PH facilitates degradation of HIF1α at normoxic conditions, inhibition of HIF-PH is expected to maintain relatively high levels of HIF1α. HIF1α has been found to interact with jumonji-domain containing histone demethylase proteins (JMJD1A and JMJD2A) which are responsible for the removal of tri-methyl groups from Histone H3K9 [207]; it should be

reiterated from section 4.3.1E that inhibitors of jumonji-domain containing demethylases, however, did not affect transgene expression in the screen. Also, HIF1α has been demonstrated to transcriptionally reduce levels of the class I HDAC, HDAC2, in epithelial lung and macrophage cells [208]. As discussed above, HDACs generally promote transcriptional repression. The putative repression of HDAC expression due to inhibition of HIF-PH with 2,4-DPD and DMOG (and consequently maintenance of HIF1α) is consistent with the screening observations, in that HDAC as well as HIF-PH inhibitors led to drastic enhancement in UMUC3 transgene expression, but failed to do so in CHO-K1 cells, suggesting that the observed enhancement in transgene expression with HIF-PH inhibitors may be explained by the same mechanisms driving transgene expression enhancement in the presence of HDAC inhibitors.

Finally, the only inhibitor of Aurora Kinase A (AKA) in the screening, phthalazinone pyrazole, resulted in strong enhancement of transgene expression in UMUC3 cells. AKA and the closely related Aurora Kinase B (AKB) have been demonstrated to capably catalyze phosphorylation of Histone 3 Serine 10 (H3S10) at the onset of mitosis [209], playing a major role in chromosomal segregation. While the capability to carry out epigenetic modifications generally corresponding to transcriptional regulation such as (de)methylation and (de)acetylation are lacking in the literature for AKA, AKB has been demonstrated to facilitate the double histone modification H3K9 trimethylation and H3S10 phosphorylation both in cells undergoing mitosis, but also in post-mitotic cells; this modification is localized at repressed genes in differentiated cells, but at both active and silent genes in dividing cells [210], which are representative of the cells in the screen. While phthalazinone pyrazole is known to inhibit AKA and not AKB

at the concentrations used in the screen, the AKB-specific inhibitor ZM-447439, as well as a number of pan-Aurora inhibitors showed up as leads in the screen discussed in chapter 2 [106]. This suggests that Aurora Kinase enyzmes (A-C) may all be targets for enhancing transgene expression. While there may be an epigenetic role in this phenomenon, inhibition or Aurora Kinase enzymes generally results in cell cycle arrest at the G2/M transition, likely playing a major role in the transgene expression enhancement.

4.3.1H Similarities and Differences Between Epigenetic Regulation of Chromosomal and Plasmid Expression

The findings discussed in the previous subsections of section 4.3 highlight some key similarities between endogenous and transgene expression, as well as cases where plasmid and chromosomal gene expression may be regulated very differently (**Table 4.1**).

Table 4.1 – Epigenetic Enzyme Targets Affect Chromosomal Gene Expression and Transgene Expression Similarly in Some Cases and Differently in Others

Same Effect on Endogenous and Transgene Expression	Opposite Effect on Endogenous and Transgene Expression
HDAC/Sirtuin	HAT (Gcn5/PCAF)
EZH2	WDR5
LSD1	
Gadd45	
HAT (CBP/p300)	

Class I/II HDAC enzymes generally resulted in drastic transgene expression enhancement in UMUC3 cells and, with some inhibitors, moderate enhancement in CHO-K1 cells. Several inhibitors of class III HDACs, sirtuins, resulted in transgene expression enhancement in CHO-K1 cells and to a lesser extent in UMUC3 cells. The removal of acetyl groups from core histone lysines is generally associated with low chromosomal gene expression, and this phenomenon seems to occur with plasmid transgene expression. Inhibition of EZH2 led to moderate enhancement in plasmid expression in CHO-K1 cells. EZH2 is the catalytic unit of the Polycomb repressive complex (PRC2), tri-methylating a specific lysine residue on histone H3 at the promoters of silenced genes; EZH2 has a known inhibitory effect on chromosomal transcription and the screen points to a potentially similar phenomenon for transgene expression. LSD1 is most commonly known to remove mono- and di- methyl groups from histone H3K4, leading to transcriptional repression of target genes. Transgene expression enhancement observed with the LSD1 inhibitors 2-PCPA hydrochloride and, to a lesser extent, OG-L002 (next section) suggest that LSD1 may similarly regulate chromosomal and transient gene expression. Gadd45 inhibition with gemcitabine significantly *decreased* transgene expression. Gadd45 overexpression promotes DNA demethylation, a known activator of transcription. Also, Gadd45 overexpression promotes cell cycle arrest at the G2/M phase, known to be a prime point in the cell cycle for transient gene expression. Finally, while several inhibitors of HAT enzymes surprisingly increased transgene expression, the CBP/p300 HAT inhibitor dephinidin (chloride) drastically reduced transgene expression, one of only three inhibitors in the screening library to do so.

The inhibition of two epigenetic enzyme targets, HAT and WDR5, led to an effect on transgene expression opposing their known roles in chromosomal transcription regulation. While the HAT inhibitor Delphindin (chloride) decreased transgene expression, consistent with the expected mechanism of HATs and chromosomal transcription, multiple other HAT inhibitors unexpectedly increased transgene expression. In addition to the Gadd45 inhibitor gemcitabine and delphindin (chloride), the inhibitor of CARM1, ellagic acid, reduced transgene expression. As discussed in section 4.3.1D, CARM1 methylates the CBP/p300 HAT, leading to its activation. Therefore, two of the three molecules in the screen that reduced transgene expression (dephinidin (chloride) and ellagic acid) directly or indirectly inhibit the activity of CBP/p300 HATs. Taking into consideration that the lead HAT inhibitor identified in the screen for enhancing transgene expression (CPTH2 hyrdochloride) targets only the Gcn5/PCAF family of HATs, it seems that the family of HAT inhibited plays a major role in whether enhancement or reduction in transgene expression is observed.

WDR5-0103 inhibits WDR5, which is a subunit of the mixed myeloid leukemia (MLL) complex which facilitates H3K4 methylation. This is generally an activation mark for transcription, but WDR5-0103 surprisingly increased transgene expression in both CHO-K1 and UMUC3 cells. The explanation for this phenomenon is unknown.

4.3.2 Select Lead Inhibitor Dose Optimization with Additional Plasmid

The results outlined in Section 4.3.1 identified several inhibitors of epigenetic related enzymes as candidates for enhancing transgene expression in UMUC3 bladder cancer cells and/or CHO-K1 cells. However, local chromatin structure and

transcriptional activity are often dependent on the promoter and gene. Consequently, a subset of the lead inhibitors identified in the screen were dose-optimized for their abilities to enhance transgene expression with both the pEF-Luc plasmid as well as a second luciferase expressing plasmid driven by a different promoter; the pGL3 plasmid with luciferase expression under control of the SV40 promoter. The experiments were carried out using the same polymer carrier as used for the screening (Neomycin resorcinol diglycidyl ether), and the vehicle-control normalized luciferase expression are shown for CHO-K1 cells in **Figure 4.4** and UMUC3 cells in **Figure 4.5**. In CHO-K1 cells, the combination HDAC/DNMT inhibitor (RSC-133), a sirtuin inhibitor (Tenovin-1), a HAT inhibitor (CPTH2 hydrochloride), an LSD1 inhibitor (2-PCPA hydrochloride), and the WDR5 inhibitor (WDR5-0103) were dose-optimized for transfection enhancement efficiency. While these dose response experiments served the purpose of finding the optimal lead inhibitor concentrations for further mechanistic experimental evaluation, it is evident based on two independent trials that transgene expression enhancement is not highly dependent on promoter (SV40 or EF1α). As in CHO-K1 cells, the ability of lead inhibitors to enhance transgene expression in UMUC3 cells did not appear to depend on promoter identity. The lead inhibitors chosen for dose-optimization with both DNA plasmids in UMUC3 cells were a pan nuclear HDAC inhibitor (SB939), a cytoplasmic HDAC6 inhibitor (CAY10603), RSC-133, 2-PCPA hydrochloride, and a second LSD1 inhibitor that was not included in the initial screen (OG-L002).

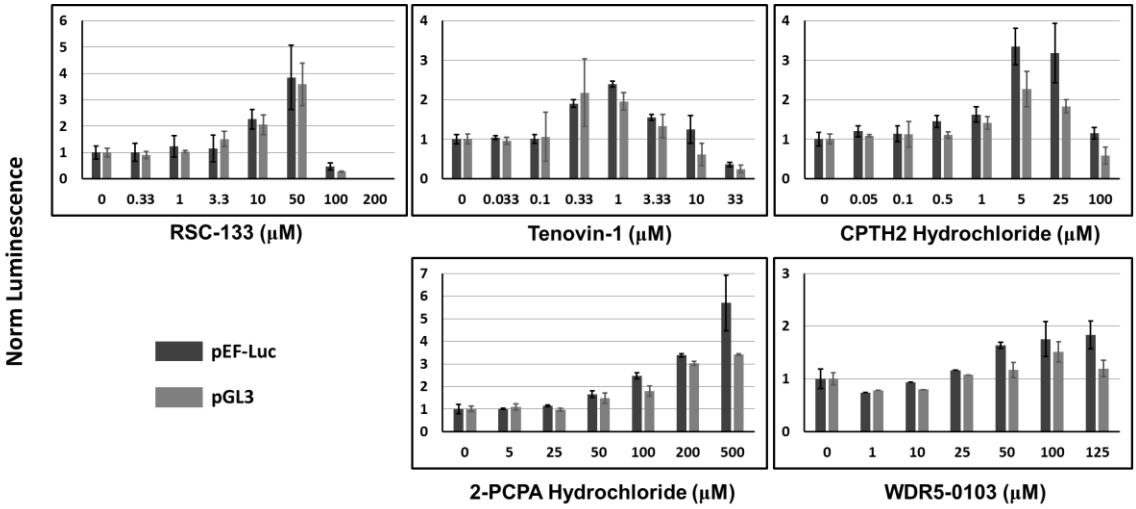

Figure 4.4 Several lead inhibitors from the screening were assayed for their ability to enhance transgene expression in CHO-K1 cells at additional doses and with a second plasmid, pGL3, containing a luciferase gene with expression driven by the SV40 promoter. The original plasmid (pEF-Luc) was also included. Transfection efficiencies (n=2) are reported normalized to the vehicle control (0.2% DMSO), and normalization to protein and viability are not taken into account

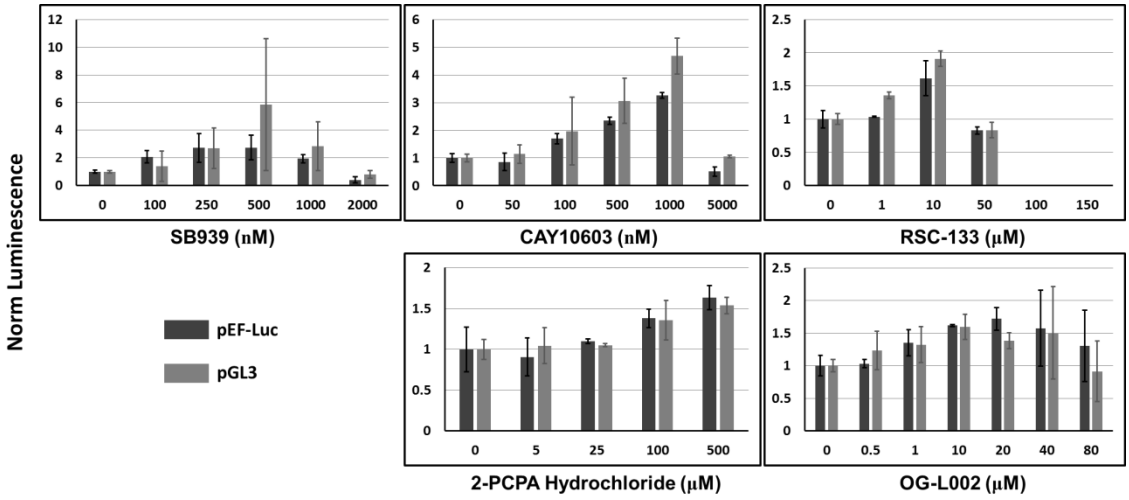

Figure 4.5 Several lead inhibitors from the screening were assayed for their ability to enhance transgene expression in UMUC3 cells at additional doses and with a second plasmid, pGL3, containing a luciferase gene with expression driven by the SV40 promoter. The original plasmid (pEF-Luc) was also included. Transfection efficiencies (n=2) are reported normalized to the vehicle control (0.2% DMSO), and normalization to protein and viability are not taken into account

4.3.3 Effect of Epigenetic Enzyme Inhibitors on Plasmid Nuclear Entry

With the exception of the cytoplasmic activity of a subset of HDACs, the known activity of most of the enzymes found to be leads for enhancing transgene expression occurs in the nucleus, affecting histone/DNA interactions. However, it is possible that there are off-target effects of inhibiting some of these targets that alter the amount of plasmid entering the nucleus, thus increasing transgene expression irrespective of changes in putative histone/plasmid DNA particles. To elucidate this potential phenomenon in our systems, several lead inhibitors at their optimal concentrations for enhancing transgene expression were introduced to cells which were then transfected with the pGL3 plasmid. Following two days of transfection, nuclei were isolated and using primers described in chapter 3, qPCR was carried out to quantify relative amount of plasmid inside the nuclei of transfected cells, denoted as "FI (fold increase) plasmid nuclear localization". In CHO-K1 cells (**Figure 4.6**), inhibitors of HDAC/DNMT, sirtuins, LSD1, pan-HDAC, and HAT, all of which were leads for enhancing transgene expression, did not appear to affect the

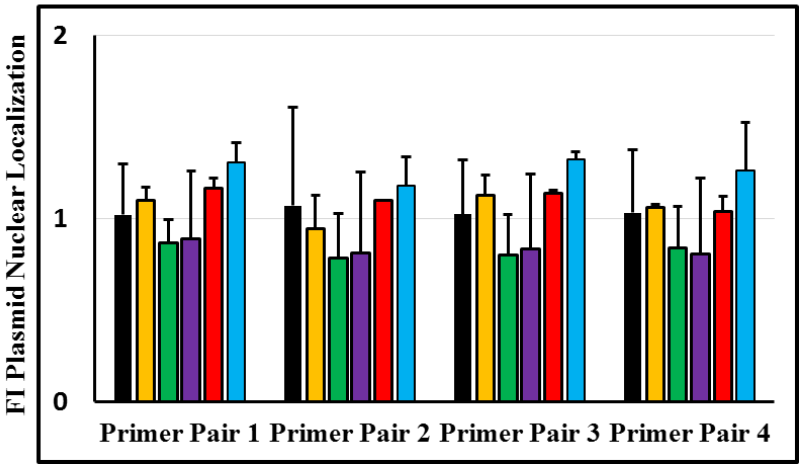

Figure 4.6 pGL3 plasmid enrichment in CHO-K1 nuclear fraction with lead inhibitor + transfection treatment, including the pan-HDAC inhibitor SB939, which was not a strong lead in CHO-K1 cells. N=2 independent experiments. Black = 0.2% DMSO (vehicle control); Orange = 50 μM RSC-133; Green = 1 μM Tenovin-1; Purple = 200 μM 2-PCPA hydrochloride; Red = 500 nM SB939; Blue = 5 μM CPTH2 hydrochloride

presence of plasmid inside the nucleus. This suggests that in CHO-K1 cells, the mechanistic explanation for plasmid expression enhancement lies at some point following nuclear entry, likely involving epigenetic mechanisms.

In UMUC3 cells (**Figure 4.7**), drug treatments included a lead pan-HDAC inhibitor (SB939), cytoplasmic HDAC6 inhibitor (CAY10603), and LSD1 inhibitor (OG-L002). While the LSD1 inhibitor did not affect plasmid presence in target nuclei, both HDAC inhibitors increased detectable intact plasmid inside nuclei, likely playing a role in the observed enhancement in transgene expression. We have previously reported increased plasmid uptake in two prostate cancer cell lines treated with the nuclear HDAC1/HDAC3 inhibitor entinostat (chapter 3, [148]). The increase in nuclear plasmid levels accompanying inhibition of HDAC6 is likely related to increased levels of acetylated tubulin, previously demonstrated to improve cargo transport toward the nucleus [84, 180].

With the observation of increased plasmid inside the nucleus of human bladder cancer cells and our previous studies in human prostate cancer cells, it seems evident that human cancer cells possess an HDAC-regulated mechanism directly or indirectly regulating transport of internalized cargo to the nucleus; this mechanism is lacking in Chinese Hamster Ovary cells (**Table 4.2**). Given the lack of cell lines tested, however, it is unclear if this phenomenon is cancer-specific or species-specific (human vs hamster).

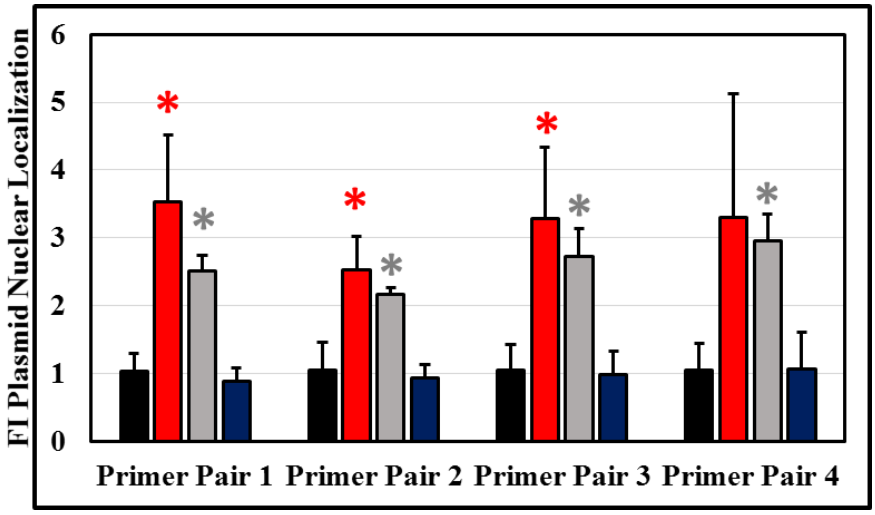

Figure 4.7 pGL3 plasmid enrichment in UMUC3 nuclear fraction with lead inhibitor + transfection treatment. N=3 independent experiments (primer pair 4 n=2 for SB939). Black = 0.2% DMSO (vehicle control); Red = 500 nM SB939; Grey = 1 µM CAY10603; Blue = 40 µM OG-L002. ***** indicates $p<0.05$, plasmid presence in nuclear fraction relative to vehicle control condition (Student's T-test)

Table 4.2 – Effect of HDAC Inhibition on Delivered Plasmid Levels in Nuclei of Human Cancer Cells vs Chinese Hamster Ovary Cells

Increase in pGL3 plasmid Nuclear Entry? Yes or No				
	Cell Line	Cytoplasmic HDAC Inhibitor	Nuclear HDAC Inhibitor	Source
Human Prostate Cancer Cells	PC3	N/A	Entinostat	Elmer, Christensen, et al. *Biotech & Bioeng 2015*
	PC3-PSMA	N/A	Entinostat	
Human Bladder Cancer Cells	UMUC3	CAY10603	SB939	Chapter 4 Study (unpublished)
Hamster Non-Cancerous Cells	CHO-K1	CAY10603	SB939	

4.3.4 Inhibitor Combinations for Further Enhancement of Plasmid Expression

While inhibiting individual epigenetic enzymes has clearly been demonstrated to enhance transgene expression, the strategy of inhibiting multiple enzymes at once in parallel with detection of luciferase expression is advantageous in two ways: first, there is potential for increased enhancement in transgene expression and, second, the results may provide hints regarding which mechanisms are independent, redundant, or synergistic. Combinations of several inhibitors at 1-3 optimal concentrations were carried out in CHO-K1 cells (**Figure 4.8**). When not accounting for changes in viability, there is no detectable enhancement in transgene expression with HDAC inhibitor (SB939) treatment. However, enhancement of transgene expression observed with inhibition of LSD1 using 500 μM 2-PCPA hydrochloride is amplified by inhibition of HDAC with SB939. This suggests there is synergy between these two processes affecting transient transgene expression. Additionally, the combination of LSD1 enhancement with 2-PCPA hydrochloride and EZH2 inhibition with UNC1999 is at least additive in enhancing transgene expression in CHO-K1 cells, and may be synergistic with 500 μM 2-PCPA hydrochloride and 5 μM UNC1999; individual treatments enhance transgene expression by factors of 4.2-fold and 1.4-fold respectively, and the combination yields 7.7-fold enhancement.

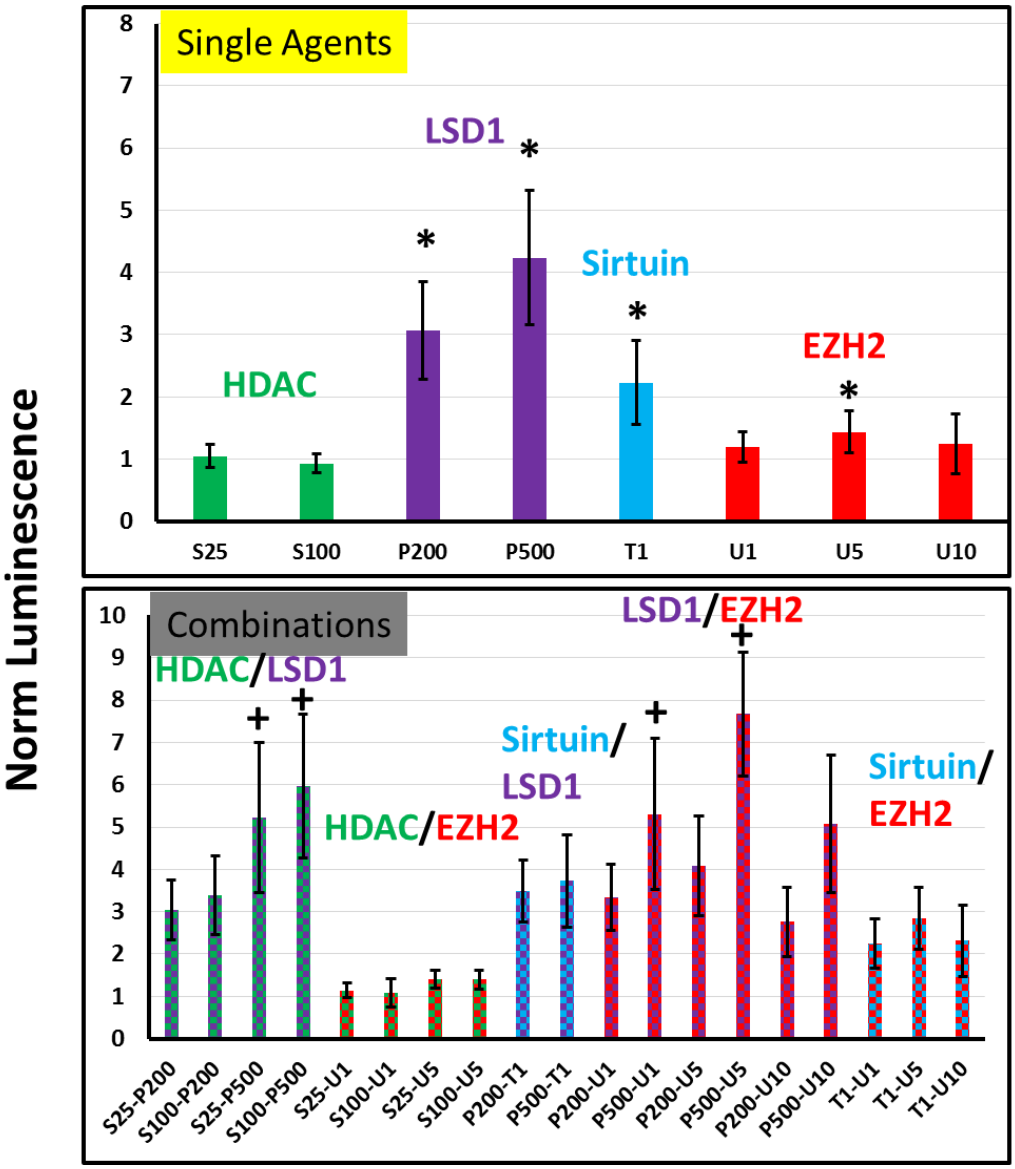

Figure 4.8 Transfections with the NR polymer complexed with the pEF-Luc plasmid were carried out in CHO-K1 cells in the presence of single epigenetic inhibitors (top) or dual combinations of inhibitors (bottom) at expressed doses. Dual combinations are represented by checkers of the two colors corresponding to the individual treatments in the top plot. Transfection efficiency is not normalized to viability, but rather expressed as total luminescnece normalized to DMSO control transfection. *Student's T-test, $p<0.05$ relative to DMSO control treatment (top); + Student's T-test, $p<0.05$ relative to both individual inhibitor treatment transfections. S = SB939 (nM); P = 2-PCPA Hydrochloride (μM); T = Tenovin-1 (μM); U = UNC1999 (μM)

Similar inhibitor combination transfections were carried out in UMUC3 cells (**Figure 4.9**). HDAC inhibition and LSD1 inhibition, which both increase transgene expression individually, additively increased transgene expression when used in combination.

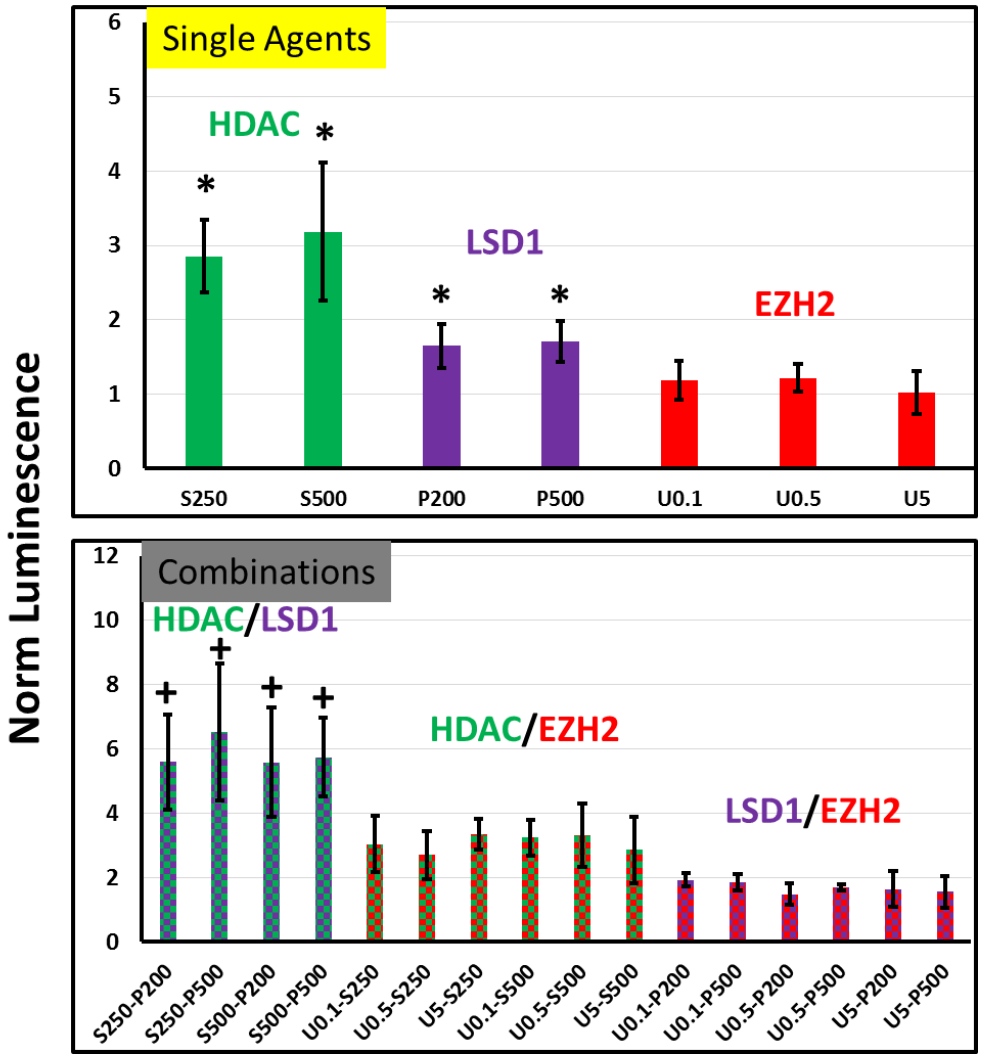

Figure 4.9 Transfections with the NR polymer complexed with the pEF-Luc plasmid were carried out in UMUC3 cells in the presence of single epigenetic inhibitors (top) or dual combinations of inhibitors (bottom) at expressed doses. Dual combinations are represented by checkers of the two colors corresponding to the individual treatments in the top plot. Transfection efficiency is not normalized to viability, but rather expressed as total luminescnece normalized to DMSO control transfection. *Student's T-test, $p<0.05$ relative to DMSO control treatment (top); + Student's T-test, $p<0.05$ relative to both individual inhibitor treatment transfections. S = SB939 (nM); P = 2-PCPA Hydrochloride (μM); U = UNC1999 (μM)

Combinations involving HDAC/EZH2 and LSD1/EZH2 were not promising for further increase in transgene expression.

4.4 DISCUSSION AND CONCLUSIONS

The work explained in chapter 4 has identified a number of epigenetic enzyme classes that play an activating or repressive role in transgene expression in two cell lines. Histone Deacetylase, Lysine Specific Demethylase, and Enhancer of Zeste Homolog 2 enzymes have well-established roles in repressing transcription by removing or adding functional groups to promoters of target genes. In agreement with these roles in chromosomal transcription regulation, inhibitors of these enzymes enhanced transgene expression in one or both cell lines. Inhibition of WDR5 (an MLL methyltransferase component) enhanced transgene expression, contrary to its role of activating target genes in the chromosome. Histone acetyltransferase inhibition led to enhancement, reduction, or no effect on transgene expression; however, the effect on transgene expression appeared to depend on the family of HAT inhibited.

One major limitation of the screening experiments was the inclusion of only one plasmid, given that epigenetic modifications are often dependent on the promoter driving target gene expression. To gauge the generality of the phenomena observed in the screen, dose-response experiments were carried out with select lead inhibitors in each cell line in conjunction with transfections using the original screening plasmid (pEF-Luc) and a second luciferase plasmid, pGL3 (driven by a different promoter). These experiments were carried out twice and it was evident that the observed enhancement in transgene expression occurred regardless of the plasmid (i.e. promoter) used.

Because epigenetic regulation of transcription occurs in the nucleus, it was necessary to determine if there were off-target effects of lead inhibitors altering the amount of plasmid delivered to the nucleus, changing transgene expression independent of epigenetic effects. The pGL3 plasmid was chosen for transfections, which were carried out for 48 hours as with the screen and dose-optimizations. Following transfections, cell nuclei were isolated, DNA purified, and nuclear plasmid quantified using qPCR. Lead inhibitors in CHO-K1 cells did not yield an increase in the presence of plasmid inside target nuclei, indicating that the mechanism(s) responsible for enhanced transgene expression occurred following nuclear entry. In UMUC3 cells, however, HDAC inhibition increased the levels of plasmid inside transfected cell nuclei, explaining a large portion (although not all) of the enhancement in transgene expression. This was consistent with the studies carried out in chapter 3, in which increased plasmid in target prostate cancer cell nuclei transfected in the presence of a different HDAC inhibitor was observed. These data suggested that a currently undetermined mechanism by which HDAC inhibition facilitates transfected plasmid to more efficiently enter the nucleus in human cancer cells; this mechanism was not observed with HDAC inhibition in CHO-K1 cells, which showed only a very moderate enhancement in transgene expression with HDAC inhibition in the screen.

Finally, several of the lead inhibitors were added in combinations to determine if further transfection enhancement was possible. In CHO-K1 cells, HDAC inhibition with SB939 did not enhance transgene expression when not accounting for viability loss (which was accounted for in the screening). However, LSD1 inhibition with 2-PCPA hydrochloride, which strongly enhanced transgene expression individually, was rendered even more effective when carried out in combination with HDAC inhibition. This suggests

synergy in the mechanisms of LSD1 and HDAC related to transgene expression (hypothesis discussed in chapter 5). Additionally, the combination of LSD1 and EZH2 inhibition led to significant further enhancement of transgene expression, with some synergy likely occurring (hypothesis discussed in chapter 5). In UMUC3 cells, simultaneous inhibition of LSD1 and HDAC resulted in additive, although probably not synergistic, enhancement in transgene expression. This suggests that the mechanisms by which LSD1 and HDAC affect transgene expression in UMUC3 cells are not highly linked, but rather likely act independently of each other.

CHAPTER 5 – SUMMARY AND FUTURE DIRECTIONS

The research carried out in chapters 2-4 identified a number of enzymatic targets that positively or negatively affect polymer mediated transgene expression in cancer cells as well as a biotechnologically relevant cell line, CHO-K1. Identified targets included kinase enzymes that regulate functions from cell cycle regulation to extracellular-intracellular signal transduction as well as enzymes that regulate functions such as histone modifications and hypoxia response. Mechanistic evaluation of these inhibitory targets has elucidated information regarding cell cycle, visual transgene trafficking within the cytoplasm, and qPCR quantification of relative transgene levels in the nuclei.

Current experimentation is seeking to create a more tangible link between the regulation of chromosomal gene expression and transgene expression by: 1) assaying for the formation of nucleosomes between plasmid DNA and a core histone as occurs with native DNA chromatin and 2) determining if known histone modifications in native chromatin interact with plasmid DNA. These ongoing experiments are discussed in Future Direction 1.

5.1 FUTURE DIRECTION 1 – PLASMID-HISTONE INTERACTION QUANTIFICATION

5.1.1 Introduction

As discussed in chapters 3 and 4, chromatin structure and transcriptional activity are regulated by a number of post-translational modifications, such as acetylation and methylation, on core histones. These post-translationally modified histones typically

interact with the promoter region of the regulated gene, but can also interact with DNA upstream or downstream of the promoter. While the formation of chromatin with endogenous DNA in eukaryotic cell nuclei is well understood, the formation of plasmid DNA/histone "chromatin" is not well established within the cell. There are numerous examples of nucleosomal DNA/histone particles composed of foreign DNA forming outside of the cell or in cell free assays, but less evidence of exogenous DNA forming such particles inside of a transfected cell; however, a study performed by Russev et al in 2009 suggested that transfected plasmid DNA can form nucleosome-like particles in HEK 293 cells following double strand break-induced linearization [143]. While this study used micrococcal nuclease treatment to form nucleosome-like particles before running a DNA gel to compare the DNA fragment size profile with a chromatin ladder, a stronger argument for the formation of plasmid/histone particles is to directly assay the interaction using chromatin immunoprecipitation (ChIP).

ChIP is a procedure using immunoprecipitation to isolate a desired protein with its complexed nucleic acid components and either subsequent massive DNA sequencing to determine which DNA sequences in a genome interact with this protein (ChIP-seq) [211] or subsequent qPCR (ChIP-qPCR) [212] with a specific set of primers to determine if and to what extent the protein of interest interacts with specific known DNA sequences (ChIP discussion henceforth will refer to ChIP-qPCR). ChIP can be conducted in two different modes. The first mode, termed Native ChIP (N-ChIP) involves immunoprecipitation of chromatin in its native state, directly retrieved from cells or tissue, without cross-linking chromatin protein and DNA. Chromatin is then treated with micrococcal nuclease (MNase) to cut particles into mono-, di-, tri-, etc nucleosomes (depending on MNase

treatment concentration and time). Following immunoprecipitation of proteins, DNA can be isolated from its interacting proteins for final qPCR analyses using phenol:chloroform extraction followed by ethanol precipitation. The second method for carrying out ChIP involves cross-linking of DNA and protein within chromatin with paraformaldehyde, and is referred to as X-ChIP. Following cross-linking, chromatin is sonicated, yielding a size distribution of nucleosome particles (mono-, di-, tri-, etc) depending on the sonication time. After completing the subsequent immunoprecipitation, protein-DNA cross-links are reversed and DNA is purified for qPCR analyses.

X-ChIP and N-ChIP each possess advantages and disadvantages, and these must be weighed when considering the application. N-ChIP is advantageous in that the avoidance of cross-linking evades the isolation of DNA sequences non-specifically interacting with the protein of interest. Additionally, antibody specificity and efficiency are generally tested against unfixed proteins by Western blot, so antibody efficiency for N-ChIP is better predicted by antibody testing than for X-ChIP, which can damage the epitope with paraformaldehyde treatment [213]. However, nucleosomal rearrangements may occur during the process of N-ChIP in the absence of cross-linking [213], a problem which is generally avoided with X-ChIP.

Experiments in Future Direction I, which are currently underway, are directed toward determining if exogenously delivered plasmid DNA interacts with a core histone using N-ChIP (experiment 1), and determining if lead epigenetic inhibitors facilitate interactions of plasmid DNA with specific functionally marked (methylation, acetylation)

core histones that are generally associated with transcriptionally active chromatin using X-ChIP (experiment 2).

5.1.2 Experiment 1 – Endogenous Histone H3 Interaction with Transfected Plasmids

5.1.2A Hypothesis –

The first experiment in Future Direction 1 will be the use of ChIP to detect any intracellular interactions between Histone H3 and the two luciferase reporter plasmids used in Chapter 4 (pEF-Luc and pGL3). Because the purpose of this experiment is to detect if any measurable interaction is occurring, it is important that any signal picked up with qPCR is due to *specific* histone/DNA interactions. For this reason, N-ChIP, as opposed to X-ChIP, will be used for this experiment in an effort to avoid non-specific cross-linking of proximal histone and DNA not interacting with each other. *It is hypothesized that ChIP-qPCR will detect a statistically significant increase in plasmid signal when immunoprecipitation is carried out with a Histone H3 antibody relative to a negative control (IgG) antibody using the fold-enrichment method of quantification, indicating intracellular histone-plasmid interaction*.

5.1.2B Experimental Plan and Anticipated Results–

Polymer-mediated transfections will be carried out similarly to those conducted in chapter 4 with the neomycin-resorcinol diglycidyl ether (NR) polymer complexed with the pEF-Luc and the pGL3 plasmids in both CHO-K1 and UMUC3 cells. However, transfections will be scaled up from 96- and 24-well plate formats to a 6-well plate format in order to increase the number of cells to meet ChIP requirements. Following 48 hours of

transfection, cells will be trypsinized and washed once with 1X PBS. Cell preparation for N-ChIP will then be carried out following a modified protocol combining components of two established N-ChIP protocols (**Figure 5.1**) [213, 214]. Briefly, sucrose gradient separation will be used in parallel with cell lysis to extract nuclei of targeted cells. Nuclei will then be subjected to MNase treatment at the optimally found treatment time (6, 9, 12, and 15 minutes will be tested). The goal is to obtain a distribution of nucleosomes with a detectable mononucleosomal band. Subsequently, the enzymatic cleavage of nucleosomal

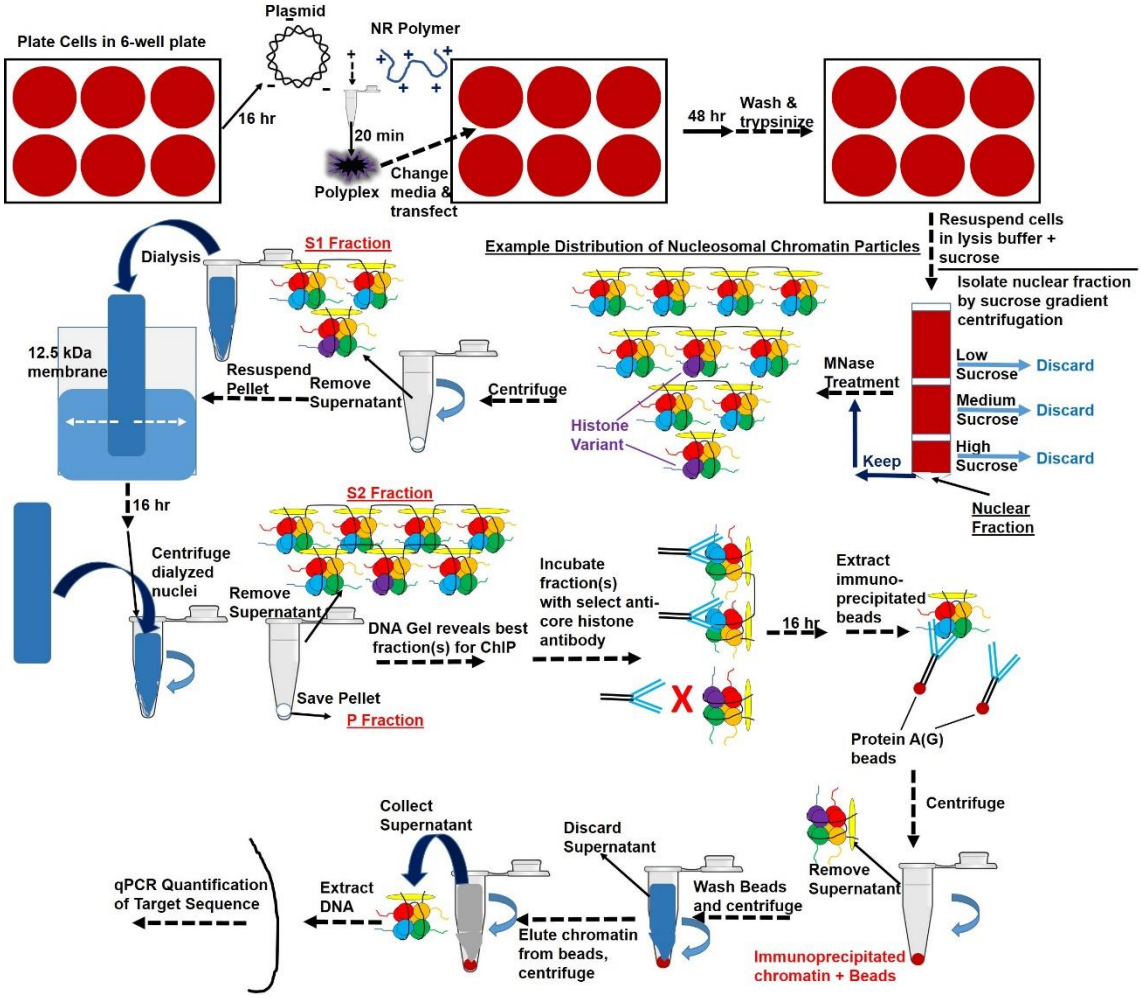

Figure 5.1 General Native ChIP (N-ChIP) protocol to be followed in order to quantify transfected pEF-Luc and pGL3 plasmid interaction with a core histone in nuclei of CHO-K1 and UMUC3 cells

DNA will be halted, and a centrifugation step will be carried out. The supernatant, rich in small nucleosomes (eg. mono- and di-nucleosomes), will be isolated and saved (S1 fraction). The pellet, rich in heavier nucleosome oligomers, will be resuspended and further purified by dialysis and centrifugation (supernatant S2 fraction); the pellet will be saved and also gauged by gel electrophoresis for the presence of large nucleosomal particles. The chromatin fraction(s) richest in mono-,di-, and tri-nucleosomes will be treated with an anti-Histone H3 antibody (Cell Signaling #4620); a negative control antibody (IgG) will also be used for an immunoprecipitation for normalization in the fold-enrichment calculation following qPCR. Using Protein A(G)-conjugated beads, which recognize the antibodies, antibody-bound chromatin will be separated from the unbound chromatin via centrifugation steps; unbound and bound fractions will both be saved. Following several wash steps of the bound fraction, the chromatin will be eluted from the beads, and subsequently DNA will be separated from the protein components of chromatin (including histones) via phenol:chloroform:iaa extraction and ethanol precipitation. qPCR analyses will then be carried out using the SYBR Green detection system (Roche) to quantify fold-enrichment of plasmid sequence-specific signal relative to the negative control IgG antibody.

While promoter sites are common targets for histone interactions, histones can interact with DNA regions upstream of the promoter and even on or downstream of regulated genes. Therefore, primers must be designed to detect histone-plasmid interactions at many sites over the plasmid to assure an exhaustive probing for histone-plasmid nucleosomes. Many primers have been designed and purchased to detect these interactions via ChIP-qPCR, and they are illustrated in **Figure 5.2.**

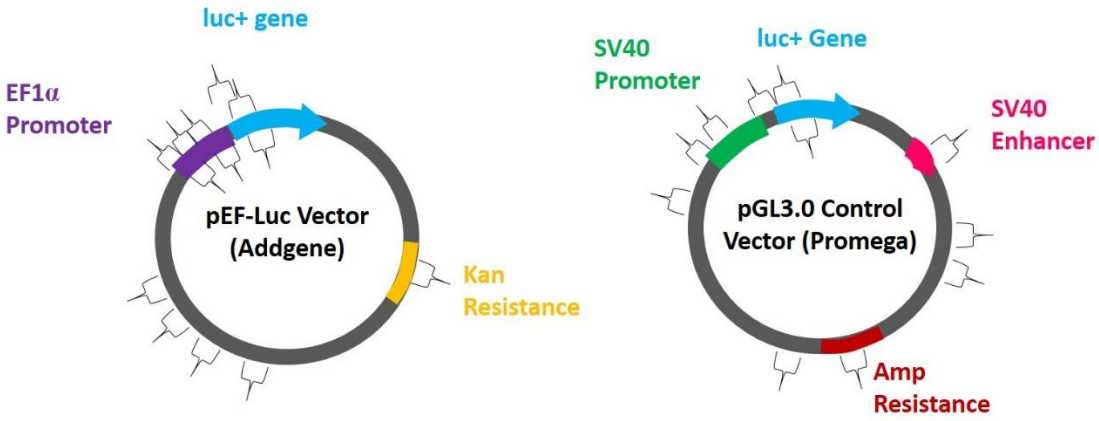

Figure 5.2 Primer amplicon regions for detection of pEF-Luc/histone and pGL3/histone interactions using ChIP-qPCR are roughly shown by brackets

Quantification of qPCR signal will be carried out by comparison of C_t values, using the formula $2^{\wedge}\Delta C_t$ to calculate fold-change in signal between the Histone H3 antibody immunoprecipitation (IP) and the negative control IgG IP. It is anticipated that the Histone H3 IP reaction will generate a stronger qPCR signal than the negative control IgG IP for at least one set of primers, indicating specific interaction between Histone H3 and transfected plasmid.

5.1.3 Experiment 2 – Association of Transcriptionally Active Histone Marks with Plasmid in Presence of Single and Dual Inhibitor Combination Treatments

5.1.3A Hypothesis –

While Experiment 1 aims to determine if transfected plasmid DNA interacts with target cell core histones, forming nucleosome-like particles, Experiment 2 is designed to elucidate the pattern of plasmid interaction with modified histones in the presence of lead epigenetic enzyme inhibitors. The experiments outlined in this section go beyond the question from experiment 1 of "do histones and delivered plasmid DNA interact in the nucleus?" and seek the answer to "how do they interact, and how do these interactions regulate plasmid transcription?" As discussed in chapters 3 and 4, core histones marked

with particular functional groups on specific amino acid residues are more commonly found in chromatin regions of high transcription (euchromatin) than in regions of silenced genes (heterochromatin). To determine if similar mechanisms regulate plasmid expression, polymer-mediated plasmid transfections will be carried out in CHO-K1 cells in the presence of lead inhibitors in the manner discussed in section 5.1.3B.

In chapter 4, inhibitors of HDAC, LSD1, and EZH2 were each discovered to enhance transient plasmid expression in at least one of the two cell lines included in the small molecule epigenetics inhibitor screening. In subsequent experiments, dual inhibitor combinations of these targets were introduced to plasmid-transfected cells (chapter 4). Interestingly, in CHO-K1 cells, combinations of HDAC and LSD1 inhibition resulted in synergistic enhancement in plasmid expression; this phenomenon also appeared to occur with combinatorial LSD1 and EZH2 inhibition in CHO-K1 cells. In UMUC3 cells, combinations of HDAC and LSD1 inhibitors resulted in additive enhancement in plasmid expression, but synergy did not appear to be present. However, enhancement in plasmid expression with individual target inhibition was different in the two cell lines. In UMUC3 cells, HDAC inhibition drastically enhanced transgene expression while very little enhancement was observed in CHO-K1 cells. In UMUC3 cells, EZH2 inhibition did not enhance transgene expression; however, in CHO-K1 cells enhancement was observed. LSD1 inhibition resulted in enhanced expression in both cell lines. These cell line differences in the propensity of plasmid expression to be enhanced by inhibitors of these epigenetic enzymes suggests that epigenetic regulation may differ due to differences in pathways, or possibly in expression or activity levels of downstream targets. The synergistic enhancement of transgene expression observed with dual enzyme inhibition in

CHO-K1 cells, however, suggests that these other pathway members may indeed be the other inhibited enzyme; in other words, inhibition of one target (eg. LSD1) may affect the activity of the other target (eg. HDAC or EZH2). There are instances of this indeed being the case, as many enzyme-induced epigenetic marks on histones are facilitated by the cooperation of other enzymes placing other marks at another site.

HDAC1 and LSD1 are both eraser enzymes that catalyze the removal of a functional group from core histones, promoting transcriptional silencing of local target genes. HDAC1 removes acetyl groups from a number of histone lysine residues, while LSD1 primarily removes methyl groups from di- or mono-methylated histone H3 lysine 4 (H3K4me2 or H3K4me). However, LSD1 and HDAC1 are mutually present in transcriptionally repressive complexes containing the protein CoREST [215]. In a 2005 study that identified an LSD1-CoREST-HDAC1 complex by MS/MS, it was found that LSD1-CoREST-mediated H3K4 demethylation in HeLa cell-isolated nucleosomes was reduced 4-fold when they were first hyperacetylated by treatment with an HDAC inhibitor [198]**,** suggesting synergistic cooperation between HDAC and LSD1 activity. Additionally, a 2013 study demonstrated a two-way cooperation between HDAC1 and LSD1 in embryonic stem cells and embryonic carcinoma cells; in this study, inhibition of either HDAC1 or LSD1 increased both the acetylation of H4K16 (HDAC target) and methylation of H3K4 (LSD1 target) in pluripotent systems (although the same behavior was not observed in tested non-pluripotent systems) [215]. Given the synergistic nature by which simultaneous inhibition of LSD1 and HDAC were found to enhance transgene (plasmid) expression in CHO-K1 cells (**Figure 4.8**) and the known complexation of LSD1 and HDAC, *it is hypothesized that 1) individual inhibition of LSD1 and HDAC inhibition*

in pEF-Luc plasmid transfected CHO-K1 cells will increase the interaction of H3K4me2- and H3K9ac-marked Histone H3, respectively, with pEF-Luc isolated from cell nuclei and 2) combined inhibition of HDAC and LSD1 will further increase pEF-Luc association with H3K4me2 due to hyperacetylation-induced sensitization of nucleosomes to H3K4me2. While acetylation of H3K9ac is one of many HDAC1 targets to choose from, it was selected because HDAC inhibition with SB939 has already been verified to drastically increase H3K9ac in CHO-K1 by Western blot in the laboratory (**Appendix V, Figure A4**).

A second combination of enzyme inhibitors identified to potentially induce synergistic transgene expression enhancement in CHO-K1 cells (**Figure 4.8**) was LSD1 and EZH2. While HDAC1 and LSD1 are known to interact in a number of complexes with the protein CoREST, EZH2 and LSD1 are physically tethered by a long intergenic noncoding RNA (lincRNA), HOTAIR (**Figure 5.3**). HOTAIR has been demonstrated to

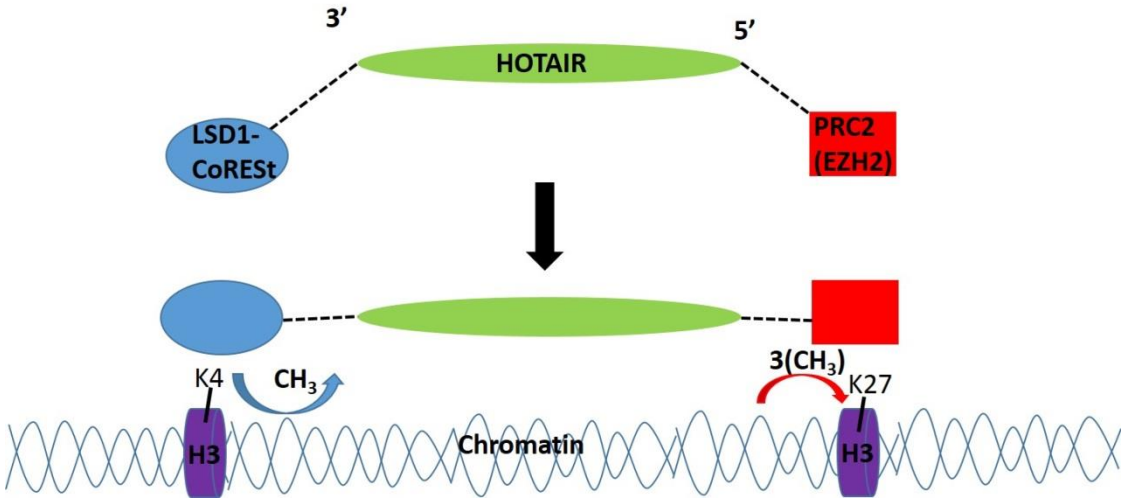

Figure 5.3 The lincRNA, HOTAIR, tethers the epigenetic silencing enzymes LSD1, which promotes H3K4 demethylation, and EZH2, which catalyzes H3K27me3. HOTAIR assists in targeting these enzymes to their enzymatic sites, likely facilitating simultaneous transcriptional repressive histone marks on target gene promoters

not only physically link the EZH2-containing PRC2 complex and the LSD1-CoREST

complex, but also to target these enzymes to their respective functionalization target sites (H3K27 and H3K4) promoting these functional transcriptional silencing transfers on *HOXD* loci [216]. While this hasn't been explicitly demonstrated, one hypothesis is that the binding of active LSD1 to its target site promotes binding of PRC2/EZH2 to its target site via HOTAIR and vice versa, therefore promoting synergistic silencing of target genes. If inhibition of one of these two enzymes in any way obstructs targeting of the other enzyme by HOTAIR, synergistic *enhancement* in transcriptional activation would be expected for target genes. Given the synergy in plasmid expression observed in CHO-K1 cells with LSD1 and EZH2 inhibitors and this dual enzymatic targeting by HOTAIR, *it is hypothesized that dual inhibition of LSD1 with 2-PCPA hydrochloride and EZH2 with UNC1999 will increase the association with plasmid promoter regions of H3K4me2 above and H3K27me3 below levels observed with either individual inhibitor treatment*. While it will not be tested, silencing of HOTAIR transcription may be a strategy to enhance polymer-mediated transgene expression by interrupting linked EZH2-LSD1 targeting to gene promoters.

5.1.3B Experimental Plan and Anticipated Results –

Neomycin resorcinol diglycidyl ether polymer-mediated transfections of the pEF-Luc plasmid will be carried out in the absence of enzyme inhibitors, in the presence of individual inhibitors, or with the dual inhibitor combinations discussed in section 5.1.3A. Following 48 hours, cross-linking ChIP (X-ChIP) will be carried out to quantify levels of plasmid/histone interactions. In the experiments outlined in section 5.1.2, Native ChIP (N-ChIP) was proposed to detect whether plasmid-histone interactions occur in the nuclei of transfected cells; N-ChIP, due to the absence of a cross-linking reaction, does not detect

non-specific interacting molecules, a very important characteristic when trying only to detect if an interaction is occurring at all. However, the experiments outlined in this section are designed to be carried out under the assumption that there *are* histone-plasmid interactions occurring in transfected cells. X-ChIP is a better-established method than N-ChIP and cross-linking provides certain advantages, mainly the avoidance of nucleosome rearrangements during sample preparation.

The general X-ChIP procedure to be followed for quantification of histone-plasmid interactions is illustrated in **Figure 5.4**. Briefly, following 48 hours of transfection, media and inhibitors will be removed from cells and replenished with fresh media to avoid any drug interference with the paraformaldehyde (PFA) cross-linking reaction. Histone and DNA (which includes chromosomal as well as plasmid) will be cross-linked for 10 minutes with 1% PFA. Following reaction quenching with glycine and washes, cells will be detached from their plates by scraping. Sonication will then be carried out in lysis buffer for several different times to optimize this step. Following sonication, supernatant from each sample (each sonicated for a different amount of time) containing chromatin of different sizes will be collected. Once sonication optimization is complete, chromatin sonicated for the optimal amount of time will be incubated with one of several antibodies. For experiments containing HDAC inhibitor, LSD1 inhibitor, or the combination, immunoprecipitations (IPs) will be conducted using an H3K9ac antibody, H3K4me2 antibody, a second antibody detecting a common histone acetylation mark (H4K16), and

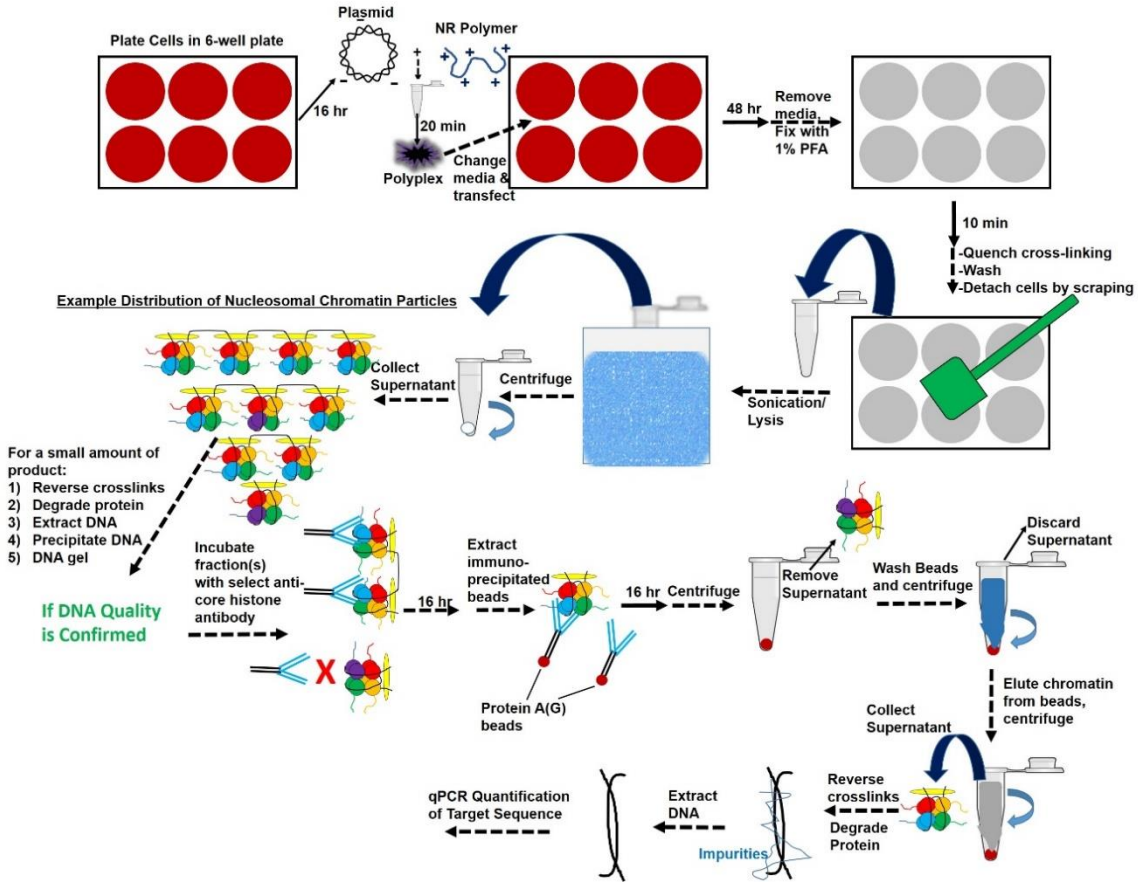

Figure 5.4 General cross-linking ChIP (X-ChIP) protocol to be followed in order to quantify transfected pEF-Luc plasmid interaction with un-modified and modified histone H3 and modified histone H4 in nuclei of CHO-K1 cells

IgG. For transfections in the presence of LSD1 inhibitor, EZH2 inhibitor, or the combination, IPs will be done with H3K4me2, H3K27me3, and IgG antibodies. As with the N-ChIP procedure, immuno-linked chromatin will be incubated with protein A(G)-conjugated beads. Following washes, chromatin will be eluted from the beads and the protein-DNA cross-links reversed, protein degraded with proteinase k, DNA extracted, and histone-DNA interactions quantified via qPCR detection. The percent input method will be used, with the pure chromatin isolated following sonication and centrifugation used as the positive control. qPCR signals from all IPs will be expressed as a percentage of this

input sample. For qPCR detection, the same primer pairs shown for the pEF-Luc plasmid in **Figure 5.2** will be used.

It is anticipated that X-ChIP experiments will reveal interesting mechanistic information about epigenetic regulation of plasmid expression. Regardless of ChIP results with inhibitor combination experiments, if individual inhibitor treatments increase plasmid association with the hypothesized marked histones, this evidence will point to some similarities between epigenetic transcriptional regulation of chromosomal and exogenously delivered plasmid. If ChIP results on combination-inhibited samples provide evidence supporting the hypotheses proposed in this section, it will not only further substantiate the proposition that transgene and chromosomal expression are regulated by similar epigenetic mechanisms, but will supply a more thorough general understanding of the mechanisms behind epigenetic transcriptional repression by the addition of a new system on which histone writer and eraser enzymes and their marked histones function.

5.2 FUTURE DIRECTION 2 – PATHWAY ARTICULATION IN REGULATION OF TRANSGENE EXPRESSION - SYSTEMS BIOLOGY

While *Future Direction 1* highlighted a specific set of experiments focusing on understanding histone-plasmid interactions inside the nuclei of transfected cells, *Future Direction 2* is a suggested broad perspective to take on the field of polymer-mediated transgene expression and, more vaguely, gene delivery in all forms, including viral and non-viral, transient and stable. The findings in chapters 2-4 illuminated numerous targets affecting transient gene expression. As more knowledge about gene delivery and

expression is accumulated, such as the targets and mechanisms described in the previous chapters, the ability to solve the puzzle of how a target cell can be modulated to control transgene expression will be on the horizon. The first step in understanding this extremely complex puzzle is to identify individual targets; many were identified in this thesis and many more will be identified in the future. The second step, which should be executed in parallel, is to connect these targets using a systems biology approach: are these targets completely independent of each other? It is unlikely that they are. The work in this thesis took small steps in that direction by carrying out transfections in the presence of multiple target inhibitors simultaneously, and proposed specific experiments seek to understand how epigenetic enzymatic targets may functionally coordinate with each other to regulate transient gene expression. Others have also begun applying a systems biology approach to understanding this complex puzzle [217].

This approach can be vastly improved by avoiding the classification of enzymes based on their most obvious function. For instance, Gadd45 proteins (discussed briefly in chapters 1 and 4) can be activated in response to DNA damage. They are known to promote global DNA demethylation, but they eventually promote G2/M cell cycle arrest. Overexpression of this protein has been shown to enhance polymer-mediated transgene expression (and inhibition found to decrease it in the epigenetic inhibitor screening in chapter 4). While DNA methylation is a known transcriptional repressor, G2/M cell cycle arrest is generally regarded as the optimal phase for transient gene expression, so it is not obvious to which phenomenon this is attributable; perhaps DNA methylation and cell cycle arrest are not completely independent of each other.

An example of an enzyme that may have multiple implicit effects on transgene expression is PLK1. PLK1, as has been covered in depth in chapter 2, is a very potent regulator of the cell cycle at the G2/M checkpoint, driving cells into mitosis, with its inhibition arresting cells at this transition. However, within the wake of carrying out its cell cycle functions, PLK1 affects other functions that could very well alter transgene expression. For example. PLK1 phosphorylates vimentin, leading to the restriction of endosomal fusion upon mitotic entry [218]. Endosomes continually fuse along the endolysosomal pathway and the continued allowance of endosomal fusion accompanying *inhibition* of PLK1 may play a role in the intracellular trafficking of internalized transgenes and, ultimately, in transgene expression. However, PLK1 has recently been found to positively regulate the formation of acetylated (i.e. stable) microtubules through phosphorylation of kindlin 1, a negative regulator of HDAC6 [219]. As we and others have found (previously discussed), stable, acetylated microtubules through HDAC6 inhibition improve transgene cargo trafficking along microtubules toward the nucleus and enhance transgene expression. Because PLK1 inhibition in this case would counter the effects of HDAC6 inhibition, it is likely that this combination strategy would yield poor results on transgene expression efficacy.

An example of an off-target epigenetic effect potentially improving transgene expression is with HDAC inhibition. HDAC inhibition using trichostatin in colorectal cancer cells has been revealed to activate transcription of Suppressors of Cytokine Signaling (SOCS) genes by promoter hyperacetylation. Because these gene products are negative regulators of the JAK/STAT pathway, JAK2/STAT3 signaling was ultimately

downregulated with HDAC inhibition [220]. As discussed in chapter 2, JAK2 inhibition was found to enhance transgene expression and class I/II HDACs inhibition also enhances transgene expression. As displayed in **Figure 3.7**, JAK2/STAT3 inhibition using the drug AG490 enhanced 1,4C-1,4Bis-mediated transgene expression 9.2-fold and HDAC inhibition with Entinostat enhanced it 15.4-fold; while the combination of these two drugs enhanced transfection 34.9-fold, greater than either individual inhibitor, if these two pathways were acting entirely independently of each other, the combination treatment likely would have yielded much greater enhancement. It's possible that inhibition of class I/II HDAC in combination with JAK2 inhibition was slightly redundant in that a portion of HDAC's mechanism behind transgene expression enhancement may be to inhibit the JAK pathway through SOCS activation.

These are a just a few of countless examples demonstrating that while identifying molecular targets that affect gene delivery and expression is absolutely necessary, it is nowhere near sufficient for solving the puzzle. Significant progress was made in the experiments completed in the previous chapters as well as by many other researchers. This work has begun to and continues to set the foundation for building a thorough understanding of not only the identified transgene expression protein targets and their molecular mechanisms, but what these mechanisms do physically to impose a certain fate on intracellular transgene cargo. The mammalian cell is not simply a black box with a linear response upon an inhibitory perturbation, but rather it's an amalgamation of many functioning pathways that affect each other mutually or through interference, and how these functions affect transgene expression requires a continued persistent effort and likely a systems biological approach.

REFERENCES

[1] R. Kircheis, L. Wightman, E. Wagner, Design and gene delivery activity of modified polyethylenimines, Adv Drug Deliv Rev, 53 (2001) 341-358.

[2] M.H. Schiff, G.R. Burmester, J.D. Kent, A.L. Pangan, H. Kupper, S.B. Fitzpatrick, C. Donovan, Safety analyses of adalimumab (HUMIRA) in global clinical trials and US postmarketing surveillance of patients with rheumatoid arthritis, Ann Rheum Dis, 65 (2006) 889-894.

[3] M.A. Cheever, C.S. Higano, PROVENGE (Sipuleucel-T) in prostate cancer: the first FDA-approved therapeutic cancer vaccine, Clin Cancer Res, 17 (2011) 3520-3526.

[4] T. Vesikari, S.L. Block, F. Guerra, M. Lattanzi, S. Holmes, A. Izu, N. Gaitatzis, A.K. Hilbert, N. Groth, Immunogenicity, safety and reactogenicity of a mammalian cell-culture-derived influenza vaccine in healthy children and adolescents three to seventeen years of age, Pediatr Infect Dis J, 31 (2012) 494-500.

[5] L. Baldi, D.L. Hacker, M. Adam, F.M. Wurm, Recombinant protein production by large-scale transient gene expression in mammalian cells: state of the art and future perspectives, Biotechnol Lett, 29 (2007) 677-684.

[6] J. Zhang, X. Liu, A. Bell, R. To, T.N. Baral, A. Azizi, J. Li, B. Cass, Y. Durocher, Transient expression and purification of chimeric heavy chain antibodies, Protein Expr Purif, 65 (2009) 77-82.

[7] Z. Kiss, S. Elliott, K. Jedynasty, V. Tesar, J. Szegedi, Discovery and basic pharmacology of erythropoiesis-stimulating agents (ESAs), including the hyperglycosylated ESA, darbepoetin alfa: an update of the rationale and clinical impact, Eur J Clin Pharmacol, 66 (2010) 331-340.

[8] K. Zsebo, A. Yaroshinsky, J.J. Rudy, K. Wagner, B. Greenberg, M. Jessup, R.J. Hajjar, Long-term effects of AAV1/SERCA2a gene transfer in patients with severe heart failure: analysis of recurrent cardiovascular events and mortality, Circ Res, 114 (2014) 101-108.

[9] A.R. Barnard, M. Groppe, R.E. MacLaren, Gene therapy for choroideremia using an adeno-associated viral (AAV) vector, Cold Spring Harb Perspect Med, 5 (2015) a017293.

[10] Gene Therapy Clinical Trials Worldwide:, Journal of Gene Medicine, 2015.

[11] D.L. Bartlett, Z. Liu, M. Sathaiah, R. Ravindranathan, Z. Guo, Y. He, Z.S. Guo, Oncolytic viruses as therapeutic cancer vaccines, Mol Cancer, 12 (2013) 103.

[12] M. Duebgen, J. Martinez-Quintanilla, K. Tamura, S. Hingtgen, N. Redjal, H. Wakimoto, K. Shah, Stem cells loaded with multimechanistic oncolytic herpes simplex virus variants for brain tumor therapy, J Natl Cancer Inst, 106 (2014) dju090.

[13] B.J. Passer, T. Cheema, S. Wu, C.L. Wu, S.D. Rabkin, R.L. Martuza, Combination of vinblastine and oncolytic herpes simplex virus vector expressing IL-12 therapy increases antitumor and antiangiogenic effects in prostate cancer models, Cancer Gene Ther, 20 (2013) 17-24.

[14] L. Qu, Y. Wang, L. Gong, J. Zhu, R. Gong, J. Si, Suicide gene therapy for hepatocellular carcinoma cells by survivin promoter-driven expression of the herpes simplex virus thymidine kinase gene, Oncol Rep, 29 (2013) 1435-1440.

[15] H. Kong, L. Tao, K. Qi, Y. Wang, Q. Li, J. Du, Z. Huang, Thymidine kinase/ganciclovir and cytosine deaminase/5-fluorocytosine suicide gene therapy-induced cell apoptosis in breast cancer cells, Oncol Rep, 30 (2013) 1209-1214.

[16] H. Köck, M.P. Harris, S.C. Anderson, T. Machemer, W. Hancock, S. Sutjipto, K.N. Wills, R.J. Gregory, H.M. Shepard, M. Westphal, D.C. Maneval, Adenovirus-mediated p53 gene transfer suppresses growth of human glioblastoma cells in vitro and in vivo, Int J Cancer, 67 (1996) 808-815.

[17] L.C. Pagliaro, A. Keyhani, D. Williams, D. Woods, B. Liu, P. Perrotte, J.W. Slaton, J.A. Merritt, H.B. Grossman, C.P. Dinney, Repeated intravesical instillations of an adenoviral vector in patients with locally advanced bladder cancer: a phase I study of p53 gene therapy, J Clin Oncol, 21 (2003) 2247-2253.

[18] D.L. Tait, P.S. Obermiller, A.R. Hatmaker, S. Redlin-Frazier, J.T. Holt, Ovarian cancer BRCA1 gene therapy: Phase I and II trial differences in immune response and vector stability, Clin Cancer Res, 5 (1999) 1708-1714.

[19] M. Tanaka, H.B. Grossman, In vivo gene therapy of human bladder cancer with PTEN suppresses tumor growth, downregulates phosphorylated Akt, and increases sensitivity to doxorubicin, Gene Ther, 10 (2003) 1636-1642.

[20] S. Anai, S. Goodison, K. Shiverick, K. Iczkowski, M. Tanaka, C.J. Rosser, Combination of PTEN gene therapy and radiation inhibits the growth of human prostate cancer xenografts, Hum Gene Ther, 17 (2006) 975-984.

[21] M. Tijsterman, R.H. Plasterk, Dicers at RISC; the mechanism of RNAi, Cell, 117 (2004) 1-3.

[22] G.J. Hannon, RNA interference, Nature, 418 (2002) 244-251.

[23] S.E. Castel, R.A. Martienssen, RNA interference in the nucleus: roles for small RNAs in transcription, epigenetics and beyond, Nat Rev Genet, 14 (2013) 100-112.

[24] M. Nogawa, T. Yuasa, S. Kimura, M. Tanaka, J. Kuroda, K. Sato, A. Yokota, H. Segawa, Y. Toda, S. Kageyama, T. Yoshiki, Y. Okada, T. Maekawa, Intravesical administration of small interfering RNA targeting PLK-1 successfully prevents the growth of bladder cancer, J Clin Invest, 115 (2005) 978-985.

[25] B. Urban-Klein, S. Werth, S. Abuharbeid, F. Czubayko, A. Aigner, RNAi-mediated gene-targeting through systemic application of polyethylenimine (PEI)-complexed siRNA in vivo, Gene Ther, 12 (2005) 461-466.

[26] M. Centlivre, N. Legrand, S. Klamer, Y.P. Liu, K. Jasmijn von Eije, M. Bohne, E.S. Rijnstra, K. Weijer, B. Blom, C. Voermans, H. Spits, B. Berkhout, Preclinical in vivo evaluation of the safety of a multi-shRNA-based gene therapy against HIV-1, Mol Ther Nucleic Acids, 2 (2013) e120.

[27] S.Y. Chen, A.L. Shiau, Y.T. Li, Y.S. Lin, C.H. Lee, C.L. Wu, C.R. Wang, Suppression of collagen-induced arthritis by intra-articular lentiviral vector-mediated delivery of Toll-like receptor 7 short hairpin RNA gene, Gene Ther, 19 (2012) 752-760.

[28] M.J. Bennett, A.M. Aberle, R.P. Balasubramaniam, J.G. Malone, R.W. Malone, M.H. Nantz, Cationic lipid-mediated gene delivery to murine lung: correlation of lipid hydration with in vivo transfection activity, J Med Chem, 40 (1997) 4069-4078.

[29] T. Potta, Z. Zhen, T.S. Grandhi, M.D. Christensen, J. Ramos, C.M. Breneman, K. Rege, Discovery of antibiotics-derived polymers for gene delivery using combinatorial synthesis and cheminformatics modeling, Biomaterials, 35 (2014) 1977-1988.

[30] S. Barua, A. Joshi, A. Banerjee, D. Matthews, S.T. Sharfstein, S.M. Cramer, R.S. Kane, K. Rege, Parallel Synthesis and Screening of Polymers for Nonviral Gene Delivery, Molecular Pharmaceutics, 6 (2009) 86-97.

[31] N.W. Kam, Z. Liu, H. Dai, Functionalization of carbon nanotubes via cleavable disulfide bonds for efficient intracellular delivery of siRNA and potent gene silencing, J Am Chem Soc, 127 (2005) 12492-12493.

[32] I. Roy, S. Mitra, A. Maitra, S. Mozumdar, Calcium phosphate nanoparticles as novel non-viral vectors for targeted gene delivery, Int J Pharm, 250 (2003) 25-33.

[33] C.H. Jones, C.K. Chen, A. Ravikrishnan, S. Rane, B.A. Pfeifer, Overcoming nonviral gene delivery barriers: perspective and future, Mol Pharm, 10 (2013) 4082-4098.

[34] S. Xiang, H. Tong, Q. Shi, J.C. Fernandes, T. Jin, K. Dai, X. Zhang, Uptake mechanisms of non-viral gene delivery, J Control Release, 158 (2012) 371-378.

[35] D.M. Underhill, A. Ozinsky, Phagocytosis of microbes: complexity in action, Annu Rev Immunol, 20 (2002) 825-852.

[36] I. Kopatz, J.S. Remy, J.P. Behr, A model for non-viral gene delivery: through syndecan adhesion molecules and powered by actin, J Gene Med, 6 (2004) 769-776.

[37] P.R. Dash, M.L. Read, L.B. Barrett, M.A. Wolfert, L.W. Seymour, Factors affecting blood clearance and in vivo distribution of polyelectrolyte complexes for gene delivery, Gene Ther, 6 (1999) 643-650.

[38] E.C. Dell'Angelica, J. Klumperman, W. Stoorvogel, J.S. Bonifacino, Association of the AP-3 adaptor complex with clathrin, Science, 280 (1998) 431-434.

[39] S.D. Conner, S.L. Schmid, Regulated portals of entry into the cell, Nature, 422 (2003) 37-44.

[40] H.T. McMahon, E. Boucrot, Molecular mechanism and physiological functions of clathrin-mediated endocytosis, Nat Rev Mol Cell Biol, 12 (2011) 517-533.

[41] S.L. Schmid, Clathrin-coated vesicle formation and protein sorting: an integrated process, Annu Rev Biochem, 66 (1997) 511-548.

[42] M. Murata, J. Peränen, R. Schreiner, F. Wieland, T.V. Kurzchalia, K. Simons, VIP21/caveolin is a cholesterol-binding protein, Proc Natl Acad Sci U S A, 92 (1995) 10339-10343.

[43] Z. Bengali, J.C. Rea, L.D. Shea, Gene expression and internalization following vector adsorption to immobilized proteins: dependence on protein identity and density, J Gene Med, 9 (2007) 668-678.

[44] A.L. Kiss, E. Botos, Endocytosis via caveolae: alternative pathway with distinct cellular compartments to avoid lysosomal degradation?, J Cell Mol Med, 13 (2009) 1228-1237.

[45] S. Engel, T. Heger, R. Mancini, F. Herzog, J. Kartenbeck, A. Hayer, A. Helenius, Role of endosomes in simian virus 40 entry and infection, J Virol, 85 (2011) 4198-4211.

[46] A.W. Wong, S.J. Scales, D.E. Reilly, DNA internalized via caveolae requires microtubule-dependent, Rab7-independent transport to the late endocytic pathway for delivery to the nucleus, J Biol Chem, 282 (2007) 22953-22963.

[47] J. Rejman, A. Bragonzi, M. Conese, Role of clathrin- and caveolae-mediated endocytosis in gene transfer mediated by lipo- and polyplexes, Mol Ther, 12 (2005) 468-474.

[48] J. Rejman, V. Oberle, I.S. Zuhorn, D. Hoekstra, Size-dependent internalization of particles via the pathways of clathrin- and caveolae-mediated endocytosis, Biochem J, 377 (2004) 159-169.

[49] J. Suh, D. Wirtz, J. Hanes, Efficient active transport of gene nanocarriers to the cell nucleus, Proceedings of the National Academy of Sciences of the United States of America, 100 (2003) 3878-3882.

[50] S. Barua, K. Rege, Cancer-cell-phenotype-dependent differential intracellular trafficking of unconjugated quantum dots, Small, 5 (2009) 370-376.

[51] M.A. van der Aa, E. Mastrobattista, R.S. Oosting, W.E. Hennink, G.A. Koning, D.J. Crommelin, The nuclear pore complex: the gateway to successful nonviral gene delivery, Pharm Res, 23 (2006) 447-459.

[52] S. Huth, F. Hoffmann, K. von Gersdorff, A. Laner, D. Reinhardt, J. Rosenecker, C. Rudolph, Interaction of polyamine gene vectors with RNA leads to the dissociation of plasmid DNA-carrier complexes, J Gene Med, 8 (2006) 1416-1424.

[53] D.V. Schaffer, N.A. Fidelman, N. Dan, D.A. Lauffenburger, Vector unpacking as a potential barrier for receptor-mediated polyplex gene delivery, Biotechnol Bioeng, 67 (2000) 598-606.

[54] H. Herweijer, J.A. Wolff, Progress and prospects: naked DNA gene transfer and therapy, Gene Ther, 10 (2003) 453-458.

[55] W.D. Henner, I. Kleber, R. Benzinger, Transfection of Escherichia coli spheroplasts. 3. Facilitation of transfection and stabilization of spheroplasts by different basic polymers, J Virol, 12 (1973) 741-747.

[56] A. Akinc, M. Thomas, A.M. Klibanov, R. Langer, Exploring polyethylenimine-mediated DNA transfection and the proton sponge hypothesis, J Gene Med, 7 (2005) 657-663.

[57] M.P. Xiong, M.L. Forrest, G. Ton, A. Zhao, N.M. Davies, G.S. Kwon, Poly(aspartate-g-PEI800), a polyethylenimine analogue of low toxicity and high transfection efficiency for gene delivery, Biomaterials, 28 (2007) 4889-4900.

[58] A. Zintchenko, A. Philipp, A. Dehshahri, E. Wagner, Simple modifications of branched PEI lead to highly efficient siRNA carriers with low toxicity, Bioconjug Chem, 19 (2008) 1448-1455.

[59] S. Oliveira, I. van Rooy, O. Kranenburg, G. Storm, R.M. Schiffelers, Fusogenic peptides enhance endosomal escape improving siRNA-induced silencing of oncogenes, Int J Pharm, 331 (2007) 211-214.

[60] R.M. Capito, M. Spector, Collagen scaffolds for nonviral IGF-1 gene delivery in articular cartilage tissue engineering, Gene Ther, 14 (2007) 721-732.

[61] M. Kaouass, R. Beaulieu, D. Balicki, Histonefection: Novel and potent non-viral gene delivery, J Control Release, 113 (2006) 245-254.

[62] D. Balicki, E. Beutler, Histone H2A significantly enhances in vitro DNA transfection, Molecular Medicine, 3 (1997) 782-787.

[63] P. Erbacher, S. Zou, T. Bettinger, A.M. Steffan, J.S. Remy, Chitosan-based vector/DNA complexes for gene delivery: biophysical characteristics and transfection ability, Pharm Res, 15 (1998) 1332-1339.

[64] J.M. Dang, K.W. Leong, Natural polymers for gene delivery and tissue engineering, Adv Drug Deliv Rev, 58 (2006) 487-499.

[65] D.G. Anderson, D.M. Lynn, R. Langer, Semi-automated synthesis and screening of a large library of degradable cationic polymers for gene delivery, Angew Chem Int Ed Engl, 42 (2003) 3153-3158.

[66] T. Potta, Z. Zhen, T. Grandhi, M. Christensen, J. Ramos, C. Breneman, K. Rege, Discovery of Antibiotics-derived Polymers for Gene Delivery using Combinatorial Synthesis and Cheminformatics Modeling, *Biomaterials: in press*, (2013).

[67] L. Ciani, S. Ristori, A. Salvati, L. Calamai, G. Martini, DOTAP/DOPE and DC-Chol/DOPE lipoplexes for gene delivery: zeta potential measurements and electron spin resonance spectra, Biochim Biophys Acta, 1664 (2004) 70-79.

[68] M. Ogris, S. Brunner, S. Schüller, R. Kircheis, E. Wagner, PEGylated DNA/transferrin-PEI complexes: reduced interaction with blood components, extended circulation in blood and potential for systemic gene delivery, Gene Ther, 6 (1999) 595-605.

[69] N. Sakaguchi, C. Kojima, A. Harada, K. Koiwai, N. Emi, K. Kono, Effect of transferrin as a ligand of pH-sensitive fusogenic liposome-lipoplex hybrid complexes, Bioconjug Chem, 19 (2008) 1588-1595.

[70] R.J. Cristiano, J.A. Roth, Epidermal growth factor mediated DNA delivery into lung cancer cells via the epidermal growth factor receptor, Cancer Gene Ther, 3 (1996) 4-10.

[71] S. Mishra, J.D. Heidel, P. Webster, M.E. Davis, Imidazole groups on a linear, cyclodextrin-containing polycation produce enhanced gene delivery via multiple processes, J Control Release, 116 (2006) 179-191.

[72] J. Cheng, R. Zeidan, S. Mishra, A. Liu, S.H. Pun, R.P. Kulkarni, G.S. Jensen, N.C. Bellocq, M.E. Davis, Structure-function correlation of chloroquine and analogues as transgene expression enhancers in nonviral gene delivery, J Med Chem, 49 (2006) 6522-6531.

[73] C.L. Grigsby, K.W. Leong, Balancing protection and release of DNA: tools to address a bottleneck of non-viral gene delivery, J R Soc Interface, 7 Suppl 1 (2010) S67-82.

[74] E.E. Vaughan, D.A. Dean, Intracellular trafficking of plasmids during transfection is mediated by microtubules, Mol Ther, 13 (2006) 422-428.

[75] M.A. Badding, E.E. Vaughan, D.A. Dean, Transcription factor plasmid binding modulates microtubule interactions and intracellular trafficking during gene transfer, Gene Ther, 19 (2012) 338-346.

[76] M.A. Zanta, P. Belguise-Valladier, J.P. Behr, Gene delivery: a single nuclear localization signal peptide is sufficient to carry DNA to the cell nucleus, Proc Natl Acad Sci U S A, 96 (1999) 91-96.

[77] T. Nagasaki, T. Myohoji, T. Tachibana, S. Futaki, S. Tamagaki, Can nuclear localization signals enhance nuclear localization of plasmid DNA?, Bioconjug Chem, 14 (2003) 282-286.

[78] M. Tanimoto, H. Kamiya, N. Minakawa, A. Matsuda, H. Harashima, No enhancement of nuclear entry by direct conjugation of a nuclear localization signal peptide to linearized DNA, Bioconjug Chem, 14 (2003) 1197-1202.

[79] N. Hanna, P. Ohana, F.M. Konikoff, G. Leichtmann, A. Hubert, L. Appelbaum, Y. Kopelman, A. Czerniak, A. Hochberg, Phase 1/2a, dose-escalation, safety, pharmacokinetic and preliminary efficacy study of intratumoral administration of BC-819 in patients with unresectable pancreatic cancer, Cancer Gene Ther, 19 (2012) 374-381.

[80] S. Zolotukhin, M. Potter, W.W. Hauswirth, J. Guy, N. Muzyczka, A "humanized" green fluorescent protein cDNA adapted for high-level expression in mammalian cells, J Virol, 70 (1996) 4646-4654.

[81] S. Brunner, T. Sauer, S. Carotta, M. Cotten, M. Saltik, E. Wagner, Cell cycle dependence of gene transfer by lipoplex polyplex and recombinant adenovirus, Gene Therapy, 7 (2000) 401-407.

[82] W. Kim, Y. Kim, G. Lee, Gadd45-induced Cell Cycle G2/M Arrest for Improved Transient Gene Expression in Chinese Hamster Ovary Cells, Biotechnology and Bioprocess Engineering, 19 (2014) 386-393.

[83] M.A. Badding, D.A. Dean, Highly acetylated tubulin permits enhanced interactions with and trafficking of plasmids along microtubules, Gene Ther, 20 (2013) 616-624.

[84] S. Barua, K. Rege, The influence of mediators of intracellular trafficking on transgene expression efficacy of polymer-plasmid DNA complexes, Biomaterials, 31 (2010) 5894-5902.

[85] H. Hemmi, O. Takeuchi, T. Kawai, T. Kaisho, S. Sato, H. Sanjo, M. Matsumoto, K. Hoshino, H. Wagner, K. Takeda, S. Akira, A Toll-like receptor recognizes bacterial DNA, Nature, 408 (2000) 740-745.

[86] K.J. Ishii, S. Akira, Innate immune recognition of, and regulation by, DNA, Trends Immunol, 27 (2006) 525-532.

[87] Y. Kumagai, O. Takeuchi, S. Akira, TLR9 as a key receptor for the recognition of DNA, Adv Drug Deliv Rev, 60 (2008) 795-804.

[88] M. Suzuki, V. Cerullo, T.K. Bertin, R. Cela, C. Clarke, M. Guenther, N. Brunetti-Pierri, B. Lee, MyD88-dependent silencing of transgene expression during the innate and adaptive immune response to helper-dependent adenovirus, Hum Gene Ther, 21 (2010) 325-336.

[89] S.C. Hyde, I.A. Pringle, S. Abdullah, A.E. Lawton, L.A. Davies, A. Varathalingam, G. Nunez-Alonso, A.M. Green, R.P. Bazzani, S.G. Sumner-Jones, M. Chan, H. Li, N.S. Yew, S.H. Cheng, A.C. Boyd, J.C. Davies, U. Griesenbach, D.J. Porteous, D.N. Sheppard, F.M. Munkonge, E.W. Alton, D.R. Gill, CpG-free plasmids confer reduced inflammation and sustained pulmonary gene expression, Nat Biotechnol, 26 (2008) 549-551.

[90] G. Manning, D.B. Whyte, R. Martinez, T. Hunter, S. Sudarsanam, The protein kinase complement of the human genome, Science, 298 (2002) 1912-1934.

[91] E. Li, D. Stupack, R. Klemke, D.A. Cheresh, G.R. Nemerow, Adenovirus endocytosis via alpha(v) integrins requires phosphoinositide-3-OH kinase, J Virol, 72 (1998) 2055-2061.

[92] R.G. Parton, B. Joggerst, K. Simons, Regulated internalization of caveolae, J Cell Biol, 127 (1994) 1199-1215.

[93] S.D. Conner, S.L. Schmid, Identification of an adaptor-associated kinase, AAK1, as a regulator of clathrin-mediated endocytosis, J Cell Biol, 156 (2002) 921-929.

[94] X. Jiang, R.S. Yeung, Regulation of microtubule-dependent protein transport by the TSC2/mammalian target of rapamycin pathway, Cancer Res, 66 (2006) 5258-5269.
[95] M. Malumbres, Physiological relevance of cell cycle kinases, Physiol Rev, 91 (2011) 973-1007.

[96] J.S. Rawlings, K.M. Rosler, D.A. Harrison, The JAK/STAT signaling pathway, J Cell Sci, 117 (2004) 1281-1283.

[97] S. Gupta, T. Barrett, A.J. Whitmarsh, J. Cavanagh, H.K. Sluss, B. Dérijard, R.J. Davis, Selective interaction of JNK protein kinase isoforms with transcription factors, EMBO J, 15 (1996) 2760-2770.

[98] Z. ur Rehman, D. Hoekstra, I.S. Zuhorn, Protein kinase A inhibition modulates the intracellular routing of gene delivery vehicles in HeLa cells, leading to productive transfection, J Control Release, 156 (2011) 76-84.

[99] E.H. van den Bogaard, D. Rodijk-Olthuis, P.A. Jansen, I.M. van Vlijmen-Willems, P.E. van Erp, I. Joosten, P.L. Zeeuwen, J. Schalkwijk, Rho kinase inhibitor Y-27632 prolongs the life span of adult human keratinocytes, enhances skin equivalent development, and facilitates lentiviral transduction, Tissue Eng Part A, 18 (2012) 1827-1836.

[100] M.C. Gong, J.B. Latouche, A. Krause, W.D. Heston, N.H. Bander, M. Sadelain, Cancer patient T cells genetically targeted to prostate-specific membrane antigen specifically lyse prostate cancer cells and release cytokines in response to prostate-specific membrane antigen, Neoplasia (New York, N.Y, 1 (1999) 123-127.

[101] D.A. Grueneberg, S. Degot, J. Pearlberg, W. Li, J.E. Davies, A. Baldwin, W. Endege, J. Doench, J. Sawyer, Y. Hu, F. Boyce, J. Xian, K. Munger, E. Harlow, Kinase requirements in human cells: I. Comparing kinase requirements across various cell types, Proc Natl Acad Sci U S A, 105 (2008) 16472-16477.

[102] A. Baldwin, W. Li, M. Grace, J. Pearlberg, E. Harlow, K. Münger, D.A. Grueneberg, Kinase requirements in human cells: II. Genetic interaction screens identify kinase requirements following HPV16 E7 expression in cancer cells, Proc Natl Acad Sci U S A, 105 (2008) 16478-16483.

[103] A. Bommi-Reddy, I. Almeciga, J. Sawyer, C. Geisen, W. Li, E. Harlow, W.G. Kaelin, D.A. Grueneberg, Kinase requirements in human cells: III. Altered kinase requirements in VHL-/- cancer cells detected in a pilot synthetic lethal screen, Proc Natl Acad Sci U S A, 105 (2008) 16484-16489.

[104] D.A. Grueneberg, W. Li, J.E. Davies, J. Sawyer, J. Pearlberg, E. Harlow, Kinase requirements in human cells: IV. Differential kinase requirements in cervical and renal human tumor cell lines, Proc Natl Acad Sci U S A, 105 (2008) 16490-16495.

[105] J. Pearlberg, S. Degot, W. Endege, J. Park, J. Davies, E. Gelfand, J. Sawyer, A. Conery, J. Doench, W. Li, L. Gonzalez, F.M. Boyce, L. Brizuela, J. Labaer, D. Grueneberg, E. Harlow, Screens using RNAi and cDNA expression as surrogates for genetics in mammalian tissue culture cells, Cold Spring Harb Symp Quant Biol, 70 (2005) 449-459.

[106] M.D. Christensen, J.J. Elmer, S. Eaton, L. Gonzalez-Malerva, J. LaBaer, K. Rege, Kinome-level screening identifies inhibition of polo-like kinase-1 (PLK1) as a target for enhancing non-viral transgene expression, J Control Release, 204 (2015) 20-29.

[107] A. Gazit, N. Osherov, I. Posner, P. Yaish, E. Poradosu, C. Gilon, A. Levitzki, Tyrphostins. 2. Heterocyclic and alpha-substituted benzylidenemalononitrile tyrphostins as potent inhibitors of EGF receptor and ErbB2/neu tyrosine kinases, J Med Chem, 34 (1991) 1896-1907.

[108] E. Wagner, K. Zatloukal, M. Cotten, H. Kirlappos, K. Mechtler, D.T. Curiel, M.L. Birnstiel, Coupling of adenovirus to transferrin-polylysine/DNA complexes greatly enhances receptor-mediated gene delivery and expression of transfected genes, Proc Natl Acad Sci U S A, 89 (1992) 6099-6103.

[109] D.T. Curiel, E. Wagner, M. Cotten, M.L. Birnstiel, S. Agarwal, C.M. Li, S. Loechel, P.C. Hu, High-efficiency gene transfer mediated by adenovirus coupled to DNA-polylysine complexes, Hum Gene Ther, 3 (1992) 147-154.

[110] F. Toyoshima-Morimoto, E. Taniguchi, N. Shinya, A. Iwamatsu, E. Nishida, Polo-like kinase 1 phosphorylates cyclin B1 and targets it to the nucleus during prophase, Nature, 410 (2001) 215-220.

[111] F. Toyoshima-Morimoto, E. Taniguchi, E. Nishida, Plk1 promotes nuclear translocation of human Cdc25C during prophase, EMBO Rep, 3 (2002) 341-348.

[112] M. Takagi, T. Honmura, S. Watanabe, R. Yamaguchi, M. Nogawa, I. Nishimura, F. Katoh, M. Matsuda, H. Hidaka, In vivo antitumor activity of a novel sulfonamide, HMN-214, against human tumor xenografts in mice and the spectrum of cytotoxicity of its active metabolite, HMN-176, Invest New Drugs, 21 (2003) 387-399.

[113] H.J. Stewart, L. Kishikova, F.L. Powell, S.P. Wheatley, T.J. Chevassut, The polo-like kinase inhibitor BI 2536 exhibits potent activity against malignant plasma cells and represents a novel therapy in multiple myeloma, Exp Hematol, 39 (2011) 330-338.

[114] A.T. Dinh, C. Pangarkar, T. Theofanous, S. Mitragotri, Understanding intracellular transport processes pertinent to synthetic gene delivery via stochastic simulations and sensitivity analyses, Biophysical journal, 92 (2007) 831-846.

[115] J. Shi, B. Chou, J.L. Choi, A.L. Ta, S.H. Pun, Investigation of Polyethylenimine/DNA Polyplex Transfection to Cultured Cells Using Radiolabeling and Subcellular Fractionation Methods, Molecular pharmaceutics, 10 (2013) 2145-2156.

[116] N.P. Ingle, L. Xue, T.M. Reineke, Spatiotemporal cellular imaging of polymer-pDNA nanocomplexes affords in situ morphology and trafficking trends, Molecular pharmaceutics, 10 (2013) 4120-4135.

[117] M.J. Reilly, J.D. Larsen, M.O. Sullivan, Polyplexes traffic through caveolae to the Golgi and endoplasmic reticulum en route to the nucleus, Molecular pharmaceutics, 9 (2012) 1280-1290.

[118] R.P. Kulkarni, D.D. Wu, M.E. Davis, S.E. Fraser, Quantitating intracellular transport of polyplexes by spatio-temporal image correlation spectroscopy, Proceedings of the National Academy of Sciences of the United States of America, 102 (2005) 7523-7528.

[119] S. Barua, K. Rege, Cancer-Cell-Phenotype-Dependent Differential Intracellular Trafficking of Unconjugated Quantum Dots, Small, 5 (2009) 370-376.

[120] P.M. Ellis, Q.S. Chu, N. Leighl, S.A. Laurie, H. Fritsch, B. Gaschler-Markefski, S. Gyorffy, G. Munzert, A phase I open-label dose-escalation study of intravenous BI 2536 together with pemetrexed in previously treated patients with non-small-cell lung cancer, Clin Lung Cancer, 14 (2013) 19-27.

[121] J.M. Vose, J.W. Friedberg, E.K. Waller, B.D. Cheson, V. Juvvigunta, H. Fritsch, C. Petit, G. Munzert, A. Younes, The Plk1 inhibitor BI 2536 in patients with refractory or relapsed non-Hodgkin lymphoma: a phase I, open-label, single dose-escalation study, Leuk Lymphoma, 54 (2013) 708-713.

[122] W.C. Tseng, F.R. Haselton, T.D. Giorgio, Mitosis enhances transgene expression of plasmid delivered by cationic liposomes, Biochim Biophys Acta, 1445 (1999) 53-64.

[123] L. Pelkmans, E. Fava, H. Grabner, M. Hannus, B. Habermann, E. Krausz, M. Zerial, Genome-wide analysis of human kinases in clathrin- and caveolae/raft-mediated endocytosis, Nature, 436 (2005) 78-86.

[124] A. Annunziato, Nat. Educ 1st Ed., DNA Packaging: Nucleosomes and Chromatin, 2008.

[125] T.J. Richmond, C.A. Davey, The structure of DNA in the nucleosome core, Nature, 423 (2003) 145-150.

[126] A. Wolffe, Chromatin: Structure and Function 3rd Ed., San Diego: Academic Press1999.

[127] D. Rossetto, N. Avvakumov, J. Cote, Histone phosphorylation A chromatin modification involved in diverse nuclear events, Epigenetics, 7 (2012) 1098-1108.

[128] D. Rossetto, N. Avvakumov, J. Côté, Histone phosphorylation: a chromatin modification involved in diverse nuclear events, Epigenetics, 7 (2012) 1098-1108.

[129] T. Kouzarides, Histone methylation in transcriptional control, Current Opinion in Genetics & Development, 12 (2002) 198-209.

[130] J. Bonnet, D. Devys, L. Tora, Histone H2B Ubiquitination: Signaling Not Scrapping, Drug Discov. Today Technol., 2012.

[131] B. Xhemalce, M. Dawson, A. Bannister, Histone Modifications, in: R.A. Meyers (Ed.) Encyclopedia of Molecular Cell Biology and Molecular Medicine, Wiley-VCH Verlag GmbH & Co. KGaA, Weinheim, Germany, 2011.

[132] X.J. Yang, E. Seto, HATs and HDACs: from structure, function and regulation to novel strategies for therapy and prevention, Oncogene, 26 (2007) 5310-5318.

[133] A.J. Bannister, T. Kouzarides, Regulation of chromatin by histone modifications, Cell Res, 21 (2011) 381-395.

[134] T. Hayakawa, J. Nakayama, Physiological roles of class I HDAC complex and histone demethylase, J Biomed Biotechnol, 2011 (2011) 129383.

[135] X. Nan, H.H. Ng, C.A. Johnson, C.D. Laherty, B.M. Turner, R.N. Eisenman, A. Bird, Transcriptional repression by the methyl-CpG-binding protein MeCP2 involves a histone deacetylase complex, Nature, 393 (1998) 386-389.

[136] M. Glozak, N. Sengupta, X. Zhang, E. Seto, Acetylation and deacetylation of non-histone proteins, Gene, 363 (2005) 15-23.

[137] P. Hasselgren, Ubiquitination, phosphorylation, and acetylation - Triple threat in muscle wasting, Journal of Cellular Physiology, 213 (2007) 679-689.

[138] A. Kumar, P. Rinwa, Histone Deacetylase (HDAC) Inhibitors as Potential Drugs for Neurodegernerative Disorders: An Update, World J. Pharm. Pharm Sci, 1 (2012) 486-498.

[139] S. Ropero, M. Esteller, The role of histone deacetylases (HDACs) in human cancer, Molecular Oncology, 1 (2007) 19-25.

[140] C. Bishop, M. Ramalho, N. Nadkarni, W. Kong, C. Higgins, N. Krauzewicz, Role for centromeric heterochrornatin and PML nuclear bodies in the cellular response to foreign DNA, Molecular and Cellular Biology, 26 (2006) 2583-2594.

[141] A. Poleshko, I. Palagin, R. Zhang, P. Boimel, C. Castagna, P. Adams, A. Skalka, R. Katz, Identification of cellular proteins that maintain retroviral epigenetic silencing: Evidence for an antiviral response, Journal of Virology, 82 (2008) 2313-2323.

[142] T. Nakagawa, M. Bulger, M. Muramatsu, T. Ito, Multistep chromatin assembly on supercoiled plasmid DNA by nucleosome assembly protein-1 and ATP-utilizing chromatin assembly and remodeling factor, Journal of Biological Chemistry, 276 (2001) 27384-27391.

[143] V. Mladenova, E. Mladenov, G. Russev, Organization of plasmid DNA into nucleosome-like structures after transfection in eukaryotic cells, Biotechnology and Biotechnological Equipment, 23 (2009) 1044-1047.

[144] M. Kaouass, R. Beaulieu, D. Balicki, Histonefection: Novel and potent non-viral gene delivery, Journal of Controlled Release, 113 (2006) 245-254.

[145] M. Reilly, J. Larsen, M. Sullivan, Histone H3 Tail Peptides and Poly(ethylenimine) Have Synergistic Effects for Gene Delivery, Molecular Pharmaceutics, 9 (2012) 1031-1040.

[146] E. Hu, E. Dul, C. Sung, Z. Chen, R. Kirkpatrick, G. Zhang, K. Johanson, R. Liu, A. Lago, G. Hofmann, R. Macarron, M. de los Frailes, P. Perez, J. Krawiec, J. Winkler, M. Jaye, Identification of novel isoform-selective inhibitors within class I histone deacetylases, Journal of Pharmacology and Experimental Therapeutics, 307 (2003) 720-728.

[147] L. Vu, J. Ramos, T. Potta, K. Rege, Generation of a Focused Poly(amino ether) Library: Polymer-mediated Transgene Delivery and Gold-Nanorod based Theranostic Systems, Theranostics, 2 (2012) 1160-1173.

[148] J.J. Elmer, M.D. Christensen, S. Barua, J. Lehrman, K.A. Haynes, K. Rege, The histone deacetylase inhibitor Entinostat enhances polymer-mediated transgene expression in cancer cell lines, Biotechnol Bioeng, 113 (2016) 1345-1356.

[149] R.R. Rosato, J.A. Almenara, S. Grant, The histone deacetylase inhibitor MS-275 promotes differentiation or apoptosis in human leukemia cells through a process regulated by generation of reactive oxygen species and induction of p21CIP1/WAF1 1, Cancer Res, 63 (2003) 3637-3645.

[150] A. Khandelwal, L. Gediya, V. Njar, MS-275 synergistically enhances the growth inhibitory effects of RAMBA VN/66-1 in hormone-insensitive PC-3 prostate cancer cells and tumours, British Journal of Cancer, 98 (2008) 1234-1243.

[151] K. Anthony, A. More, X. Zhang, Activation of silenced cytokine gene promoters by the synergistic effect of TBP-TALE and VP64-TALE activators, PLoS One, 9 (2014) e95790.

[152] Z.M. Lu, J. Zhou, X. Wang, Z. Guan, H. Bai, Z.J. Liu, N. Su, K. Pan, J. Ji, D. Deng, Nucleosomes correlate with in vivo progression pattern of de novo methylation of p16 CpG islands in human gastric carcinogenesis, PLoS One, 7 (2012) e35928.

[153] H. Shu, W. Gruissem, L. Hennig, Measuring Arabidopsis chromatin accessibility using DNase I-polymerase chain reaction and DNase I-chip assays, Plant Physiol, 162 (2013) 1794-1801.

[154] H. Hayashi, Y. Ma, T. Kohno, M. Igarashi, K. Yasui, K. Chua, Y. Kubo, M. Ishibashi, R. Urae, S. Irie, T. Matsuyama, Targets in Gene Therapy, in: Y. Yu (Ed.) InTech, 2011.

[155] L. Kasman, P. Lu, C. Voelkel-Johnson, The histone deacetylase inhibitors depsipeptide and MS-275, enhance TRAIL gene therapy of LNCaP prostate cancer cells without adverse effects in normal prostate epithelial cells, Cancer Gene Ther, 14 (2007) 327-334.

[156] L. Kasman, G. Onicescu, C. Voelkel-Johnson, Histone deacetylase inhibitors restore cell surface expression of the coxsackie adenovirus receptor and enhance CMV promoter activity in castration-resistant prostate cancer cells, Prostate Cancer, 2012 (2012) 137163.

[157] Y.M. Wang, P. Zhou, L.Y. Wang, Z.H. Li, Y.N. Zhang, Y.X. Zhang, Correlation between DNase I hypersensitive site distribution and gene expression in HeLa S3 cells, PLoS One, 7 (2012) e42414.

[158] C. Huang, G. Yang, T. Jiang, K. Huang, J. Cao, Z. Qiu, Effects of IL-6 and AG490 on regulation of Stat3 signaling pathway and invasion of human pancreatic cancer cells in vitro, J Exp Clin Cancer Res, 29 (2010) 51.

[159] P.A. Marks, The clinical development of histone deacetylase inhibitors as targeted anticancer drugs, Expert Opin Investig Drugs, 19 (2010) 1049-1066.

[160] S.L. Berger, T. Kouzarides, R. Shiekhattar, A. Shilatifard, An operational definition of epigenetics, Genes Dev, 23 (2009) 781-783.

[161] T.P. Rasmussen, The epigenetics of early development: inferences from stem cells, Mol Reprod Dev, 81 (2014) 194-201.

[162] A. Carrer, K.E. Wellen, Metabolism and epigenetics: a link cancer cells exploit, Curr Opin Biotechnol, 34 (2015) 23-29.

[163] A. Brunet, S.L. Berger, Epigenetics of aging and aging-related disease, J Gerontol A Biol Sci Med Sci, 69 Suppl 1 (2014) S17-20.

[164] C. Johnson, M.O. Warmoes, X. Shen, J.W. Locasale, Epigenetics and cancer metabolism, Cancer Lett, 356 (2015) 309-314.

[165] J. Landgrave-Gómez, O. Mercado-Gómez, R. Guevara-Guzmán, Epigenetic mechanisms in neurological and neurodegenerative diseases, Front Cell Neurosci, 9 (2015) 58.

[166] F. Fuks, DNA methylation and histone modifications: teaming up to silence genes, Curr Opin Genet Dev, 15 (2005) 490-495.

[167] Y. Chang, T. Ganesh, J.R. Horton, A. Spannhoff, J. Liu, A. Sun, X. Zhang, M.T. Bedford, Y. Shinkai, J.P. Snyder, X. Cheng, Adding a lysine mimic in the design of potent inhibitors of histone lysine methyltransferases, J Mol Biol, 400 (2010) 1-7.

[168] T. Jenuwein, C.D. Allis, Translating the histone code, Science, 293 (2001) 1074-1080.

[169] C.M. Gorman, B.H. Howard, R. Reeves, Expression of recombinant plasmids in mammalian cells is enhanced by sodium butyrate, Nucleic Acids Res, 11 (1983) 7631-7648.

[170] G. Escher, A. Hoang, S. Georges, U. Tchoua, A. El-Osta, Z. Krozowski, D. Sviridov, Demethylation using the epigenetic modifier, 5-azacytidine, increases the efficiency of transient transfection of macrophages, J Lipid Res, 46 (2005) 356-365.

[171] A.C. West, R.W. Johnstone, New and emerging HDAC inhibitors for cancer treatment, J Clin Invest, 124 (2014) 30-39.

[172] J.P. Condreay, S.M. Witherspoon, W.C. Clay, T.A. Kost, Transient and stable gene expression in mammalian cells transduced with a recombinant baculovirus vector, Proc Natl Acad Sci U S A, 96 (1999) 127-132.

[173] G. Backliwal, M. Hildinger, S. Chenuet, S. Wulhfard, M. De Jesus, F.M. Wurm, Rational vector design and multi-pathway modulation of HEK 293E cells yield recombinant antibody titers exceeding 1 g/l by transient transfection under serum-free conditions, Nucleic Acids Res, 36 (2008) e96.

[174] Q. Lu, D.S. Wang, C.S. Chen, Y.D. Hu, Structure-based optimization of phenylbutyrate-derived histone deacetylase inhibitors, J Med Chem, 48 (2005) 5530-5535.

[175] C. Salmi-Smail, A. Fabre, F. Dequiedt, A. Restouin, R. Castellano, S. Garbit, P. Roche, X. Morelli, J.M. Brunel, Y. Collette, Modified cap group suberoylanilide hydroxamic acid histone deacetylase inhibitor derivatives reveal improved selective antileukemic activity, J Med Chem, 53 (2010) 3038-3047.

[176] M. Shehu-Xhilaga, D. Rhodes, F. Wightman, H.B. Liu, A. Solomon, S. Saleh, A.E. Dear, P.U. Cameron, S.R. Lewin, The novel histone deacetylase inhibitors metacept-1 and metacept-3 potently increase HIV-1 transcription in latently infected cells, AIDS, 23 (2009) 2047-2050.

[177] V.M. Richon, S. Emiliani, E. Verdin, Y. Webb, R. Breslow, R.A. Rifkind, P.A. Marks, A class of hybrid polar inducers of transformed cell differentiation inhibits histone deacetylases, Proc Natl Acad Sci U S A, 95 (1998) 3003-3007.

[178] M. Dong, Z.Q. Ning, P.Y. Xing, J.L. Xu, H.X. Cao, G.F. Dou, Z.Y. Meng, Y.K. Shi, X.P. Lu, F.Y. Feng, Phase I study of chidamide (CS055/HBI-8000), a new histone deacetylase inhibitor, in patients with advanced solid tumors and lymphomas, Cancer Chemother Pharmacol, 69 (2012) 1413-1422.

[179] H. Wang, N. Yu, D. Chen, K.C. Lee, P.L. Lye, J.W. Chang, W. Deng, M.C. Ng, T. Lu, M.L. Khoo, A. Poulsen, K. Sangthongpitag, X. Wu, C. Hu, K.C. Goh, X. Wang, L. Fang, K.L. Goh, H.H. Khng, S.K. Goh, P. Yeo, X. Liu, Z. Bonday, J.M. Wood, B.W. Dymock, E. Kantharaj, E.T. Sun, Discovery of (2E)-3-{2-butyl-1-[2-(diethylamino)ethyl]-1H-benzimidazol-5-yl}-N-hydroxyacrylamide (SB939), an orally active histone deacetylase inhibitor with a superior preclinical profile, J Med Chem, 54 (2011) 4694-4720.

[180] E.E. Vaughan, R.C. Geiger, A.M. Miller, P.L. Loh-Marley, T. Suzuki, N. Miyata, D.A. Dean, Microtubule acetylation through HDAC6 inhibition results in increased transfection efficiency, Mol Ther, 16 (2008) 1841-1847.

[181] S. Lain, J.J. Hollick, J. Campbell, O.D. Staples, M. Higgins, M. Aoubala, A. McCarthy, V. Appleyard, K.E. Murray, L. Baker, A. Thompson, J. Mathers, S.J. Holland, M.J. Stark, G. Pass, J. Woods, D.P. Lane, N.J. Westwood, Discovery, in vivo activity, and mechanism of action of a small-molecule p53 activator, Cancer Cell, 13 (2008) 454-463.

[182] S. Ropero, M. Esteller, The role of histone deacetylases (HDACs) in human cancer, Mol Oncol, 1 (2007) 19-25.

[183] T. Ueno, S. Endo, R. Saito, M. Hirose, S. Hirai, H. Suzuki, K. Yamato, I. Hyodo, The sirtuin inhibitor tenovin-6 upregulates death receptor 5 and enhances cytotoxic effects of 5-fluorouracil and oxaliplatin in colon cancer cells, Oncol Res, 21 (2013) 155-164.

[184] S. Hirai, S. Endo, R. Saito, M. Hirose, T. Ueno, H. Suzuki, K. Yamato, M. Abei, I. Hyodo, Antitumor effects of a sirtuin inhibitor, tenovin-6, against gastric cancer cells via death receptor 5 up-regulation, PLoS One, 9 (2014) e102831.

[185] S.F. MacCallum, M.J. Groves, J. James, K. Murray, V. Appleyard, A.R. Prescott, A.A. Drbal, A. Nicolaou, J. Cunningham, S. Haydock, I.G. Ganley, N.J. Westwood, P.J. Coates, S. Lain, S. Tauro, Dysregulation of autophagy in chronic lymphocytic leukemia with the small-molecule Sirtuin inhibitor Tenovin-6, Sci Rep, 3 (2013) 1275.

[186] C.M. Grozinger, E.D. Chao, H.E. Blackwell, D. Moazed, S.L. Schreiber, Identification of a class of small molecule inhibitors of the sirtuin family of NAD-dependent deacetylases by phenotypic screening, J Biol Chem, 276 (2001) 38837-38843.

[187] X. Dai, K. Hayashi, H. Nozaki, Y. Cheng, Y. Zhao, Genetic and chemical analyses of the action mechanisms of sirtinol in Arabidopsis, Proc Natl Acad Sci U S A, 102 (2005) 3129-3134.

[188] S. Kawakami, Y. Kinoshita, H. Maruki-Uchida, K. Yanae, M. Sai, T. Ito, Piceatannol and its metabolite, isorhapontigenin, induce SIRT1 expression in THP-1 human monocytic cell line, Nutrients, 6 (2014) 4794-4804.

[189] M.H. Kuo, C.D. Allis, Roles of histone acetyltransferases and deacetylases in gene regulation, Bioessays, 20 (1998) 615-626.

[190] Q. Jin, L.R. Yu, L. Wang, Z. Zhang, L.H. Kasper, J.E. Lee, C. Wang, P.K. Brindle, S.Y. Dent, K. Ge, Distinct roles of GCN5/PCAF-mediated H3K9ac and CBP/p300-mediated H3K18/27ac in nuclear receptor transactivation, EMBO J, 30 (2011) 249-262.

[191] F. Chimenti, B. Bizzarri, E. Maccioni, D. Secci, A. Bolasco, P. Chimenti, R. Fioravanti, A. Granese, S. Carradori, F. Tosi, P. Ballario, S. Vernarecci, P. Filetici, A novel histone acetyltransferase inhibitor modulating Gcn5 network: cyclopentylidene-[4-(4'-chlorophenyl)thiazol-2-yl)hydrazone, J Med Chem, 52 (2009) 530-536.

[192] Y. Dou, T.A. Milne, A.J. Ruthenburg, S. Lee, J.W. Lee, G.L. Verdine, C.D. Allis, R.G. Roeder, Regulation of MLL1 H3K4 methyltransferase activity by its core components, Nat Struct Mol Biol, 13 (2006) 713-719.

[193] G. Senisterra, H. Wu, A. Allali-Hassani, G.A. Wasney, D. Barsyte-Lovejoy, L. Dombrovski, A. Dong, K.T. Nguyen, D. Smil, Y. Bolshan, T. Hajian, H. He, A. Seitova, I. Chau, F. Li, G. Poda, J.F. Couture, P.J. Brown, R. Al-Awar, M. Schapira, C.H. Arrowsmith, M. Vedadi, Small-molecule inhibition of MLL activity by disruption of its interaction with WDR5, Biochem J, 449 (2013) 151-159.

[194] X. Chen, W. Xie, P. Gu, Q. Cai, B. Wang, Y. Xie, W. Dong, W. He, G. Zhong, T. Lin, J. Huang, Upregulated WDR5 promotes proliferation, self-renewal and chemoresistance in bladder cancer via mediating H3K4 trimethylation, Sci Rep, 5 (2015) 8293.

[195] T. Cierpicki, J. Grembecka, Targeting protein-protein interactions in hematologic malignancies: still a challenge or a great opportunity for future therapies?, Immunol Rev, 263 (2015) 279-301.

[196] R. Margueron, D. Reinberg, The Polycomb complex PRC2 and its mark in life, Nature, 469 (2011) 343-349.

[197] Y.H. Lee, S.A. Coonrod, W.L. Kraus, M.A. Jelinek, M.R. Stallcup, Regulation of coactivator complex assembly and function by protein arginine methylation and demethylimination, Proc Natl Acad Sci U S A, 102 (2005) 3611-3616.

[198] Y.J. Shi, C. Matson, F. Lan, S. Iwase, T. Baba, Y. Shi, Regulation of LSD1 histone demethylase activity by its associated factors, Mol Cell, 19 (2005) 857-864.

[199] P.L. Jones, G.J. Veenstra, P.A. Wade, D. Vermaak, S.U. Kass, N. Landsberger, J. Strouboulis, A.P. Wolffe, Methylated DNA and MeCP2 recruit histone deacetylase to repress transcription, Nat Genet, 19 (1998) 187-191.

[200] F. Fuks, W.A. Burgers, A. Brehm, L. Hughes-Davies, T. Kouzarides, DNA methyltransferase Dnmt1 associates with histone deacetylase activity, Nat Genet, 24 (2000) 88-91.

[201] J. Lee, Y. Xia, M.Y. Son, G. Jin, B. Seol, M.J. Kim, M.J. Son, M. Do, M. Lee, D. Kim, K. Lee, Y.S. Cho, A novel small molecule facilitates the reprogramming of human somatic cells into a pluripotent state and supports the maintenance of an undifferentiated state of human pluripotent stem cells, Angew Chem Int Ed Engl, 51 (2012) 12509-12513.

[202] A. Schäfer, L. Schomacher, G. Barreto, G. Döderlein, C. Niehrs, Gemcitabine functions epigenetically by inhibiting repair mediated DNA demethylation, PLoS One, 5 (2010) e14060.

[203] G. Barreto, A. Schäfer, J. Marhold, D. Stach, S.K. Swaminathan, V. Handa, G. Döderlein, N. Maltry, W. Wu, F. Lyko, C. Niehrs, Gadd45a promotes epigenetic gene activation by repair-mediated DNA demethylation, Nature, 445 (2007) 671-675.

[204] C. Barbés, J. Sánchez, M.J. Yebra, M. Robert-Geró, C. Hardisson, Effects of sinefungin and S-adenosylhomocysteine on DNA and protein methyltransferases from Streptomyces and other bacteria, FEMS Microbiol Lett, 57 (1990) 239-243.

[205] E. Bissinger, R. Heinke, W. Sippl, M. Jung, Targeting epigenetic modifiers: Inhibitors of histone methyltransferases, MedChemComm, 1 (2010) 114-124.

[206] D.C. Wahnon, V.K. Shier, S.J. Benkovic, Mechanism-based inhibition of an essential bacterial adenine DNA methyltransferase: rationally designed antibiotics, J Am Chem Soc, 123 (2001) 976-977.

[207] C. Brigati, B. Banelli, A. di Vinci, I. Casciano, G. Allemanni, A. Forlani, L. Borzì, M. Romani, Inflammation, HIF-1, and the epigenetics that follows, Mediators Inflamm, 2010 (2010) 263914.

[208] C.E. Charron, P.C. Chou, D.J. Coutts, V. Kumar, M. To, K. Akashi, L. Pinhu, M. Griffiths, I.M. Adcock, P.J. Barnes, K. Ito, Hypoxia-inducible factor 1alpha induces corticosteroid-insensitive inflammation via reduction of histone deacetylase-2 transcription, J Biol Chem, 284 (2009) 36047-36054.

[209] C. Crosio, G.M. Fimia, R. Loury, M. Kimura, Y. Okano, H. Zhou, S. Sen, C.D. Allis, P. Sassone-Corsi, Mitotic phosphorylation of histone H3: spatio-temporal regulation by mammalian Aurora kinases, Mol Cell Biol, 22 (2002) 874-885.

[210] P. Sabbattini, C. Canzonetta, M. Sjoberg, S. Nikic, A. Georgiou, G. Kemball-Cook, H.W. Auner, N. Dillon, A novel role for the Aurora B kinase in epigenetic marking of silent chromatin in differentiated postmitotic cells, EMBO J, 26 (2007) 4657-4669.

[211] T.S. Furey, ChIP-seq and beyond: new and improved methodologies to detect and characterize protein-DNA interactions, Nat Rev Genet, 13 (2012) 840-852.

[212] X. Lin, L. Tirichine, C. Bowler, Protocol: Chromatin immunoprecipitation (ChIP) methodology to investigate histone modifications in two model diatom species, Plant Methods, 8 (2012) 48.

[213] L.P. O'Neill, B.M. Turner, Immunoprecipitation of native chromatin: NChIP, Methods, 31 (2003) 76-82.

[214] D. Umlauf, Y. Goto, K. Delaval, A. Wagschal, P. Arnaud, R. Feil, Chromatin Immunoprecipitation on Native Chromatin from Cells and Tissues (PROT 22), in: A. Lewis (Ed.) The Epigenome Network of Excellence: The Focal Point for the European Epigenetics Research Community, 2005.

[215] F. Yin, R. Lan, X. Zhang, L. Zhu, F. Chen, Z. Xu, Y. Liu, T. Ye, H. Sun, F. Lu, H. Zhang, LSD1 regulates pluripotency of embryonic stem/carcinoma cells through histone deacetylase 1-mediated deacetylation of histone H4 at lysine 16, Mol Cell Biol, 34 (2014) 158-179.

[216] M.C. Tsai, O. Manor, Y. Wan, N. Mosammaparast, J.K. Wang, F. Lan, Y. Shi, E. Segal, H.Y. Chang, Long noncoding RNA as modular scaffold of histone modification complexes, Science, 329 (2010) 689-693.

[217] T.M. Martin, B.J. Wysocki, J.P. Beyersdorf, T.A. Wysocki, A.K. Pannier, Integrating mitosis, toxicity, and transgene expression in a telecommunications packet-switched network model of lipoplex-mediated gene delivery, Biotechnol Bioeng, 111 (2014) 1659-1671.

[218] K. Ikawa, A. Satou, M. Fukuhara, S. Matsumura, N. Sugiyama, H. Goto, M. Fukuda, M. Inagaki, Y. Ishihama, F. Toyoshima, Inhibition of endocytic vesicle fusion by Plk1-mediated phosphorylation of vimentin during mitosis, Cell Cycle, 13 (2014) 126-137.

[219] H. Patel, I. Stavrou, R.L. Shrestha, V. Draviam, M.C. Frame, V.G. Brunton, Kindlin1 regulates microtubule function to ensure normal mitosis, J Mol Cell Biol, (2016).

[220] H. Xiong, W. Du, Y.J. Zhang, J. Hong, W.Y. Su, J.T. Tang, Y.C. Wang, R. Lu, J.Y. Fang, Trichostatin A, a histone deacetylase inhibitor, suppresses JAK2/STAT3 signaling via inducing the promoter-associated histone acetylation of SOCS1 and SOCS3 in human colorectal cancer cells, Mol Carcinog, 51 (2012) 174-184.

APPENDIX I – KINASE INHIBITOR SCREENING EXPANDED RESULTS

Table A1 – Abbreviated/full names for the kinase targets of all 182 kinase inhibitors, along with some of the reported functions of each kinase

Kinase Target	Kinase Function	Inhibitors Used
Akt (Protein Kinase B)	Metabolism, apoptosis, cell proliferation, transcription, cell migration	MK-2206
		CCT128930
		A-674563
		AT7867
		Gefitinib
ALK (Activin Receptor Like Kinase)	Activates transforming growth factor-β family proteins	NVP-TAE684
		SB 431542
		SB 525334
		PF-2341066
ATM (Ataxia telangiectasia mutated kinase)	DNA damage repair	KU-55933
		KU-60019
		NU7441
Aurora	Cell division/proliferation	TAK-901
		AZD1152-HQPA
		MLN8237
		ZM-447439
		Aurora A Inhibitor I
		VX-680
		CCT129202
		Hesperadin
		AMG 900
		PHA-680632
		SNS-314 Mesylate
		JNJ-7706621
		PHA-739358
		ENMD-2076
		AT9283
		CYC116
		KW 2449
		AZ960
Bcr-Abl Kinase	Cell differentiation, division, adhesion, and stress responses	Nilotinib
		PHA-739358
		AT9283
		KW 2449 (ABL)
		Dasatinib (Abl)
		AZD-0530 (ABL)
		DCC-2036
		WP1130
BMP (Bone Morphogenic Protein Kinase)	Signal transduction, specifically WNT repression, apoptosis	LDN193189
B-Raf	Signal transduction and cell growth	PLX-4720
		ZM 336372
		BAY 73-4506
Caspase		VX-765
CDK (cyclin dependent kinase)	Cell division, transcription, mRNA processing, cell differentiation	Flavopiridol HCl
		Flavopiridol Alvocidib
		AZD5438
		AT7519
		BS-181 HCl
		Roscovitine
		PHA-793887
		SNS-032
		PD0332991
		JNJ-7706621
		Mubritinib
CHK	Initiation of mitosis	AZD7762

(Checkpoint Kinase 1)		LY2603618
c-Kit	Cell proliferation	Imatinib Mesylate
		Masitinib
		OSI-930
		BAY 73-4506
		Ki8751
		Vatalanib
		Telatinib
c-Met (Hepatocyte growth factor receptor)	Embryonic development and wound healing	SGX-523
		SU11274(PKI-SU11274)
		PF-04217903
		JNJ-38877605
		BMS 777607
		PF-2341066
		XL184
		XL880(GSK1363089)
		MGCD-265
		BMS 794833
DNA-PK (DNA dependent protein kinase)	DNA repair	PP121
		NU7441
EGFR (Endothelial Growth Factor Receptor)	Cell Proliferation	Apatinib
		Erlotinib Hydrochloride
		WZ3146
		WZ4002
		PD153035 HCl
		OSI-420
		WZ8040
		Gefitinib(Iressa)
		AEE788
		Lapatinib Ditosylate
		BMS-599626
		BIBW2992(Tovok)
		AG-490
		Mubritinib
		AZD8931
		CI-1033
FAK (Focal Adhesion Kinase or PTK2)	Cell adhesion and migration	PF-562271
FGFR (fibroblast growth factor receptor)	Cell proliferation and differentiation	BIBF1120(Vargatef)
		Masitinib
		TSU-68
FLT-3 (FMS-like tyrosine kinase 3)	Cell development	AC-220
		TG101209
		KW 2449
		Sunitinib Malate
		ENMD-2076
		XL184
		BMS 794833
GSK-3 (glycogen synthase kinase 3)	Cell proliferation, migration, inflammation, glucose regulation, apoptosis	CHIR-99021
		Indirubin
		SB 216763
HER2 (Human epidermal growth factor receptor 2)	Cell proliferation, anti-apoptosis	CP-724714
		Neratinib
		CI-1033(Canertinib)
		AEE788
		Lapatinib Ditosylate
		BMS-599626
		BIBW2992
		AZD8931
IGF-1R (Insulin-like growth factor receptor 1)	Cell survival and proliferation	GSK1838705A
		NVP-ADW742|
JAK (Janus Kinase)	Signal Transduction (STAT transcription factor activation)	LY2784544
		NVP-BSK805
		CP-690550(Tofacitinib)

		Cyt387
		AZD1480
		AZ 960
		AT9283
		AG-490
		TG101209
JNK (c-Jun N-terminal Kinase)	Stress response, differentiation, apoptosis	SP600125
MEK (MAP kinase kinase)	Signal transduction, growth regulation	TAK-733
		GSK1120212
		PD0325901
		U0126-EtOH
		CI-1040 (PD184352)
		AZD8330
		BIX 02189
		AZD6244(Selumetinib)
		AS703026
Mtor (mammalian target of rapamycin)	Cell growth, proliferation, migration, survival, protein synthesis, transcription	WYE-354
		WYE-687
		OSI027
		WAY-600
		PP242
		AZD8055
		KU-0063794
		WYE-125132
		Rapamycin(Sirolimus)
		Everolimus(RAD001)
		Deforolimus(MK-8669)
		PF-04691502
		GDC-0980
		PKI587
		NU7441
		PP121
		GSK1059615
		BEZ235
		PI-103
p38 MAPK (p38 mitogen-activated protein kinase)	Stress responses, cell differentiation, apoptosis, autophagy	PH-797804
		BIRB 796
		SB 203580
		SB 202190
		LY2228820
		VX-745
		VX-702
		Vinorelbine(Navelbine)
PDGFR (Platelet derived growth factor receptor)	Cell proliferation, differentiation, growth, and development	Crenolanib (CP-868569)
		Imatinib Mesylate
		Masitinib
		KI8751
		PP121
		Bibf1120
		Sunitinib Malate
		ABT-869
		Ap24534
		AV-951
		Imatinib
		TSU-68
		Sorafenib Tosylate
		Motesanib Diphosphate
		Telatinib
PI3K (phosphoinositide 3-kinase)	Cell growth, proliferation, differentiation, motility, survival, intracellular trafficking	AS252424
		TGX-221
		PIK-75 Hydrochloride
		PIK-293
		PIK-93
		PIK-90

		GDC-0941
		TG100-115
		AS604850
		AZD6482(PI3-kinase β inhibitor)
		AS-605240
		IC-87114
		XL765
		ZSTK474
		GSK2126458
		BKM-120
		CAL-101
		PIK-294
		A66
		GSK1059615
		BEZ235
		PI-103
		Pf-04691502
		Gdc-0980
		Pki587
PKC (protein kinase c)	Regulating signal transduction and transcription	CX-4945
		Enzastaurin
PLK (polo-like kinase 1)	Cell cycle progression	ON-01910
		HMN-214
		GSK461364
		BI 2536
		BI6727
S6 Kinase (ribosomal s6 kinase	Regulates transcription	AT7867
SRC	Cell differentiation, motility, proliferation, and survival	PCI-32765
		KX2-391
		Bosutinib(SKI-606)
		Dasatinib
		AZD0530(Saracatinib)
		DCC-2036
		ENMD-2076
		Vandetanib
		Motesanib
		NVP-BHG712
Syk (spleen tyrosine kinase)	Cell to cell communication	R935788
		R406
		R406(free base)
Tgf-β	Cell growth	Sb 525334
Tie2 (TEK tyrosine kinase)	Cell to cell communication	XL184
		MGCD-265
VEGFR (vascular endothelial growth factor receptor)	Cell division and migration, microvascular permeability	Pazopanib Hydrochloride
		Cediranib(AZD2171)
		KRN 633
		Axitinib
		Vatalanib
		BMS 794833
		Vandetanib
		AP24534
		AV-951(Tivozanib)
		Imatinib(STI571)
		TSU-68
		Sorafenib Tosylate
		Motesanib Diphosphate
		NVP-BHG712
		Telatinib
		CYC116
		OSI-930
		BAY 73-4506
		KI8751
		XL880
		MGCD-265

		AEE788
		BIBF1120
		Sunitinib Malate
		ABT-869

Table A2 – Effects of all 182 Kinase inhibitors on luciferase expression relative to the control (no drug) in PC3-PSMA cells

***Statistically different than Polyplex/DMSO control (p <0.05)**

Poly/DNA (w/w) = 10:1, Conc. = 10xIC_{50}, n=5

Drug	Ave	StD
BI6727	12.42	13.80
*BI 2536	12.29	5.25
*GSK461364	9.90	4.78
*HMN-214	9.49	8.26
Bosutinib(SKI-606)	6.64	10.96
AG-490	6.43	10.66
PD0332991	6.05	5.59
SNS-314 Mesylate	5.97	6.07
Imatinib Mesylate	5.31	4.67
*Vinorelbine(Navelbine)	4.87	2.54
VX-702	4.82	4.05
PHA-680632	4.40	5.53
KW 2449	4.38	4.09
NVP-ADW742|	4.36	5.87
*SNS-032(BMS-387032)	4.13	2.37
KX2-391	3.97	4.37
Neratinib	3.79	4.42
*AS703026	3.56	2.33
AMG 900	3.37	5.39
*BMS 777607	3.32	1.97
Hesperadin	3.30	2.48
CCT129202	3.28	3.14
*ON-01910	3.24	1.46
*AT9283	3.24	1.35
*VX-680	3.02	1.91
WP1130	2.93	4.70
*CI-1033(Canertinib)	2.71	0.93
PKI587	2.70	4.42
*AC-220	2.69	1.34
*XL184	2.65	0.67
AZD1480	2.65	2.99

*Aurora A Inhibitor I	2.62	0.82
Deforolimus(MK-8669)	2.60	1.90
MGCD-265	2.60	1.68
LY2603618	2.57	2.22
Everolimus(RAD001)	2.46	2.92
*AZD7762	2.45	1.05
*Vatalanib	2.43	1.35
AZ 960	2.37	2.24
*AZD6244(Selumetinib)	2.36	1.08
ZM-447439	2.34	2.23
Masitinib(AB1010)	2.34	2.17
A-674563	2.32	1.88
*PHA-793887	2.29	1.02
SB 525334	2.27	2.26
A66	2.26	2.08
Axitinib	2.25	1.34
TSU-68	2.21	1.66
MLN8237	2.19	1.16
R406(free base)	2.19	1.58
Crenolanib	2.17	3.07
VX-745	2.17	1.03
AP24534	2.14	1.00
PHA-739358	2.12	1.20
ENMD-2076	2.12	0.94
TG101209	2.09	2.00
AZD8931	2.07	2.23
CP-724714	2.03	0.66
NVP-TAE684	2.02	1.27
LY2228820	1.99	1.16
LDN193189	1.92	1.85
PF-2341066	1.92	1.44
KRN 633	1.91	1.28
BIX 02189	1.91	0.91
JNJ-7706621	1.89	2.97
ZM 336372	1.89	3.30
Rapamycin(Sirolimus)	1.88	2.43
XL880(GSK1363089)	1.85	1.34
AEE788	1.78	1.18
WYE-125132	1.78	1.32
BAY 73-4506	1.77	1.22
BIBW2992(Tovok)	1.76	1.40
AT7867	1.75	1.36
Sorafenib Tosylate	1.74	1.06
AZD0530(Saracatinib)	1.70	1.10
AZD8330	1.69	1.87

Motesanib Diphos	1.67	1.45
JNJ-38877605	1.65	0.83
SB 431542	1.63	2.23
R406	1.61	2.42
Enzastaurin	1.59	1.69
KU-60019	1.58	1.66
Roscovitine(CYC202)	1.58	0.53
Imatinib(STI571)	1.53	1.13
WZ8040	1.53	0.40
VX-765	1.51	0.64
PF-04217903	1.49	0.87
SB 216763	1.48	0.95
OSI-420	1.47	1.22
BS-181 hydrochloride	1.47	1.39
CX-4945	1.44	1.20
PD153035 HCl	1.42	0.52
KU-0063794	1.42	1.18
Cediranib(AZD2171)	1.41	1.23
Mubritinib	1.41	1.08
CI-1040 (PD184352)	1.40	0.70
AZD1152-HQPA	1.40	0.76
SP600125	1.39	1.65
PKI-SU11274	1.37	0.65
BMS-599626	1.37	0.87
PI-103	1.34	0.49
Cyt387	1.33	1.38
SGX-523	1.31	0.72
KU-55933	1.28	0.75
U0126-EtOH	1.28	0.39
WZ4002	1.26	0.41
PIK-294	1.26	0.78
NVP-BHG712	1.23	1.24
PD0325901	1.23	0.97
Indirubin	1.23	1.06
Ki8751	1.23	0.79
Telatinib	1.20	0.89
AV-951(Tivozanib)	1.20	0.52
AZD8055	1.19	1.09
CAL-101	1.18	1.11
Pazopanib HCl	1.17	0.82
CHIR-99021	1.15	1.39
Gefitinib(Iressa)	1.14	0.65
PLX-4720	1.14	0.61
SB 202190	1.12	0.51
PP242	1.11	1.00

BKM-120	1.11	0.86
GSK2126458	1.10	1.05
ZSTK474	1.10	1.09
XL765	1.10	1.03
Vandetanib	1.08	0.26
NU7441	1.08	0.33
PF-562271	1.08	0.84
Polyplex only Control	1.05	1.19
ABT-869(Linifanib)	1.05	1.40
GSK1838705A	1.05	0.69
Polyplex/DMSO	1.04	0.06
MK-2206	1.04	0.74
BMS 794833	1.04	0.48
SB 203580	1.03	0.91
CCT128930	1.02	0.55
IC-87114	1.01	0.50
Polyplex/DMSO	1.01	0.03
Dasatinib	1.01	0.88
GSK1120212	1.01	0.86
CYC116	1.00	0.23
PCI-32765	0.99	0.67
AT7519	0.99	0.60
AS-605240	0.99	0.80
AZD6482	0.98	0.69
AS604850	0.97	0.33
TG100-115	0.96	1.38
GDC-0941	0.95	0.84
BIRB 796	0.95	0.80
Lapatinib Ditosylate	0.94	0.22
Sunitinib Malate	0.93	0.55
WAY-600	0.91	0.61
OSI027	0.90	0.42
PIK-90	0.90	0.85
PP121|	0.89	0.65
Flavopiridol(Alvocidib)	0.89	1.24
WZ3146	0.87	0.89
Erlotinib HCl	0.86	0.31
Nilotinib	0.86	0.36
Apatinib	0.86	0.53
PIK-93	0.86	0.77
BEZ235	0.85	0.38
PH-797804	0.83	0.35
TAK-733	0.80	0.54
Polyplex only Control	0.79	0.14
GDC-0980	0.78	0.41

DCC-2036	0.78	0.17
WYE-687	0.78	0.67
PIK-293	0.76	0.57
BIBF1120(Vargatef)	0.73	0.35
OSI-930	0.71	0.24
TAK-901	0.70	0.59
CP-690550(Tofacitinib)	0.68	0.39
R935788	0.66	0.48
NVP-BSK805	0.66	0.22
GSK1059615	0.66	0.52
WYE-354	0.66	0.51
PIK-75 Hydrochloride	0.58	0.56
PF-04691502	0.57	0.76
TGX-221	0.48	0.68
AZD5438	0.46	0.54
LY2784544	0.43	0.19
Flavopiridol HCl	0.42	0.46
AS252424	0.42	0.39

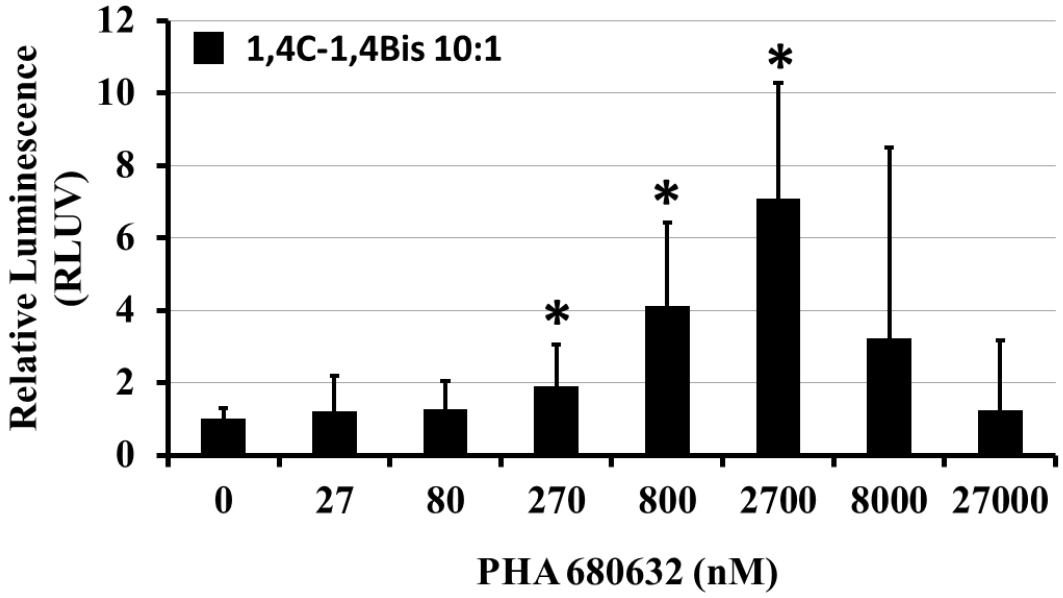

Figure A1 1,4C-1,4Bis-mediated transfections carried out in PC3-PSMA cells in the presence of several doses of the pan-aurora kinase inhibitor PHA 680632. * = Student's T-test, transgene expression enhancement significant relative to DMSO + polyplex control, denoted as "0"

APPENDIX II – ENTINOSTAT EFFECT ON GLOBAL PROTEIN AND TRANSIENT EXPRESSION

Table A3 - Transgene expression, protein content, and cell count for PC3-PSMA cells treated with DMSO vehicle control or 33 µM Entinostat and transfected with pGL3 DNA using 1,4C-1,4Bis polymer as delivery vehicle (n=3 independent experiments, 48 hours following transfection)

	Vehicle Control	**33 µM Entinostat**
RLU/well	$4.01X10^{3}\pm1.25X10^{3}$	$*3.33X10^{4}\pm1.30X10^{4}$
µg Protein/Well	365±40	297±58
Cell Count/Well	$4.66X10^{5}\pm3.04X10^{4}$	$*1.34X10^{5}\pm2.40X10^{4}$
RLU/Cell	$8.6X10^{-3}\pm2.7X10^{-3}$	$*248.4X10^{-3}\pm97.0X10^{-3}$
ng Protein/Cell	0.78±0.09	*2.21±0.43
Vehicle Control Normalized RLU/Cell	1.0±0.3	*28.4±5.3
Vehicle Control Normalized Protein/Cell	1.0±0.1	*2.8±0.3

APPENDIX III – POLYMER MATERIALS USED FOR TRANSFECTIONS

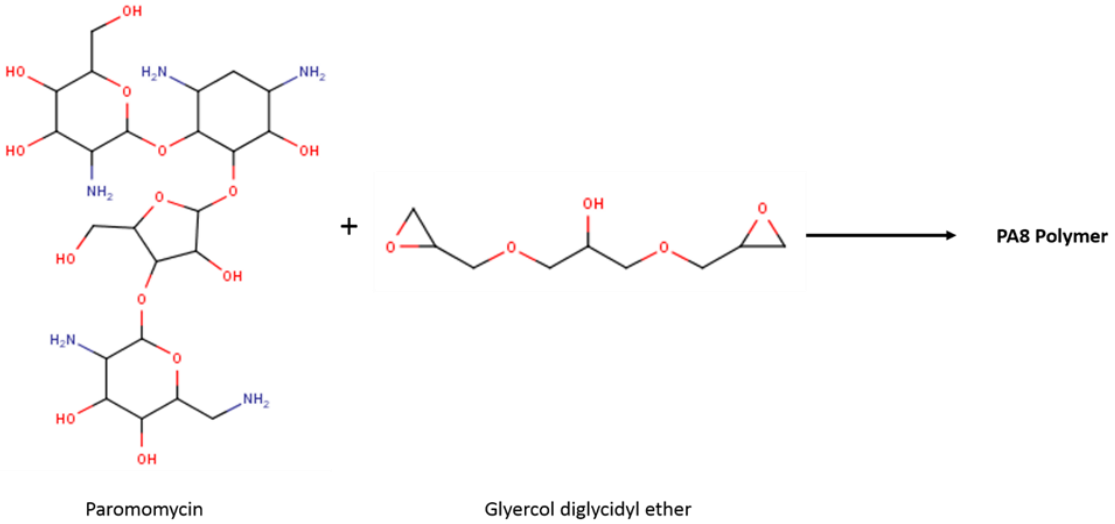

Figure A2 Amine-containing monomer (paromomycin) and ether-containing cross-linker (glycerol diglycidyl ether) used in ring-opening reaction for synthesizing the P8 polymer used in gene delivery studies. Structures drawn using MarvinSketch drawing software (ChemAxon). Structures obtained from Sigma-Aldrich website

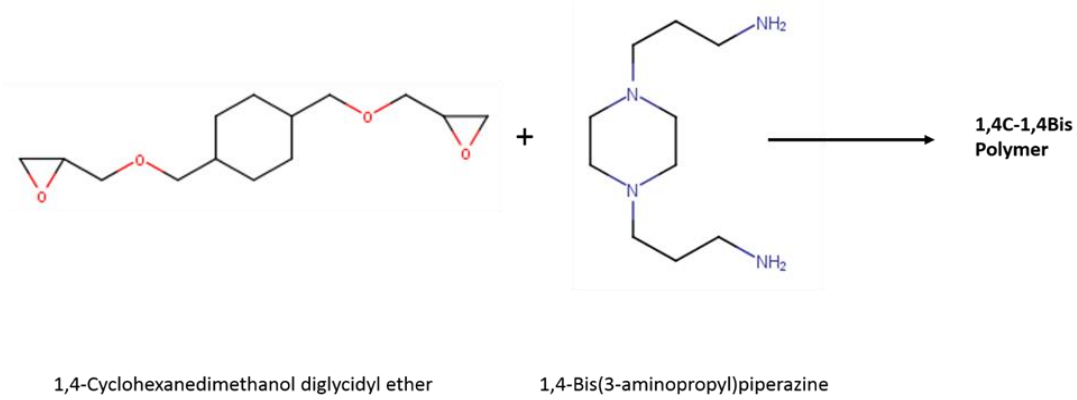

Figure A3 Ether-containing monomer (1,4-cyclohexanedimethanol diglycidyl ether) and amine-containing monomer (1,4-Bis(3-aminopropyl)piperazine) used in ring-opening reaction to synthesize the 1,4C-1,4Bis polymer used in gene delivery studies. Structures drawn using MarvinSketch drawing software (ChemAxon). Structures obtained from Sigma-Aldrich website

APPENDIX IV – EPIGENETIC ENZYME INHIBITORS INCLUDED IN CHAPTER 4

Table A4 – Screening inhibitors and their optimal concentrations for transgene expression enhancement plotted in figures 4.1 and 4.2

Inhibitor	Target	High or Low Dose Candidate?	Optimal Conc (μM) for Transgene Expression
Phthalazinone pyrazole	Aurora A	Low	0.05 (CHO-K1) / 0.5 (UMUC3)
(+)-JQ-1	BET	High	0.5 (both cell lines)
PFI-1	BET	High	0.5 (both cell lines)
2',3',5'-triacetyl-5-azacytidine	DNMT	High	50 (both cell lines)
5-Azacytidine	DNMT	High	0.5 (CHO-K1) / 5 (UMUC3)
Decitabine	DNMT	High	0.5 (CHO-K1) / 50 (UMUC3)
RG-108	DNMT	High	0.5 (both cell lines)
Zebularine	DNMT	High	5 (CHO-K1) / 50 (UMUC3)
Lomeguatrib	DNMT - MGMT	Low	0.05 (CHO-K1) / 5 (UMUC3)
RSC-133	DNMT/HDAC	High	50 (both cell lines)
GSK343	EZH2	Low	5 (both cell lines)
UNC1999	EZH2	Low	5 (both cell lines)
3-Deazaneplanocin A	EZH2 - indirectly	High	0.5 (both cell lines)
Gemicitabine	Gadd45	Low	Reduced Transgene Expression
Mirin	H2Ax phosphorylation	High	5 (CHO-K1) / 50 (UMUC3)
I-CBP112 (hydrochloride)	HAT - CBP/p300	High	50 (CHO-K1) / 5 (UMUC3)
CPTH2 (hydrochloride)	HAT - Gcn5	High	50 (CHO-K1) / 5 (UMUC3)
C646	HAT - p300	High	5 (CHO-K1) / 0.5 (UMUC3)
Anacardic acid	HAT - p300 and PCAF	High	0.5 (CHO-K1) / 5 (UMUC3)
CAY10669	HAT - PCAF	High	50 (both cell lines)
Delphinidin (chloride)	HAT -p300/CBP	High	Reduced Transgene Expression
(S)-HDAC-42	HDAC	Low	0.5 (both cell lines)
CAY10433	HDAC	High	5 (CHO-K1) / 50 (UMUC3)
Chidamide	HDAC	High	5 (both cell lines)
HNHA	HDAC	High	50 (CHO-K1) / 5 (UMUC3)

Oxamflatin	HDAC	Low	0.5 (both cell lines)
Sodium butyrate	HDAC	High	50 (CHO-K1) / 5 (UMUC3)
Apicidin	HDAC - Class I	Low	0.05 (both cell lines)
CBHA	HDAC - Class I	Low	0.5 (CHO-K1) / 5 (UMUC3)
MS-275	HDAC - Class I	High	0.5 (both cell lines)
Pimelic diphenylamide 106	HDAC - Class I	High	5 (both cell lines)
Pyroxamide	HDAC - Class I	High	5 (both cell lines)
Valproic Acid (sodium salt)	HDAC - Class I	High	0.5 (CHO-K1) / 5 (UMUC3)
4-iodo-SAHA	HDAC - Class I/II	High	0.5 (both cell lines)
ITF-2357	HDAC - Class I/II	Low	0.05 (both cell lines)
M 344	HDAC - Class I/II	Low	0.05 (CHO-K1) / 0.5 (UMUC3)
Scriptaid	HDAC - Class I/II	High	5 (CHO-K1) / 0.5 (UMUC3)
Suberohydroxamic Acid (SBHA)	HDAC - Class I/II	High	0.5 (CHO-K1) / 50 (UMUC3)
Suberoylanilide Hydroxamic Acid (SAHA)	HDAC - Class I/II	Low	0.5 (both cell lines)
Trichostatin A	HDAC - Class I/II	Low	0.05 (both cell lines)
CAY10603	HDAC - HDAC6	Low	0.05 (CHO-K1) / 0.5 (UMUC3)
PCI 34051	HDAC - HDAC8	Low	0.5 (CHO-K1) / 5 (UMUC3)
SB939	HDAC - minus HDAC6/7	Low	0.05 (CHO-K1) / 0.5 (UMUC3)
Sodium 4-phenylbutyrate	HDAC - weak	High	50 (CHO-K1) / 0.5 (UMUC3)
CAY10398	HDAC 1	High	5 (both cell lines)
KD-5170	HDAC Class I/II	High	0.5 (both cell lines)
2,4-DPD	HIF1α prolyl hydroxylase	High	50 (both cell lines)
DMOG	HIF1α prolyl hydroxylase	High	50 (both cell lines)
Daminozide	Histone Demethylase - Jumonji	High	0.5 (CHO-K1) / 50 (UMUC3)
GSK-J1 (sodium salt)	Histone Demethylase - Jumonji	High	0.5 (CHO-K1) / 50 (UMUC3)
GSK-J4 (hydrochloride)	Histone Demethylase - Jumonji	High	0.5 (CHO-K1) / 5 (UMUC3)
IOX1	Histone Demethylase - Jumonji	High	5 (both cell lines)

N-Oxalylglycine	Histone Demethylase - Jumonji	High	0.5 (CHO-K1) / 50 (UMUC3)
2-PCPA (hydrochloride)	Histone Demethylase - LSD1	High	50 (both cell lines)
Chaetocin	HMT	High	Very toxic
Ellagic Acid	HMT - CARM	High	Reduced Transgene Expression
BIX01294 (hydrochlorie hydrate)	HMT - G9a	High	5 (both cell lines)
UNC0224	HMT - G9a	Low	0.5 (CHO-K1) / 5 (UMUC3)
UNC-0321 Itrifluoroacetate salt)	HMT - G9a	Low	5 (CHO-K1) / 0.05 (UMUC3)
UNC0638	HMT - G9a/GLP	Low	0.05 (CHO-K1) / 0.5 (UMUC3)
WDR5-0103	HMT - WDR5-MLL complex	High	50 (both cell lines)
Sinefungin	Methyltransferases - General	High	50 (both cell lines)
CCG-100602	Other	High	0.5 (CHO-K1) / 5 (UMUC3)
Isoliquiritigenin	Other	High	5 (both cell lines)
Octyl-α-ketoglutarate	Other	High	0.5 (CHO-K1) / 5 (UMUC3)
S-adenosylhomocysteine	Other	High	50 (both cell lines)
Suramin (sodium salt)	Other	High	5 (both cell lines)
trans-Resveratrol	Other	High	5 (both cell lines)
UNC1215	Other - L3MBTL3 reader	High	50 (both cell lines)
MI-2 (hydrochloride)	Other - MLL	High	5 (both cell lines)
Cl-Amidine (trifluoroacetate salt)	PAD4 deimination	High	50 (both cell lines)
F-Amidine (trifluoroacetate salt)	PAD4 deimination	High	50 (CHO-K1) / 0.5 (UMUC3)
3-amino benzamide	PARP	High	50 (CHO-K1) / 5 (UMUC3)
BSI-201	PARP	High	0.5 (both cell lines)
(-)-Neplanocin A	SAH Hydrolase	Low	0.05 (both cell lines)
1-Naphthoic Acid	Sirtuin	High	50 (both cell lines)
EX-527	Sirtuin	High	0.5 (both cell lines)
Nicotinamide	Sirtuin	High	5 (both cell lines)
JGB1741	Sirtuin - SIRT1	High	0.5 (CHO-K1) / 5 (UMUC3)

Salermide	Sirtuin - SIRT1/2	High	0.5 (CHO-K1) / 5 (UMUC3)
SIRT1/2 Inhibitor IV	Sirtuin - SIRT1/2	High	0.5 (both cell lines)
Sirtinol	Sirtuin - SIRT1/2	High	50 (CHO-K1) / 0.5 (UMUC3)
Tenovin-1	Sirtuin - SIRT1/2	High	0.5 (both cell lines)
Tenovin-6	Sirtuin - SIRT1/2/3	High	5 (CHO-K1) / 0.5 (UMUC3)
AGK2	Sirtuin - SIRT2	High	5 (both cell lines)
Splitomicin	Sirtuin - yeast	High	50 (CHO-K1) / 0.5 (UMUC3)
CAY10591	Sirtuin Activator	High	0.5 (both cell lines)
Piceatannol	Sirtuin Activator	High	0.5 (CHO-K1) / 5 (UMUC3)
PFI-3	SMARC	High	50 (CHO-K1) / 5 (UMUC3)

APPENDIX V – SB939 TREATED CELLS AND HISTONE H3K9 ACETYLATION

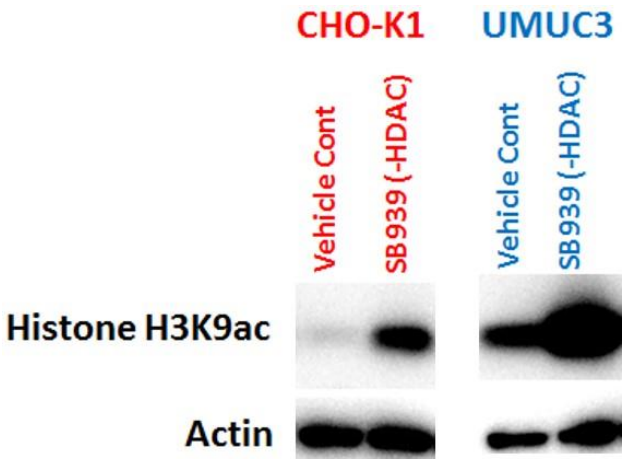

Figure A4 CHO-K1 and UMUC3 cells were treated with the HDAC inhibitor SB939 (500 nM) and transfected with the pEF-Luc plasmid. Following 48 hours of transfection, cells were lysed and assayed for histone H3K9 acetylation via immunoblot

APPENDIX VI – LIST OF GRADUATE CAREER PUBLICATIONS

1) **Christensen MD**, Goklany S, Davis R, Niti R, Meraji M, Haynes K, Rege K. Identification and Investigation of Small Molecule Inhibitors of Epigenetic Modifying Enzymes for Enhancing Plasmid Transgene Expression. In progress; planned submission Fall 2016
2) **Christensen MD**, Elmer JJ, Gonzalez L, Eaton S, LaBaer J, Rege K. Kinome-Level Screening Identifies Inhibition of Polo-Like Kinase 1 (PLK1) as a Target for Enhancing Non-Viral Transgene Expression. *Journal of Controlled Release*. 2015. 204: 20-29 (co first author)
3) Elmer JJ, **Christensen MD**, Barua S, Lehrman J, Haynes K, Rege K. The Histone Deacetylase Inhibitor Entinostat Enhances Polymer-Mediated Transgene Expression. *Biotechnology & Bioengineering*. 2016. 113(6): 1345-56 (co first author)
4) Miryala B, Grandhi S, **Christensen MD**, Tian Y, Rege K. Aminoglycoside-derived Amphiphilic Nanoparticles for Molecular Delivery. Accepted by *Colloids and Surfaces B: Biointerfaces*. June 2016
5) Potta T, Zhen Z, Grandhi T, **Christensen MD**, Ramos J, Breneman CM, Rege K. Discovery of Antibiotics-derived Polymers for Gene Delivery using Combinatorial Synthesis and Cheminformatics Modeling. *Biomaterials*. 2014. 35(6): 1977-88
6) Elmer JJ, **Christensen MD**, Rege K. Applying Horizontal Gene Transfer Phenomena to Enhance Non-viral Gene Therapy. *J. Controlled Release*. 2013. 172: 246-57